

**Preparation and Characterization of Sterically and  
Electrostatically Stabilized TiO<sub>2</sub> Suspensions**

**By**

**AYHAN ULUÇAY**

**A Dissertation Submitted to the  
Graduate School in Partial Fulfillment of the  
Requirements for the Degree of**

**MASTER OF SCIENCE**

**Department: Materials Science and Engineering**

**Major: Materials Science and Engineering**

**Izmir Institute of Technology**

**Izmir, Turkey**

**September, 1999**

**İZMİR YÜKSEK TEKNOLOJİ ENSTİTÜSÜ  
REKTÖRLÜĞÜ  
Kütüphane ve Dokümantasyon Daire Bşk.**

We approve the thesis of Ayhan ULUÇAY

Date of Signature

*Muhsin Çiftçioğlu*  
.....

29.09.1999

**Prof.Dr. Muhsin ÇİFTÇİOĞLU**

Supervisor

Department of Chemical Engineering

*Hürriyet Polat*  
.....

29.09.1999

**Assist.Prof.Dr. Hürriyet POLAT**

Department of Chemistry

*Funda*  
.....

29.09.1999

**Assist.Prof.Dr. Funda TIHMİNLİOĞLU**

Department of Chemical Engineering

*Muhsin Çiftçioğlu*  
.....

29.09.1999

**Prof.Dr. Muhsin ÇİFTÇİOĞLU**

Head of Interdisciplinary

Materials Science and Engineering program

# ACKNOWLEDGEMENT

The aim of this study was the investigation of stable  $TiO_2$  powder suspension. I would like to thank Prof.Dr. Muhsin Çiftçiöğlü for his close supervisory helps, support and encouragements during this study. Special thanks are to all research assistants, especially Uğur Ünal, for their contributions to this thesis and to the laboratory technicians Nilgün Özgül and Şerife Şahin for their help in the laboratory work..

I would like to thank my manager ,Mrs.Gülşen Çeliker, and Yaşar Group.

Finally, I would like to thank my family and my wife for their help and support.

# ABSTRACT

The aim of this study was the investigation of stable  $\text{TiO}_2$  powder suspension formation in water. The water based paints are environmentally safe and expected to replace organic based solvents.

Four different commercial titania pigment powders with different characteristics were used. Only a high molecular weight surfactant was used. Suspensions were prepared for four titania powders at 5,10, and 20 % by volume solid content and the same suspensions were used in the investigation of the effects of the surfactant on the stability of suspensions. The surfactant was added in the range of 0.1 to 0.5 % by weight of pigment. Two characterization methods were used in the analysis: sedimentation and rheological characterization.

It has been found that there are some stable pH ranges for the suspensions prepared by four  $\text{TiO}_2$  powders. In these ranges, it is expected to behave as dilatant - shear thickening and the sediment was densely packed. Three zones, sediment, falling and supernatant zones, were observed in disperse suspensions.

As a result of this, the pH ranges of these powders in water is observed visually. If it has rutile structure in powder C G (95%  $\text{TiO}_2$  content, 5%  $\text{Al}_2\text{O}_3$  coated), it works very well in basic mediums. Also rutile powder G (99%  $\text{TiO}_2$  content, uncoated), it is expected at pH=2 and basic mediums. The anatase powders ,E and F (both are 99%  $\text{TiO}_2$  content, uncoated), are stable in basic mediums. The F has wider stable zone than the powder E.

The results of this work have shown that rutile alumina coated powder C suspensions were stable in basic media. Rutile powder G suspensions were stable at pH=2 and basic media. Anatase powders E and F were stable in basic media with powder F being stable in a wider pH range. The combined analysis of sedimentation -rheological behaviour of suspensions were found to be very helpful in understanding the suspension behaviours. Relatively high sediment packing densities in the 50-60% of theoretical titania density were obtained for some of the suspensions.

# TABLE OF CONTENTS

Bu çalışmanın amacı kararlı yapıda olan  $TiO_2$  tozlarının su içindeki davranışlarını incelemektir. Su bazlı boyalar çevresel olarak daha güvenlidir ve organik çözücülerle olanların yerini alması beklenmektedir.

Dört değişik ticari titanyum dioksit kullanılmıştır ve bunlar değişik özelliklerdedir. Yanlız bir adet yüksek molekül ağırlıklı yüzey aktif maddesi kullanılmış olup, yüksek molekül ağırlığına sahiptir. Bütün süspansiyonlar %5,10 ve 20 hacimce titanyum dioksit içeren oranlarda hazırlanmış ve ayrı bir çalışmada ağırlıkça %0,1 'den %0,5 'e yüzey aktif maddesi girilerek süspansiyonların kararlılıkları incelenmiştir.

Bu çalışmayı analiz edebilmek için iki ölçüm metodu kullanılmıştır: biri akış ile ilgili, diğeri ise sedimentasyon özellikleri ile ilgilidir. Dört farklı tozla hazırlanmış olan süspansiyonların kararlı oldukları belirli pH aralıkları vardır. Bu aralıklarda reolojik yapı dilatant yapı gösterirken, oluşan çökeltinin yüksekliğinin kısa olması ve çökeltinin ise yoğun bir yapıda olması beklenir. Kararlı olduğu aralıklarda üç değişik bölge beklenir; "supernatant", "falling zone" ve "sediment".

Çalışmanın sonucunda, alüminyum oksit ile kaplanmış olan C (%95  $TiO_2$  içeriği ile %5  $Al_2O_3$  kaplaması vardır) tozunun bulunduğu süspansiyon bazik ortamlarda, daha kararlı yapı vermektedir. Saf haldeki rutil G (%99 saf  $TiO_2$  ) tozu ile hazırlananlar ise  $pH=2$  ve bazik ortamlarda kararlıdır. Anatas olan E ve F tozları (%99 saf  $TiO_2$  ) yalnızca bazik ortamlarda kararlı yapı göstermektedir ve F tozunun aralığı daha geniştir. Reolojik ve sedimentasyon davranışlarının incelenmesi süspansiyonların davranışlarının daha kolay anlaşılır hale gelmesini sağlamaktadır ve çökeltilerin sahip oldukları sıklıklarının oranları %50-60 lardadır.

# TABLE OF CONTENTS

	page
LIST OF FIGURES	v
LIST OF TABLES	viii
CHAPTER I INTRODUCTION	1
CHAPTER II PRODUCTION OF TiO <sub>2</sub>	4
2.1 Physical Properties of TiO <sub>2</sub>	4
2.2 Production of TiO <sub>2</sub>	4
2.3 TiO <sub>2</sub> Processing Methods	6
2.4 Application of TiO <sub>2</sub>	8
CHAPTER III PAINT	13
3.1 Composition of Paints	13
3.2 Basic Components	13
3.3 Why TiO <sub>2</sub> is used in paint	15
3.4 Paint Production	16
3.5 New Technologies	17
CHAPTER IV COLLOIDAL MECHANISMS	21
CHAPTER V SEDIMENTATION AND RHEOLOGY	32
5.1 Rheology	32
5.2 Sedimentation	37
CHAPTER VI EXPERIMENTAL	38
CHAPTER VII RESULTS AND DISCUSSION	43
7.1 Characterization of Powder C	46
7.2 Characterization of Powder E	47
7.3 Characterization of Powder F	47
7.4 Characterization of Powder G	49
CHAPTER VIII CONCLUSION AND RECOMMENDATIONS	82
REFERENCES	84
APPENDIX	A1

# LIST OF FIGURES

	page
Figure 2.1	5
Figure 2.2	5
Figure 2.3	7
Figure 2.4	9
Figure 3.1	16
Figure 4.1	24
Figure 4.2	24
Figure 4.3	26
Figure 4.4	26
Figure 4.5	26
Figure 4.6	29
Figure 4.7	30
Figure 5.1	34
Figure 5.2	34
Figure 5.3	36
Figure 5.4	36
Figure 5.5	36
Figure 5.6	37
Figure 6.1	41

Figure 6.2	Particle size diagrams for powder G	41
Figure 6.3	Particle size diagrams for powder F	42
Figure 6.4	Particle size diagrams for powder E	42
Figure 7.1	Schematic representation of H vs. t for monosize TiO <sub>2</sub> particles for 10% solids loadings	45
Figure 7.2	H vs. t three different pH for powder C without surfactant	50
Figure 7.3	PD % vs. pH at saturation time for powder C without surfactant	51
Figure 7.4	Viscosity vs. rate and rate vs. stress graphs for powder C (for 5%)	52
Figure 7.5	Viscosity vs. rate and rate vs. stress graphs for powder C (for 10%)	53
Figure 7.6	Viscosity vs. rate and rate vs. stress graphs for powder C (for 20%)	54
Figure 7.7	H vs. t graphs for powder C with surfactant	55
Figure 7.8	PD % vs. surf.% graphs for powder C at saturation time	56
Figure 7.9	Viscosity vs. rate and rate vs. stress graphs for powder C with surfactant (for 5%)	57
Figure 7.10	Viscosity vs. rate and rate vs. stress graphs for powder C with surfactant (for 10%)	58
Figure 7.11	Viscosity vs. rate and rate vs. stress graphs for powder C with surfactant (for 20%)	59
Figure 7.12	H vs. t three different pH for powder E without surfactant	60
Figure 7.13	PD % vs. pH at saturation time for powder E without surfactant	61
Figure 7.14	Viscosity vs. rate and rate vs. stress graphs for powder E (for 5%)	62
Figure 7.15	Viscosity vs. rate and rate vs. stress graphs for powder E (for 10%)	63
Figure 7.16	Viscosity vs. rate and rate vs. stress graphs for powder E (for 20%)	64

## LIST OF TABLES

Figure 7.17	H vs. t graphs for powder E with surfactant	65
Figure 7.18	PD % vs. surf.% graphs for powder E at saturation time	66
Figure 7.19	Viscosity vs. rate and rate vs. stress graphs for powder E with surfactant (for 5%)	67
Figure 7.20	Viscosity vs. rate and rate vs. stress graphs for powder E with surfactant (for 10%)	68
Figure 7.21	Viscosity vs. rate and rate vs. stress graphs for powder E with surfactant (for 20%)	69
Figure 7.22	H vs. t three different pH for powder F without surfactant	70
Figure 7.23	PD % vs. pH at saturation time for powder F without surfactant	71
Figure 7.24	Viscosity vs. rate and rate vs. stress graphs for powder F (for 5%)	72
Figure 7.25	H vs. t graphs for powder F with surfactant	73
Figure 7.26	PD % vs. surf.% graphs for powder F at saturation time	74
Figure 7.27	Viscosity vs. rate and rate vs. stress graphs for powder F with surfactant (for 5%)	75
Figure 7.28	H vs. t three different pH for powder G without surfactant	76
Figure 7.29	PD % vs. pH at saturation time for powder G without surfactant	77
Figure 7.30	Viscosity vs. rate and rate vs. stress graphs for powder G (for 5%)	78
Figure 7.31	H vs. t graphs for powder G with surfactant	79
Figure 7.32	PD % vs. surf.% graphs for powder G at saturation time	80
Figure 7.33	Viscosity vs. rate and rate vs. stress graphs for powder G with surfactant (for 5%)	81

# LIST OF TABLES

		page
	INTRODUCTION	
Table 1.1	Some Typical Colloidal Systems	3
Table 2.1	Some Physical Properties of $\text{TiO}_2$	6
Table 2.2	Comparative Tinting Strengths of Common Pigments	11
Table 3.1	Comparison of Coating Technologies	17
Table 3.2	Differences in Physical Characteristics	19
Table 3.3	Differences in Applications	19
Table 3.4	Energy Consumption and Mechanisms for Radiation Curable Coatings	19
Table 4.1	Electrostatic and Steric Stabilization	30
Table 6.1	Powders used in preparing dispersions	40
Table 7.1	Comparison of the sedimentation velocity and time according to the particle size	44
Table 7.2	Visual Observations on the nature of the suspensions	48

# CHAPTER I

## INTRODUCTION

A colloid describes a mixture consisting of a dispersion of particles of one phase (a solid, liquid, or gas) in a second continuous phase (a solid, liquid, or gas). Some of the more important types of colloidal systems are summarised in Table 1.1

The most critical characteristic of the mixture will be that its (macroscopic) behaviour is determined by the nature of (microscopic) surface forces between the particles rather than by the presence of any external forces.(such as gravitational forces) These surface forces are controlled by the surface chemical properties of the particulate (dispersed phase) and the physical and chemical properties of the continuous phase. The magnitude of the forces and the resulting structure of the dispersion may vary with time.

Most substances acquire a surface electrical charge when brought into contact with a polar medium, resulting from one or more mechanisms involving ionization , ion adsorption and ion dissolution. Surface charge influences the distribution of nearby ions, attracting ions of opposite charge but repelling ions of similar charge to that of the surface. This leads to the formation of the Electrical Double Layer (EDL) which consists of the surface charges and a neutralizing excess of counter-ion and co-ions distributed in a diffuse manner in the polar medium. This is to describe the relationship between the stability and charge distribution around charged particles.

A suspension of a finely divided solid that remains dispersed in a liquid for an extended period of time is said to be colloidally stable. In water, stability arises because the particles acquire a surface charge through any one of a number of mechanisms. Such a dispersion may be destabilized by electrostatic interaction between the electric field surrounding the particles and oppositely charged ions. The latter are known as counterions and the process is called coagulation. It is apparent that stabilization and restabilization depend on the size and concentration of the particles, the nature of the particle surface and the composition of the solution. The most important parameter controlling the stability hydrosols is the solution pH[30]. This is because many sols have acid-base properties.

The state of aggregation of the dispersed powder and subsequent powder packing depend on the stability of the powder dispersion. Stability against coagulation for aqueous dispersions of oxide powders requires a low electrolyte concentration and a solution pH above or below the isoelectric point (IEP) of the oxide. The IEP, the pH at which no net charge exists in particle/liquid interface region, is between 4 and 5 for rutile and 6 for anatase titania[27]. This is the zero electrophoretic mobility. The sign of the charge and pH are determined by microelectrophoresis measurements.

A more practical and considerably easier approach is to observe the settling of the colloidal suspension as a function of pH[30]. Settling and agglomeration occur simultaneously while processing colloidal suspensions. Different size particles settle and agglomerate at different rates; thus causing the particle size distribution and agglomerate distribution to vary along the height of the suspension and to vary with time. There are 3 sedimentation zones, both transient and equilibrium conditions[18]. At the bottom of the vessel, a sedimentation cake is formed with a volume fraction which somewhat depends on the compressibility of the packing. Above that sediment layer, one finds a transition layer, the height of which varies during the settling process and depends on the diffusivity of the particles. Then, a clear liquid is found above that layer.

Titania powder is generally used in all industries. One of them is surface coatings industry as a white pigment to produce white paint. Water-based Coatings are more important than all paint systems because it is more economical and environmental due to the reduction of solvent emission during application to comply with legal requirements. Savings in organic solvents as diluents, savings in insurance premiums, lower energy consumption in spray cabins, ventilation zones and drying ovens all contribute to the overall economy of water-based coatings[32]. So this study is related with the water-based systems.

In this study, four different commercial titania powders were used at different titania solid contents and at different surfactant concentrations. Powder suspensions in the 5-20 vol% range were prepared and their rheological and sedimentation behaviours were characterized.

The aim of this study was to understand the behaviour of these four commercial pigments in water. The stability and rheological behaviour of suspensions prepared in the 2-12 pH range and by the addition of a surfactant was analysed.

Table 1.1: Some typical colloidal systems[8]

<i>Examples</i>	<i>Class</i>	<i>disperse phase</i>	<i>dispersion medium</i>
<b>Disperse Systems</b>			
Fog, mist, aerosol sprays	liquid aerosol or aerosol of liquid particles	liquid	gas
Industrial smokes	solid aerosol or aerosol of solid particles	solid	gas
Inorganic colloids(gold, metallic hydroxides.),paints	sols or colloidal suspensions	solid	liquid
Foams	foam	gas	liquid
Expanded plastics	solid foam	gas	solid
Microporous oxides. Silica gel, porous glass, zeolites	Xerogels		
<b>Macromolecular colloids</b>			
Jellies,glues	gels	macro-molecules	solvent
<b>Associated colloids</b>			
Soap,water-detergent/water-dye solutions	--	micelles	solvent
<b>Biocolloids</b>			
Blood	--	corpuscles	serum
Bone	--	hydroxy-apatite	collagen
<b>Multiple colloids</b>			
		<i>coexisting phases</i>	
Oil-bearing rock	porous rock	oil	water
Frost heaving	porous rock or soil mineral	ice	water

# CHAPTER II

## PRODUCTION OF TiO<sub>2</sub>

### 2.1 Physical Properties of TiO<sub>2</sub>

Titanium dioxide (titania), TiO<sub>2</sub>, formula weight 79.90, exists in 3 forms; anatase, brookite and rutile. Anatase is tetragonal, uniaxial negative; the unit cell contains four TiO<sub>2</sub> molecules and has a volume of 136.1 Å<sup>3</sup>. Rutile, tetragonal is isomeric but not isomorphous with anatase; uniaxial positive; the unit cell has two TiO<sub>2</sub> units and a volume of 62.4 Å<sup>3</sup>. Brookite is orthorhombic, biaxial positive. Figure 2.1 shows the crystal unit cells of anatase and rutile. Anatase and brookite are monotropic forms to be changed to stable rutile with increasing temperature. Brookite transforms to rutile above 650°C and anatase is inverted to rutile at 915±15 °C in the absence of minerals. However, in the presence of suitable minerals, the anatase and brookite is converted to rutile at much lower temperatures (400-500 °C). The denser atomic crystal pattern of rutile causes both a higher specific gravity and a higher refractive index than anatase. Rutile is mostly used in the coatings industry. The crystal forms of anatase and rutile TiO<sub>2</sub> and their properties are shown in Figure 2.1, Figure 2.2 and Table 2.1. Anatase TiO<sub>2</sub> has got very high photoactivity and is not suitable for exterior finishes because it may cause rapid degradation of the paint films. Anatase TiO<sub>2</sub> has found extensive applications in paper coatings.

### 2.2 Production of TiO<sub>2</sub>

Titanium metal does not exist in a free state in nature. It is bound to oxygen and found with iron oxides. There are three different mines as raw materials: Ilmenite (FeTiO<sub>3</sub>), rutile (TiO<sub>2</sub>) and leucosene (Fe<sub>2</sub>O<sub>3</sub>.TiO<sub>2</sub>). Ilmenite, in hard-rock formation and as beach sand, is the most important TiO<sub>2</sub> source. Hard-rock deposits happen to be available in the northern hemisphere, where as the deposits of beach sand ilmenite as well as natural rutilites are in the southern hemisphere. So, beach sand ilmenite and rutile have a higher TiO<sub>2</sub> content than hard-rock ilmenite.

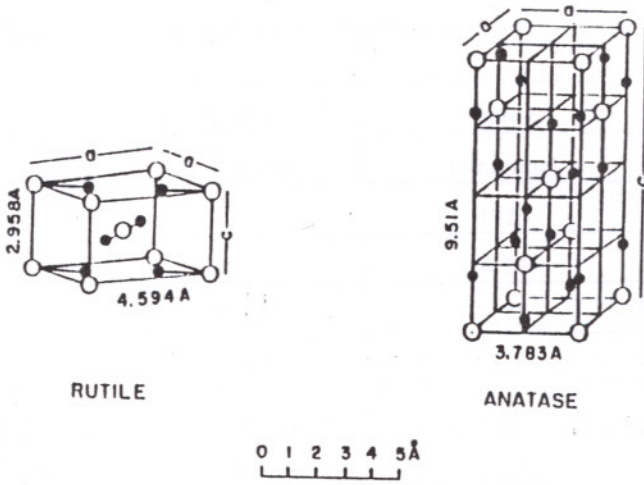


Figure 2.1 : Crystal Unit Cells of Anatase and Rutile.[26]

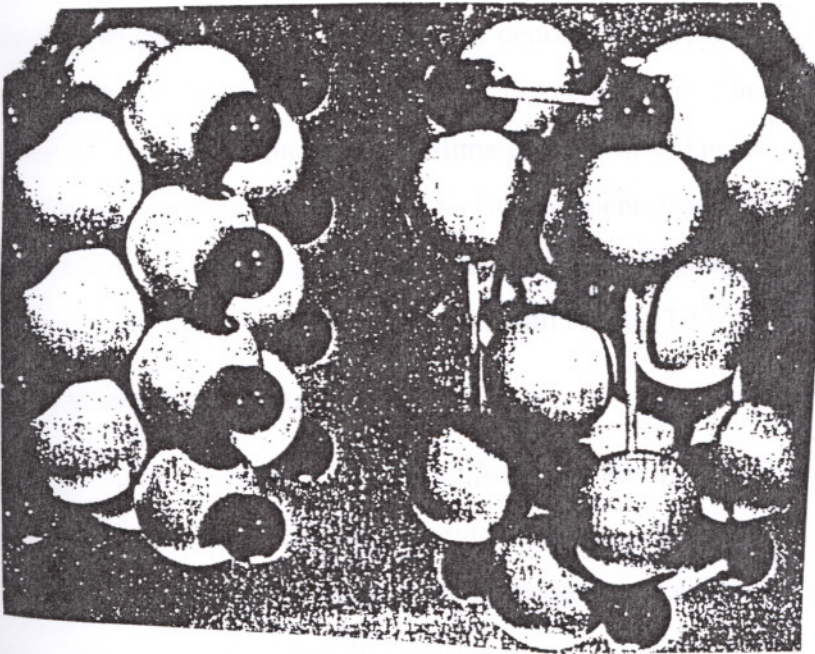


Figure 2.2 : Anatase (left) and Rutile (right) crystal forms.[26]

İZMİR YÜKSEK TEKNOLOJİ ENSTİTÜSÜ  
 REKTÖRLÜĞÜ  
 Kütüphane ve Dokümantasyon Daire Bşk.

Table 2.1 : Some Physical Properties of TiO<sub>2</sub>. [31]

Property	Anatase	Rutile	Brookite
Crystal system	tetragonal	tetragonal	Orthorhombic
M.p.(°C)	--	1825	--
Sp.Gr.	3.90	4.27	4.13
Ref.Ind.	2.52	2.72	2.63
Mohs' hardness	5.5-6.0	7.0-7.5	5.5-6.0
Sp.heat(cal/°C.g) 208°K	0.169	0.169	--
Mean dielectric constant	48	114	78
Electrical Conductivity			
At room temperature	--	10 <sup>-15</sup> -10 <sup>-14</sup>	--
At 500°C	5.5x10 <sup>-5</sup>	--	--
At 1200°C	--	0.12	--

Not too many years ago, world - wide deposits of TiO<sub>2</sub> were estimated about 420 million tonnes. In recent years, large anatase deposits in Brazil was discovered equivalent to an additional 220 million tonnes TiO<sub>2</sub> pigment a year. The TiO<sub>2</sub> deposits will last for about 260 years. Another source estimates the world ilmenite resources to total about one thousand million tonnes of TiO<sub>2</sub>. TiO<sub>2</sub> pigment production was started 66 years ago. The new industry originated simultaneously in Norway and the U.S.A. The early products were very low quality compared with today's TiO<sub>2</sub> pigments.

### 2.3 TiO<sub>2</sub> Processing Methods:

Methods for the production of TiO<sub>2</sub> from its ore fall into two groups:

- 1- Thermal hydrolysis of titanium sulphate, chloride or nitrate solutions ;
- 2- Reaction of titanium tetrachloride vapor with an oxygen-containing gas at elevated temperatures (vapor-phase oxidation reaction).

Economical and environmental factors determine the suitability of the method used. The thermal hydrolysis of titanium sulphate solutions, commonly known as the sulphate process, is the most widely used method. Titanium chloride and nitrate solutions have received little attention because of the corrosiveness of the solutions and higher operating costs. A flow sheet for the production of anatase and rutile titanium dioxide pigments is shown in Figure 2.3.

Sulphate Process: Ilmenite ore,  $\text{FeTiO}_3$  or  $\text{FeO} \cdot \text{TiO}_2$ , is used. This contains about 45-0% by weight of  $\text{TiO}_2$ . The ore is ground and dissolved in concentrated sulphuric acid to form titanyl sulphate:



Iron is added to reduce the  $\text{Fe(III)}$  to  $\text{Fe(II)}$  and some titanium is reduced to prevent reoxidation of iron. The titanyl sulphate is purified by sedimentation and crystallization and the crystallized ferrous sulphate is separated. The is precipitated by hydrolysis :



If the hydrolysis is carried out after the addition of small nuclei of rutile, called the seed, the product will take the rutile crystal form; in the absence of a seed, anatase will be obtained. Then the precipitate is separated from the solution by filtration and is washed. Additives are added to promote and control pigmentary characteristics. The treated precipitated hydrate is calcined at 800-1000 °C. Then it may be treated with inorganic oxides to improve performance properties.

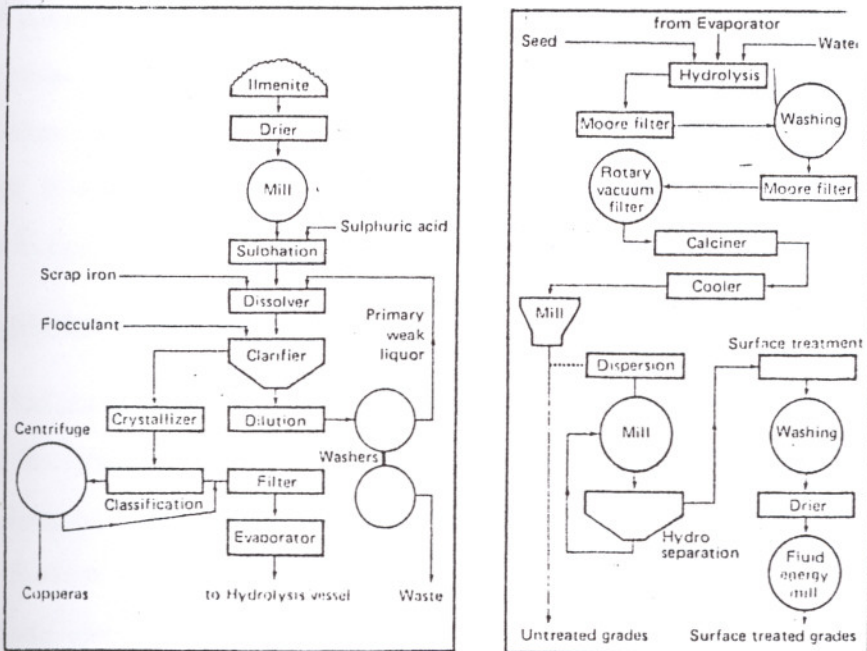
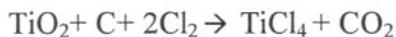


Figure 2.3 : Flow diagram of titania production.[26]

Chloride process : Natural rutile is used as the only raw material in the chloride process; however, ilmenite and other titanium ores can also be used as source ores. Crude ore is mixed with coke and reacted with chlorine at 900°C. This results in the formation of TiCl<sub>4</sub>, CO<sub>2</sub> and CO:



Because of the variations in the between the chlorides of metal impurities and that of TiCl<sub>4</sub>, impurities can effectively be removed by condensation and/or distillation steps. Purified TiCl<sub>4</sub> is then reacted with oxygen or air in a flame reaction at 1500°C to produce chlorine and fine-particle TiO<sub>2</sub>; the former is recycled.



Aluminium tetrachloride is added to promote the production of the rutile form and to correct crystal size. The TiO<sub>2</sub> can be post-treated to improve the properties. Post-treatments include application of inorganic oxides and other compounds to the surface.

Coatings containing 2-5% by weight alumina or silica are satisfactory for general purpose paints. It may be coated with the combination of several materials, e.g. alumina, silica, zirconia, aluminium phosphates or other metals for the other industries. It is shown the scanning electron microscope picture of silica coated titania particles in Figure 2.4.

## 2.4 Applications of TiO<sub>2</sub>

The surface coatings industry is the major consumer of titania. The other major markets for titania are the plastics and paper industries and to a lesser degree the rubber, ceramic, textile, masonry product and cosmetic industries.

Surface Coatings Industry : The heading covers a very broad spectrum of applications, including some of the better known segments of paints, printing inks and specialized coatings. The desirable properties are:

a-High degree of dispersion

b-Opacity ( hiding power )

c-Brightness

d-Tinting strength

e-Durability

f-Gloss

g-End product stability

a-) High degree of dispersion : The ability to achieve the desired properties of a system is dependent on the ability to fully disperse the titania down to its ultimate particle size and for those particles to be held in a deflocculated state. There are many methods to achieve dispersion, but with rising costs energy and manpower, the coatings industry is demanding rapid wetting and easy-dispersing pigments, so that ultimate particle size is achieved in a minimum time with minimum power costs.

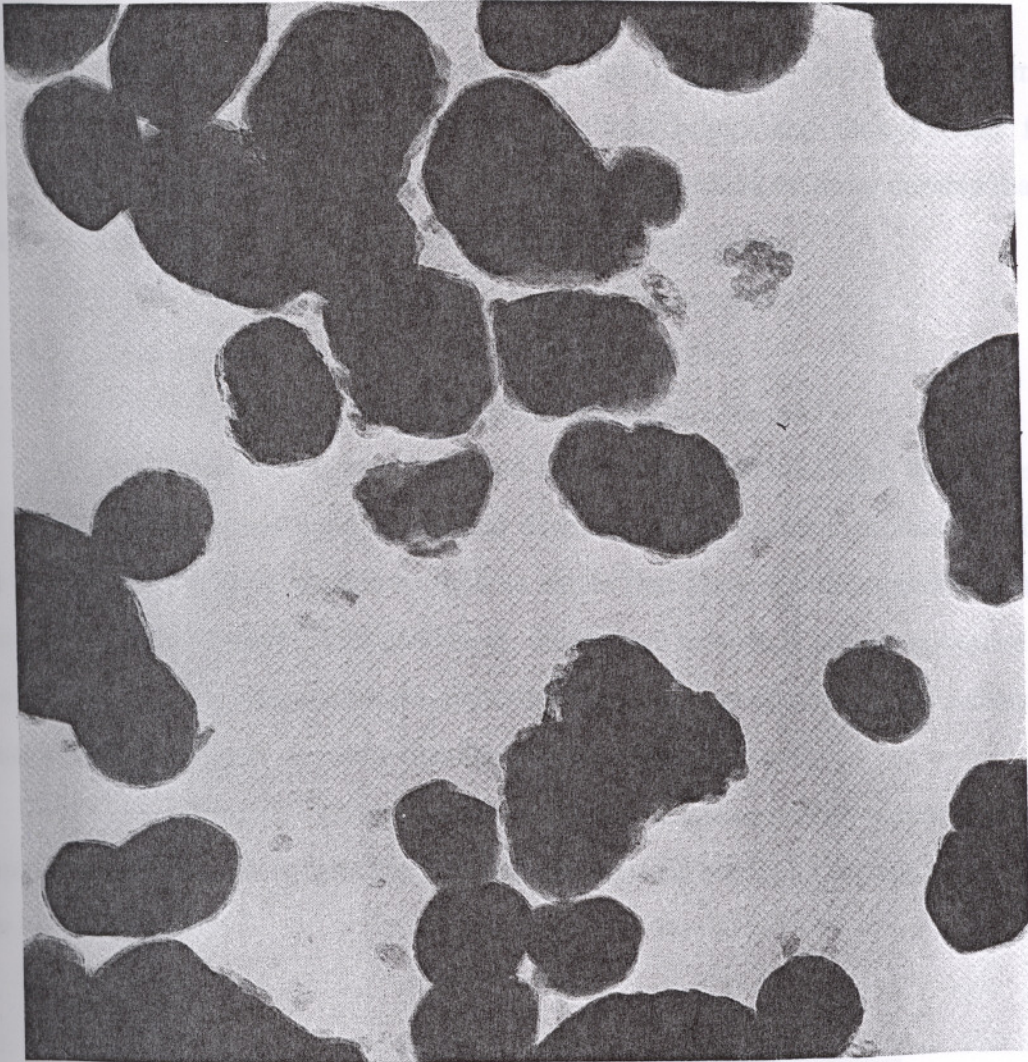


Figure 2.4 : SEM picture of silica coated rutile titania particles.[6]

b-) Opacity ( hiding power ) : The use of titania revolves around its ability to scatter light so, the greater the refractive index difference between particle and medium, the greater the amount of light reflected from the surface. This is how opacity is achieved in a paint film by using titania. For example, the high refractive index of rutile titania of 2.71 will give a greater ratio than that of anatase (2.55) in the same medium.

c-) Tinting strength : It is a measure of the comparative amounts of two coloured pigments that need to be blended with the same amount of the same pigment in the same medium to produce a tint of equal strength in each case. With this definition, a series of white pigments were compared in a standard blue pigment showing in Table 2.2.

d-) Durability : It is the degree to which paints and paint materials withstand the destructive effect of the conditions.

Most polymers are attacked by UV radiation in the sun's rays. Some polymers are more resistant to these harmful UV rays than others and thus a paint film containing a resin of high resistance to UV degradation should be more durable than a paint film containing a resin of low resistance to UV degradation.

Two principal factors which affect the durability of paint are:

- Chemical and physical nature of the paint film.
- The environment that the paint film has to withstand.

Although titanium pigment is a good absorber of ultraviolet light, the influence of titanium pigment is both protective and destructive. The pigment protects the film by absorbing ultraviolet radiation to such an extent that there is little radiation left to damage the binder directly. This protective destructive balance is largely governed by the titanium pigment manufacturer's ability by the inclusion of coatings of oxides of aluminium and/or silicon on to the titanium dioxide crystal.

e)Gloss : It is the degree to which a surface simulates a perfect mirror in its capacity to reflect incident light. The film with the least defects at its surface will give the highest gloss.

Table 2.2 : Comparative tinting strengths of common pigments.[26]

Materials	Tinting Strengths
Rutile Titania	1850
Anatase Titania	1350
ZnS	900
Lithopone	300
ZnO	200

Plastics Industry : Unlike the surface coatings industry, which uses relatively thin films the plastics industry uses relatively thick profiles. The pigment loadings tend to be lower than in paint products this is a generalization because thermoplastic polymers such as ABS which has a pronounced yellow undertone require relatively high pigmentation to mask this polymer colour.

The titanium pigment requirement for thermoplastic products is easy dispersion under low shear conditions. This is assisted by use of titanium pigments which renders the pigment hydrophobic.

Methods of incorporation of titanium pigments into plastics are varied, but the major methods are:

- a) dry blender
- b) ribbon blender
- c) high speed mixer
- d) internal mixer and
- e) continuous compounder

Rubber Industry : Applications in rubber are of relatively small volume and the dispersion equipment is of a very high shear nature that is internal mixers and here the titanium pigment used is an uncured anatase or rutile. Anatase is used where chalking is required and rutile where non chalking is required.

Paper Industry : Historically, anatase has been used for paper production. However, a shift to rutile was made in Australia a number of years ago, and considerable reduction in titanium pigment usage was made by this change. The two large areas of rutile pigment usage in the paper industry are:

- a) beater addition to wood pulp and
- b) board coating.

Ceramics Industry : Vitreous enamels account for the bulk of titanium pigment usage in ceramics. Requirements are for easy and complete solubility into vitreous frit with good colour reproduction in the final enamel. This application requires special production techniques to provide the required properties.

Other Applications : In all other applications for example, cosmetics, cement products, food, and leather, some form of dispersion of the titanium pigment will be necessary.

# CHAPTER III

## PAINT

Paint is a product is in liquid or powder form, containing pigments when it is applied to a substrate it forms an opaque film having protective, decorative or specific technical properties according to the ISO 4618/1. The composition of a paint determines whether a high-gloss film or a flat (matt) surface is formed.

### 3.1 Composition of Paints

Coatings generally contain various ingredients which can be divided into the following groups:

volatile	Solvents	→	
components	Coalescing agents	→	
	Film forming substances	→	→
	Resins	→	<b>binders</b> → <b>paints</b>
	Plasticizers	→	→
nonvolatile	Additives	→	
components	Dyes	→	
	Pigments		
	Extender pigments		

Solvents, binders, and pigments are generally present in much higher amounts.

### 3.2 Basic Components

Resins : Most important raw materials are resins. The term "resin" denotes that the material is a vitreous-amorphous solid without a defined melting point. However, paint technologists also use the term resin to denote a certain group of natural or synthetic film formers with resinous consistency.

Resins are soluble in either organic solvents or water but not both. They increase the solids content of paints and improve the gloss and adhesion of coating films. Their most essential function is to increase hardness and reduce the drying time in oxidative curing systems.

Plasticisers are normally organic liquids of oil consistency and low volatility. Esters of polyacids are typical examples. Plasticizers have the opposite effect to resins; they lower the softening temperature range of the binder, resulting in a lower film-formation temperature, improved flow and increased flexibility.

Pigments and extender pigments: They are responsible for coloring hiding power and in certain cases for improved resistance of the coating films. They consists of finally ground, crystalline solids that are dispersed in the paint and film. The hiding power and the tinting strength of a paint depend on the particle size of the pigment.

The intense hiding power of many white and colored pigments enables the paint technologist to partially replace these expensive materials with cheaper extender pigments such as barytes, kaolin. These extenders have the some particle size as the pigments. Due to their lower refractive index, they contribute less to the hiding power of coating films than pigments but they do not change the hue.

Additives : The term " additives " denotes auxiliary products that, even in small concentrations, improve the technological properties of paints or coating films. They are classified according to their effects.

Driers catalyze the decomposition of peroxide and hydroxyperoxides formed by the action of atmospheric oxygen on binders like alkyd resins. This promotes the formation of radicals and polymerization of the binders is thus initiated and accelerated. Metallic soaps (e.g.cobalt naphthanate or lead octoate) are soluble in most binders as efficient driers.

Antiskinning Agents are mostly antioxidants that counteract the tendency of drier-containing points to form an insoluble surface skin on contact with atmospheric oxygen. In the film they promote uniform drying and thus hinder wrinkling. Antiskinning agents of the oxime type (methyl ethyl ketoxime) mask the driers by chealation. During film formation, they evaporate together with the solvents and so do not extent the drying time.

Curing Agents act as catalyts in chemically cross-linking binder systems. They allow stoving enamels to be cured in shorter times or at lower temperatures.

Leveling Agents promote the formation of smooth, uniform coating films from uneven, patterned layers of wet paint.( eg. glycol ethers )

Wetting, Antifloating and Antiflooding agents maintain gloss, hiding power and uniformity of shade. Surfactants promote dispersion of the pigments and counteract the

flocculation tendency of particles that are insufficiently wetted. Antifloating and antiflooding agents hinder the vertical and horizontal separation of pigments with different densities and surface activities (e.g. silica)

Dispersion agents counteract the settling tendency of pigments. Since good wetting and a viscosity of the paint keep the pigments well suspended.

Solvents : They are volatile fluids that evaporate from the coatings during the film-forming processes. Solvents (xylene, butyl acetate...) dissolve solid or highly viscous binder components without chemical reaction, i.e. they give the binders a processable consistency and provide adjusting the viscosity for paint application. Appropriate solvent composition improves wetting and dispersion of the pigments, leveling and gloss are also increased. After application of the paint the solvents evaporate.

### 3.3 Why $\text{TiO}_2$ is used in paint

White inorganic pigments are mainly used in paint formulations to impart opacifying or light-scattering properties to the paints. Until the introduction of  $\text{TiO}_2$  pigments, white lead (basic lead carbonates) and  $\text{ZnO}$  pigments were largely used.  $\text{ZnS}$  and lithopone (  $\text{ZnS}/\text{BaSO}_4$  co-precipitate ) also found extensive application as white pigments.

The main reasons for the successful replacement of other inorganic white pigments with  $\text{TiO}_2$  are:

- It has a very high refractive index and thus imparts to coatings or other  $\text{TiO}_2$  - containing products a considerable degree of opacity or hiding power.
- It has high reflectivity, i.e. it exhibits a distinct lack of absorption of visible light. Hence,  $\text{TiO}_2$  imparts a high degree of brightness and brilliant whiteness.
- The particle size of  $\text{TiO}_2$  can be controlled to ensure a very narrow spread around the pre-selected optimum. Thus light-scattering, gloss and dispersibility can be maximized.
- It is thermally stable, chemically and biologically inert, non-toxic, and non-fibrogenic.
- Rutile  $\text{TiO}_2$  is photochemically inert and exhibits some interesting semiconductor properties.
- Ultrafine grades of  $\text{TiO}_2$  ( with particle sizes of 0.015 - 0.035 microns ) help to produce the flip effect in metallic paints.

TiO<sub>2</sub> pigments, however, do have a few disadvantages are compared to others:

- The untreated TiO<sub>2</sub> pigments are not sufficiently basic to react with the acidic products formed as a result of photo-oxidation and thus do not help to maintain the integrity of the films as lead pigments.
- They have no fungicidal or bacteriostatic properties.
- They do not form soaps with the fatty acids to be stable for wet paint and flexible for the dry film.

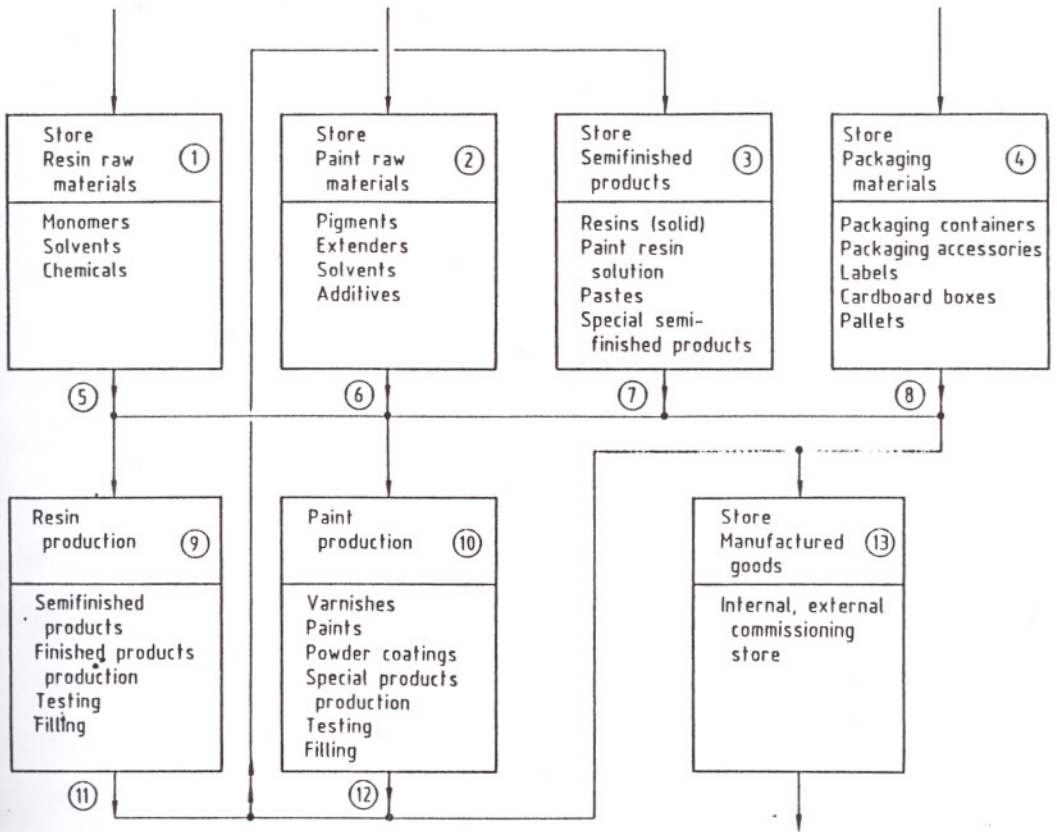


Figure 3.1 : Material Flow in paint production.[31]

### 3.4 Paint Production

The paint - making process can be subdivided into four main stages:

1. Preparation of the millbase ( premixing )
2. Continuous dispersion
3. Completion of the formation
4. Correction and adjustment of the final product

Figure 3.1 illustrates the material flow in paint and coating production, starting with reception and storage of the raw materials and finishing with the end product ready for dispatch. The type of raw material, its consistency, the amount consumed, and the packaging are decisive for natural flow and metering. In large factories, large storage tanks for resin solutions and solvents have to be installed. The raw materials are delivered in tank trains. These bulk raw materials can be pumped and conveyed to the sites of use via pipes. The raw materials for 1,2,4 and in some cases 3, are delivered to the stores by road. The material flow continues to the production facilities(9 and 10).The paint maker also produces semifinished, these are stored in 3.

### 3.5 New Technologies

Recently, higher solvent prices, increased energy costs and restrictive emission regulations have led to a great emphasis on the development of new technologies. The new technologies which actually obtained some industrial breakthrough are waterborne coatings, high-solid coatings, non-aqueous dispersions, radiation curing systems and finally powder coatings. The main intention in each of these technologies is either to reduce or eliminate the presence of organic solvents present in conventional coating systems or to replace them with certain environmentally favourable solvents such as water in the case of water in the case of water-borne coatings, or aliphatic solvents in the case of non-aqueous dispersions.

Table 3.1 : Comparison of Coating Technologies.[26]

Systems	Conventional Up To 50% Solids	HighSolids 60-80% Solids	Water-Borne 30-50%	Radiation > 95% Solids
Solvent Usage	High	Moderate	Low	Very Low
Pollution Potential	High	Moderate	Low	Very Low
Energy Usage	High	High	High	Low

Water - Borne Coatings : In order to understand the importance of water-borne coatings, the advantages and disadvantages associated with these systems are summarised as follows:

#### Disadvantages:

1. The high surface tension of water makes it a poor solvent for flow characteristics.
2. All resins in contact with water have limited shelf stability.
3. Effective application of water - based resins normally requires some type of humidity control.
4. Most water-borne coating have poor detergent resistance, since they are solubilized by the neutralization of residual carboxyl groups with amines.
5. Most water - borne coatings require extensive substrate pre-treatments to obtain grease removal and thorough cleaning to achieve proper flow.

#### Advantages:

1. Existing equipment can usually be used to apply water-borne coatings.
2. Addition of relatively large volumes of water to the coating systems alleviates the odour problems which are often associated with various solvents.
3. Insurance premiums are lowered because of decreased fire hazards.
4. They greatly reduce solvent emission and make an ecological contribution by decreasing pollution.
5. Energy requirements for curing are lowered due to the reduced air-flow through the ovens.

Water-borne coatings can be divided into three main classes:

- (a) aqueous dispersion or emulsions,
- (b) colloidal or water-solubilized dispersions, and
- (c) water reducibles.

These three types vary significantly in physical and mechanical properties and thus provide a considerable formulation range for coating chemists. The main differences in the physical and the application characteristics between the three classes are summarised in Tables 3.2 and 3.3.

**Radiation Curable Coatings :** Radiation curable coating systems have mainly been developed to meet the stringent regulations concerning water and air pollution as well as to reduce energy dependence in view of the increased fuel costs and limited fuel availability during the curing of coatings.

Table 3.2: Differences in physical characteristics.[26]

Property	Aqueous Dispersion	Colloidal Dispersion	Water Reducibles
Appearance	Opaque (exhibits light scattering)	Translucent (exhibits light scattering)	Clear (exhibits light scattering)
Particle size	$\geq 0.1\mu\text{m}$	about 20-100 $\mu\text{m}$	$< 0.005\mu\text{m}$
Molecular weight	1 million	20000-200000	20000-50000
Viscosity	Low, independent of polymer mol. wt.	More viscosity sensitive, dependent on mol. wt.	Very dependent on polymer mol. wt

Table 3.3 : Differences in applications.[26]

Property	Aqueous Dispersion	Colloidal Dispersion	Water reducibles
Viscosity	High	Intermediate	Low
Durability	Excellent	Excellent	Fair-good
Resistance Properties	Excellent	Good-excellent	Fair-good
Viscosity control	Requires external thickeners	Thickened by addition of cosolvent	Governed by polymer mol.wt
Dispersibility	Poor	Good-excellent	Excellent
Application difficulties	Many	Some	Few

Radiation curable coating systems comprise mainly of UV, electron beam (EB), infrared (IR), radio frequency and microwave cured systems. The energy consumption by each of these curing techniques and the mechanisms involved in the curing are shown in Table 3.4.

Table 3.4 : Energy Consumption and Mechanisms for Radiation-Curable Coatings.[26]

Source	Energy(eV)	Mechanism
Infra red	$10^{-1}$	Thermal
Microwave	$10^{-3}$	Thermal
Radio frequency	$10^{-6}$	Thermal
Ultraviolet	5	Electronic excitation
Electron beam	$10^5$	Ionization excitation

Powder Coatings : Like water borne and radiation curing coating systems the main reason for the development of powder coatings has also been to reduce pollution problems and to decrease energy costs. The preference for powder coatings for decoration and protecting of industrial products today are due more to economic reasons and the desire to obtain quality finishes than to regulatory compliances. Besides the emission of very low volatile organic components (0.4 pounds per gallon of coating) a number of other factors contribute to their increasing acceptance and use by industrial product finishes. Other advantages of powder coating are : high material utilization (95 per cent or more) or high overall transfer efficiency, low labour, maintenance and clean up costs reduced energy consumption, low reject rates and very frequently, high quality finishes. The economics of powder coatings look even better for the future because the material costs are not influenced by the rising prices of petroleum based solvents and thinners.

High Solids Coatings : High solids (HS) coatings have mainly been developed to meet pollution regulations and to reduce energy costs. In HS coatings both aspects have been achieved by reducing the amount of volatile content in the paint formulations in comparison with conventional systems. Since high molecular weight resins are usually used in conventional paints to obtain satisfactory film properties, a direct reduction of volatile contents, or in other words, solvents, will mean a tremendous increase in solution viscosity, which may cause application problems. Thus it is essential to reduce the molecular weight of resins in parallel with the reduction of non volatile contents. This is done to keep the solution viscosity unaltered when the amount of solvents is reduced. However, use of low molecular weight binders gave rise to poor film properties.

Thus the main factors affecting properties and formulations of HS coatings are:

1. Designing of a proper vehicle showing suitable physical and viscosity relationships;
2. Selection of a suitable solvent showing dilution behaviour;
3. Effect of pigmentation;
4. Curing requirements;
5. Factors affecting film defects

# CHAPTER IV

## COLLOIDAL MECHANISMS

Whenever an interface is formed, a potential difference is expected across this interface. The most interesting situation occurs when there is a solid (or, in certain cases, a nonpolar liquid) in contact with a polar liquid, such as water. In this case, the potential arises from a concentration of charge at the interface, the origin of which may be due to the inherent ionic character of the solid, or to the adsorption of ions on the surface. These ions may be the usual inorganic ions, e.g.,  $\text{Na}^+$ ,  $\text{Cl}^-$ , or the ions of surface-active molecules, e.g., the lauryl sulphate ion,  $\text{C}_{12}\text{H}_{25}\text{OSO}_3^-$ . Even the adsorption of nonionic surface-active molecules may be accompanied by a concentration of a charge.

The system as a whole be electrically neutral, there will be an accumulation of ions of charge opposite to those adsorbed near the interface, and these are called as gegen-ions or counter-ions. The situation may be represented schematically as in the upper part of Figure 4.1. The way in which the potential falls off from the value,  $\psi_0$ , at the surface with the distance is shown in the bottom of Figure 4.1. The dotted line represents the point at which the potential has fallen off to  $1/e$  of its original value. The situation in Figure 4.1 is frequently referred to as being a diffuse double layer. Double layer, because the ionic species are present in two layers, of one charge at the surface, and the opposite charge in the solution. Diffuse, because the gegen-ions are distributed through an envelope whose diameter may be many times that of the particle, and, in fact, extends in principle to infinity.

Flat Double Layer : The problem which has to be solved is the integration of the Poisson equation:

$$d^2\psi / dx^2 = - 4\pi p/D \quad 4.1$$

where  $\psi$  is the potential,  $x$  is the distance,  $D$  is the dielectric constant, and  $p$  is the distribution of charge with distance.

The approximation which is used due to Gouy and Chapman and consists of assuming that the distribution of charge is given by the well-known Boltzmann equation:

$$n_+ = n_0 \exp[-ze\psi/kT] \text{ and } n_- = n_0 \exp[+ze\psi/kT] \quad 4.2$$

where  $n_+$  and  $n_-$  are the concentrations of positive and negative ions, respectively, at the point where the potential is  $\psi$ , i.e., where the electrical potential for each type of ion is  $+ze\psi$  and  $-ze\psi$ , respectively, and  $n_0$  is the bulk concentration of each species of ion. The valence of the ion is  $z$ ,  $e$  is the electronic charge,  $k$  is Boltzmann's constant, and  $T$  is the absolute temperature. The concentration is expressed in ions per milliliter.

Combination of equations 4.1 and 4.2 leads to the Poisson-Boltzmann equation for the potential of a flat diffuse double layer:

$$d^2\psi/dx^2 = (8\pi zen_0/D) \sinh (ze\psi/kT) \quad 4.3$$

The boundary conditions required for the integration of this equation are  $\psi = \psi_0$  when  $x = 0$  and  $\psi \rightarrow 0$ ,  $d\psi/dx \rightarrow 0$ , as  $x \rightarrow \infty$ . Integration of equation leads to the rather cumbersome expression

$$\psi = (2kT/ze) \ln \left[ \frac{(\exp(z\psi_0/2kT)+1) + (\exp(ze\psi_0/2kT)-1)\exp(-Kx)}{(\exp(z\psi_0/2kT)+1) - (\exp(ze\psi_0/2kT)-1)\exp(-Kx)} \right] \quad 4.4$$

where

$$K = 8\pi e^2 n_0 z^2 / DkT \quad 4.5$$

The quantity,  $K$ , has the dimensions of a reciprocal length, and in fact,  $1/K$  is the distance indicated by the dotted line in Figure 4.1. The same constant arises in the Debye-Hückel theory of strong electrolytes, and is usually referred to as the Debye thickness of the double layer.  $K$  is a function of the total electrolyte concentration, and for a symmetrical electrolyte concentration, and for a symmetrical electrolyte in water at 25 °C.

$$K = 0.327 \times 10^8 zc^{1/2} \quad 4.6$$

where  $c$  is the molar concentration.

When  $ze\psi_0/kT \ll 1$ , a simplification is possible. This means that  $z\psi_0 \ll 25$  mV, since  $kT/e = 25.6$  mV at 25 °C. Under these conditions

$$\psi = \psi_0 \exp [-Kx] \quad 4.7$$

Unfortunately, this rather simple result is of little value in colloid chemistry, since, in the cases of interest,  $\psi_0$  is of the order of magnitude of 25 mV or several multiples. However, it serves to indicate the general shape of the potential curve is represented by an exponential decay.

Although equation 4.4 is, as indicated above, rather inelegant, it is perfectly usable, and, in Figures 4.2 and 4.3, it is used to show the effect of electrolyte concentration and charge on the shape of the potential curve. The curves of Figure 4.2 are calculated for a uni-univalent electrolyte at concentrations of 0.1, 0.001 and 0.0001 N, while in Figure 4.3, the valency of the gegen-ion is varied at a fixed concentration of 0.0001 N.

The effect of increasing electrolyte or increasing charge is to "collapse" the double layer potential, i.e., reduce its extension through the body of the solution. This has important consequences.

A further useful calculation can be made if one assumes that the space charge in the diffuse double layer can be equated with the surface charge,  $\sigma$ , of the flat surface

$$\sigma = \sqrt{\frac{2n_0 DkT}{\pi}} \sinh \frac{ze\psi_0}{2kT} \quad 4.8$$

when the potential is low, this reduces to

$$\sigma = D_K \psi_0 / 4\pi \quad 4.9$$

Since the surface charge can frequently be calculated or estimated from, for example, a knowledge of the ionic arrangement on a crystal surface, or from

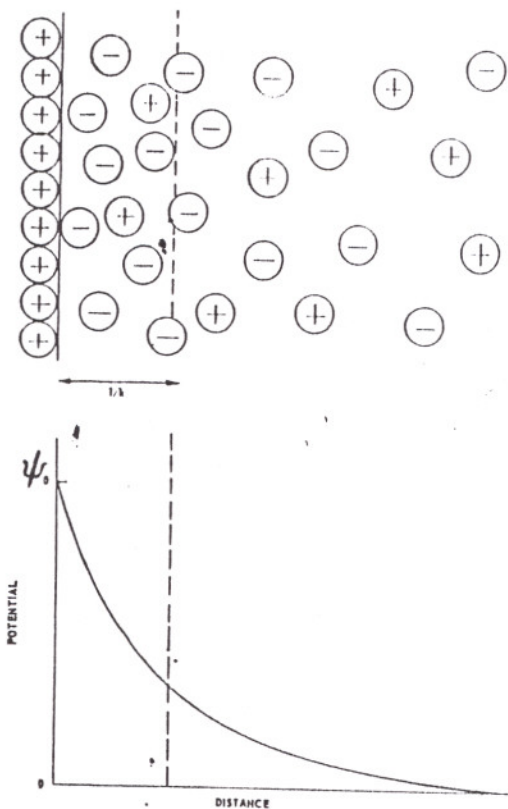


Figure 4.1 : Schematic representation of Double Layer according to Gouy-Chapman.[4]

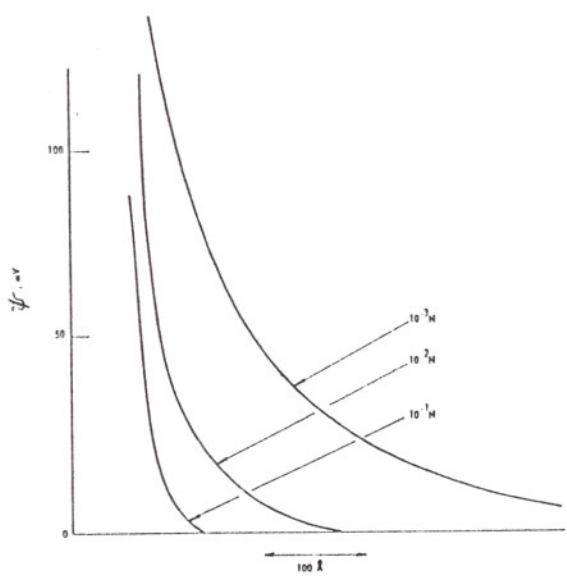


Figure 4.2: Effect of concentration of uni-univalent gegen-ions on potential.[4]

adsorption isotherms, equations 4.8 and 4.9 offer a method for the calculation of  $\psi_0$ , the potential at the surface.

Examination of equation 4.9 reveals that it is identical in form to that of a parallel plate condenser, with the plates separated by the distance,  $1/\kappa$ . The designation of the quantity  $1/\kappa$  as the "thickness" of the double layer is seen to be justified.

**Spherical Double Layer :** The calculation of the potential around a spherical double layer requires setting up the Poisson-Boltzmann equation in spherical coordinates, and performing the integration. For the case of small potentials, a form analogous to equation 4.7 is found

$$\psi = \psi_0 \frac{a}{x} \exp[\kappa(a-x)] \quad 4.10$$

where  $a$  is the radius of the spherical particle, and  $x$  is the distance from the surface of the sphere.

**Stern Theory :** A refinement of the Gouy-Chapman theory arises if one takes into consideration the fact that the first layer of gegen-ions is probably rather tightly bound to the surface, i.e., non-diffuse. Stern assumed that the configuration of this layer of gegen-ions could be described in terms of an adsorption isotherm, and gives rise to a region close to the surface where the potential declines linearly with distance. Beyond this point, the diffuse, exponential decay described by the Gouy-Chapman, theory obtains. The double layer is thus divided into Stern layer and a Gouy-Chapman layer, as illustrated schematically in Figure 4.4, while the whole situation around a spherical particle might be diagrammed as in Figure 4.5.

**Quantity  $\kappa x$  :** Distance appears in the double layer equations only in the dimensionless form,  $\kappa x$ . The behavior of the double layer potential is controlled by this quantity, and, for example if  $\kappa x$  be large in a certain approximation it is

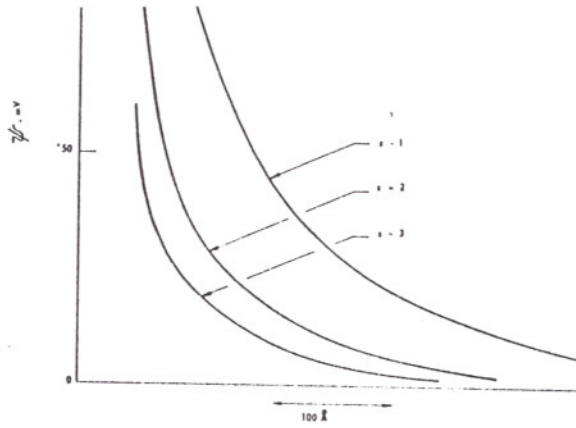


Figure 4.3 : Effect of valency of gegen-ions at an electrolyte concent. of 0.001N

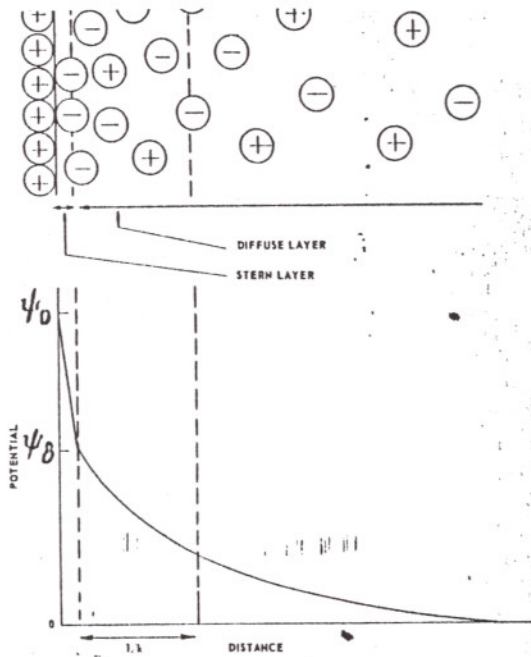


Figure 4.4 : Schematic representation of double-layer according to Stern.[4]

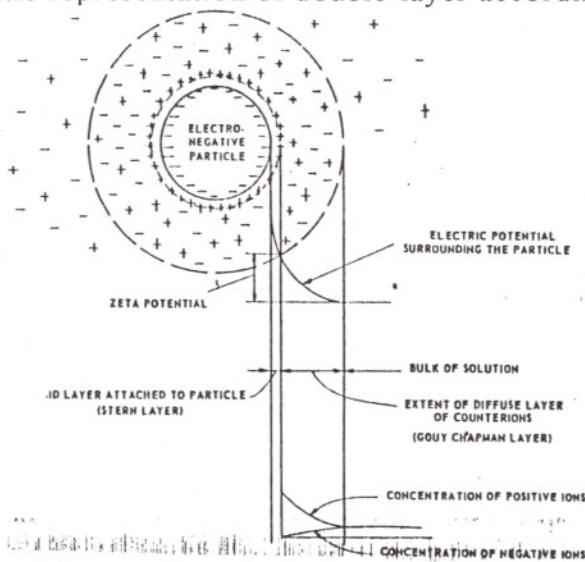


Figure 4.5 : the potential around a spherical, negatively charged particle.[4]

irrelevant whether it is  $x$  that is large (i.e., far from the surface), or  $K$  that is large (i.e., high electrolyte concentration, or, what is much the same thing gegen-ions of higher valency).

Thus, at some fixed point from the surface, an increase in  $K$  must result in a decrease in  $\psi$ . There is one other possibility, as equation 4.8 shows, the double layer thickness,  $K$ , and the potential,  $\psi$ , are related to the surface charge. Thus a change in  $K$  could be reflected in a change in  $\sigma$ , without a change in  $\psi$ . This is most likely to happen when the surface charge arises from adsorbed ions, especially when these are the ions of surface-active species.

For a spherical particle (equation 4.10), the radius of the particle,  $a$ , also appears in the dimensionless form,  $Ka$ . It is clear that  $Ka$  can be increased either by an increase in electrolyte concentration or by the presence of a particle of large radius. In fact, for a sufficiently large radius, the curvature of the surface is so small, that it is, very close to a flat plate. These useful calculations on powder particles could be made using the flat-plate approximation.

**DLVO Theory (Derjaguin-Landau-Verwey-Overbeek):** It is now necessary to consider the effect of the interaction of two particles, i.e., what happens when two particles, each bearing a double layer, approaches one another. The solution of this problem was arrived at independently by Derjaguin and Landau and Verwey and Overbeek. Figure 4.6 schematically represents the situation for the double layer between two plates, as compared with the double layer for the single plate. As can be seen, the potential has a minimum value,  $\psi_0$ , at the point  $d$ , halfway between the two plates.

If it is assumed that the individual double layers are of the Gouy-Chapman type, the Poisson-Boltzmann equation takes the form

$$d^2\psi/dx^2 = (8\pi ze n_0/D) \sinh (ze \psi/kT) \quad 4.11$$

If it is assumed that the interaction between the double layers is small, i.e., that the potential where the individual potentials meet is given by the sum of the

potentials, a simple relation for the value of the minimum in potential between the plates results

$$\psi_d = (8kT/ze)\gamma \exp(-Kd) \quad \text{where} \quad 4.12$$

$$\gamma = \{ \exp(ze\psi_0/2kT) - 1 \} / \{ \exp(ze\psi_0/2kT) + 1 \} \quad 4.13$$

It can be seen from equation 4.12 that an increase in electrolyte concentration, or an increase in the separation of the plates, has the effect of making the potential well between the plates shallower.

The most useful information which these calculations can give us, however, is the potential energy between the plates, and, since the plates have a like surface charge, this will be a potential energy of repulsion. It can be shown to be equal to

$$V_R = \frac{64n_0kT}{K} \gamma^2 c^{-2} Kd \quad 4.14$$

The effect of separation and electrolyte concentration on this repulsion can be readily visualized, and it is shown as curves A and B in Figure 4.7.

In order to have the complete description of the interaction between the two particles, however, it must be taken into account the attractive forces which also exist. This attraction arises from the so-called London-van der waals forces. For the case where the distance between the plates are fairly thick and the distance between them,  $2d$ , is of the order of less than about  $100-200 \text{ \AA}$ , the attractive potential energy is given by

$$V_A = -A/48\pi d^2 \quad 4.15$$

where  $A$  is the so-called Hamaker constant, and usually has values between  $10^{-13}$  and  $10^{-12}$ , and varies with the nature of the material of which the plates (or particles) are made.

**Total Potential Energy :** It is thus possible to determine the shape of the total potential energy curve between the plates, by means of the relation

$$V = V_A + V_B \quad 4.16$$

A quantitative expression for the net interaction of two blocks of material separated by a distance  $d$  between their surfaces is obtained by combining Equations 4.14 and 4.15 to give

$$V = \frac{64n_0kT}{K} \gamma^2 c^{-2} Kd - A/48\pi d^2 \quad 4.17$$

its value is determined by the chemical nature of the dispersed and continuous phases. A final point may be made. For certain cases, at fairly large particle distances, the total potential energy curve may show a so-called secondary minimum. This shallow minimum in the curve corresponds to a weak attraction, and a loose sort of flocculation will take place at this point. It is believed that the primary step in the coagulation occurs at this secondary minimum.

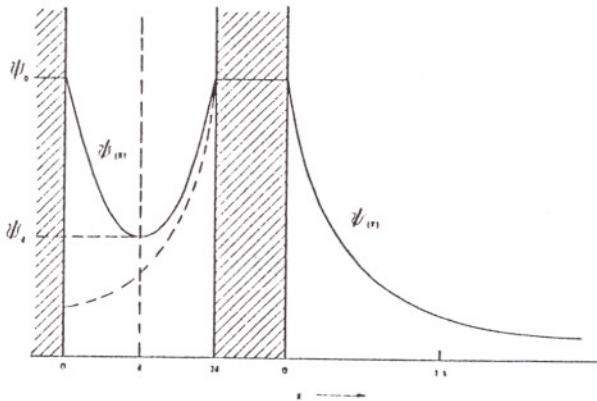


Figure 4.6 : Double layer between two flat plates ,as compared with double layer for a single plate.[4]

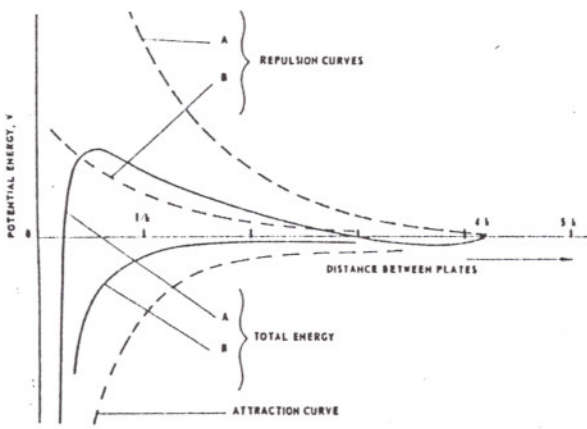


Figure 4.7: Total potential energy curve. Two repulsion curves, A and B, are shown. The solid lines are the resultant curves obtained by adding either A or B to the dotted attraction curve. In one case, a total repulsion curve is obtained, in the other case, the total curve is one of attraction.

**Steric Stabilization :** Polymers have been used to stabilize dispersions of solids in liquids against coagulation. Paints and inks used by ancient civilizations were prepared by dispersing suitable pigments in water and "protecting" the resulting system by additives such as gum arabic; egg albumin, or casein. Gelatin has also been used extensively as a stabilizing agent[13,20]. In molecular terms, these substances are changed polymers (polyelectrolytes) and their stabilizing influence is traceable to both electrostatic and polymeric effects. The advantage of polymer-induced stability over electrostatic stability imparted through low molecular weight electrolytes is summarized in Table 6.1

Table 4.1: Electrostatic and Steric Stabilization: A comparison.[13]

Electrostatic stabilization	Steric stabilization
Addition of electrolytes causes coagulation	Insensitive to electrolytes in the case of nonionic polymers
Usually effective in aqueous systems	Equally effective for both aqueous and nonaqueous dispersions
More effective at low concentrations of the dispersion	Effective at both low and high concentrations
Coagulation is not always possible	Reversible coagulation is more common
Freezing of the dispersion induces irreversible coagulation	Good freeze-thaw stability

The role of polymers on colloid stability is more complicated than electrostatic stability. First, if the added polymer moieties are polyelectrolytes, then there is a combination of electrostatic effects as well as effects that arise solely from the polymeric nature of the additive; this combined effect is referred to as electrosteric stabilization. Even in the case of nonionic polymers, addition of the polymer to a dispersion can promote stability or destabilize the dispersion, depending on the nature of interactions between the polymer and the solvent and between the polymer and the dispersed particles.

# CHAPTER V

## RHEOLOGY AND SEDIMENTATION

### 5.1 Rheology

Ceramic slurries and pastes are commonly multi-component systems that are relatively complex in structure and often poorly characterized. Particles may range from granular sizes to colloids. Added electrolytes may change interparticle forces and state of dispersion. Interparticle spacing depends directly on the concentration of the particles (solids loading), the state of dispersion and the particle packing.

A shear stress ( $\tau$ ) is required to initiate and maintain laminar flow in a simple liquid. When a shear stress is linearly dependent on the viscosity gradient (shear rate)  $-dv/dy$  (Figure 5.1), the liquid is said to be Newtonian,

$$\tau = \eta_L (-dv/dy) \quad 5.1$$

In liquids and solutions containing large molecules and suspensions containing non-attracting particles, laminar flow may orient the molecules or particles. When orientation reduces the resistance to shear, the stress required to increase the shear rate diminishes with increasing shear rate.

This behaviour is often described by an empirical power law equation,

$$\tau = K (-dv/dy)^n \quad 5.2$$

where  $K$  is the consistency index and  $n < 1$  is the shear thinning constant which indicates the departure from Newtonian behaviour. The apparent viscosity decreases with increasing shear rate, and the behaviour is said to be shear thinning or pseudoplastic. The apparent viscosity of a power law material is

$$\tau = \eta_a (-dv/dy)^{n-1} \quad 5.3$$

The power law with  $n > 1$  may also approximate the flow behaviour of moderately concentrated suspensions containing large agglomerates and concentrated, deflocculated slurries. With an increase in the shear rate, particle interference and apparent viscosity increases. This dependence on shear rate is called shear thickening behaviour.

A material having the yield stress  $\tau_y$  to initiate flow is called a Bingham plastic when the flow is described by the equation

$$\tau = \tau_y + \eta_p (-dv/dy) \quad 5.4$$

$$\eta = \tau_y / (dv/dy) + \eta_p \quad 5.5$$

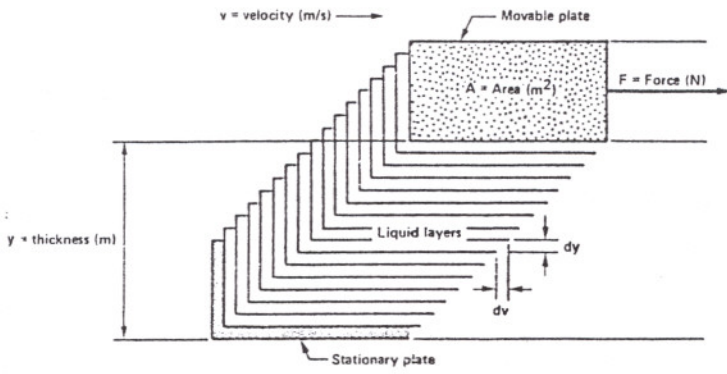
Equation 5.5 indicates that the Bingham material is shear thinning and  $\eta_p$  is the viscosity limit at a high shear rate.

For some materials, the apparent shear resistance and viscosity at a particular shear rate may decrease with shearing time. This behaviour, called thixotropy, is commonly observed for shear thinning materials when the orientation and bonding (coagulation) of molecules or particles change with the time during shear flow. For a thixotropic material with a yield stress, the apparent yield strength is higher after the suspension has at rest and a particle structure has reformed. A few materials exhibit an increase in shear resistance with time when sheared at a constant rate. This behaviour is called rheopectic and may be expected when agitation enhances bonding between structural units in the suspension. These properties are illustrated in Figure 5.2.

The viscosity of a suspension  $\eta_s$  is greater than the viscosity of the liquid medium  $\eta_L$  in the suspension, and the ratio is referred to as the relative viscosity  $\eta_r$ . For a very dilute suspension of non-interacting spheres in a Newtonian liquid, the viscosity for the laminar flow is described by the Einstein equation:

$$\eta_r = \eta_s / \eta_L = 1 + 2.5\Phi_p \quad 5.6$$

where  $\Phi_p$  is the volume fraction of dispersed spheres.



SHEAR STRESS,  $\tau = F/A$  (Pa)

SHEAR RATE,  $\dot{\gamma} = dv/dy$  ( $\text{s}^{-1}$ )

VISCOSITY,  $\eta = \tau/\dot{\gamma}$  (Pa·s)

Figure 5.1 : Model indicating viscous flow and definitions.[21,27]

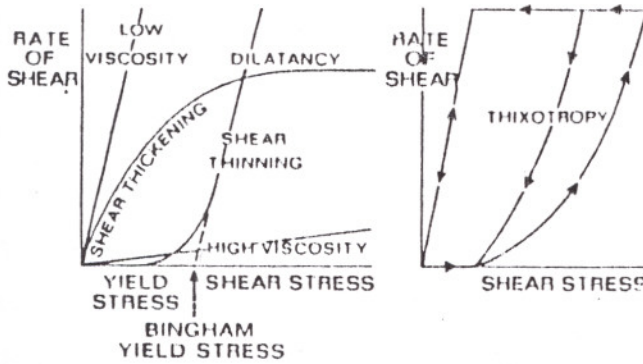


Figure 5.2 : Various types of rheological behaviour.[24]

In very high concentrated suspensions, the movement of particles around one another to accommodate shear flow requires time. Above a particular shear rate, the hindered rotation and particle interference may cause the appearance of shear thickening behaviour (Figure 5.3). Increasing the solids loading generally decreases the shear rate at which dilatant behaviour begins. In moderate concentrated suspensions below a particular shear rate, the particles show shear thinning when the shear thinning overcomes the randomizing effect of Brownian motion and the particles stay relatively longer positions.

In suspensions of oxides deflocculated using simple electrolytes, when the pH corresponds to the Isoelectric point of the particles, coagulation forces produce large, relatively porous agglomerates which may form a continuous gel structure when the solids content is sufficiently high. The viscosity of a slurry is very sensitive to the coagulation forces and the flocculated structure, as shown in Figure 5.4. The viscosity of the coagulated structure is relatively high and commonly shear thinning and thixotropic in behaviour. Partially coagulated suspension have the lower the viscosity, but exhibit shear thickening behaviour because of the interaction of agglomerates when sufficiently concentrated.

A continuous flocced structure in clay is formed when the clay is sufficiently concentrated. Increasing the pH reduces the floc size and eventually produces a dispersion of clay platelets with both negative edges and negative faces, and the apparent viscosity is relatively low, as shown in Figure 5.5. At low pH, the edges of the platelets become positive, but the forces remain negative, the viscosity remains relatively high.

Rheological control depends on determining flow properties as a function of shear rate. The shear rate dependence of the shear stress and viscosity is commonly determined using a rotating viscometer or by measuring the flow velocity through a tube. Colloids may be dispersed or agglomerated particles. In dispersed systems, the viscosity depends on the liquid viscosity of the liquid medium and the hydrodynamic properties and volume fraction of the dispersed particles with adsorbed surfactant. The proportion of liquid for flow directly with the packing efficiency of the particles.

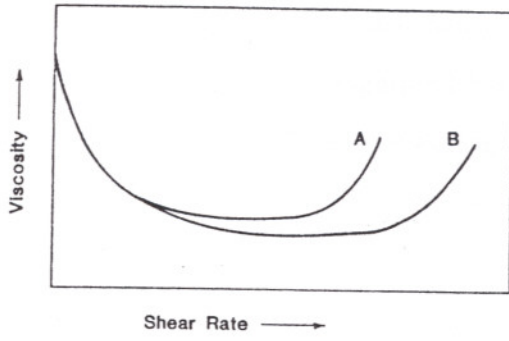


Figure 5.3 : General variation of viscosity with shear rate for two slurries indicating shear thickening behaviour at a high shear rate. The less well-dispersed system A exhibits shear thickening behaviour at a lower shear rate.[27]

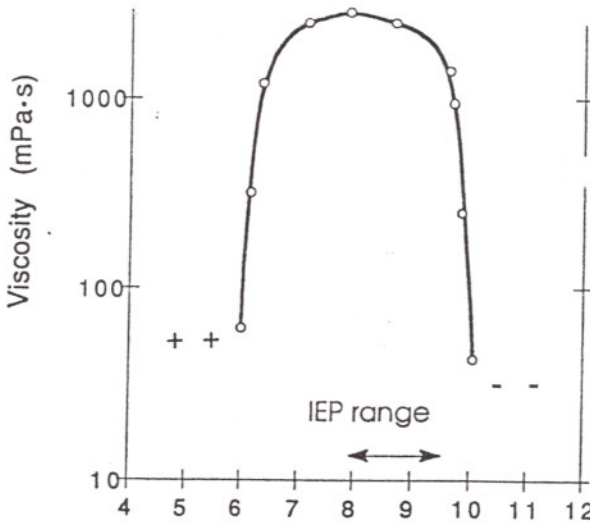


Figure 5.4 : Dependence of viscosity of slurry of reactive alumina powder on solution pH.[27]

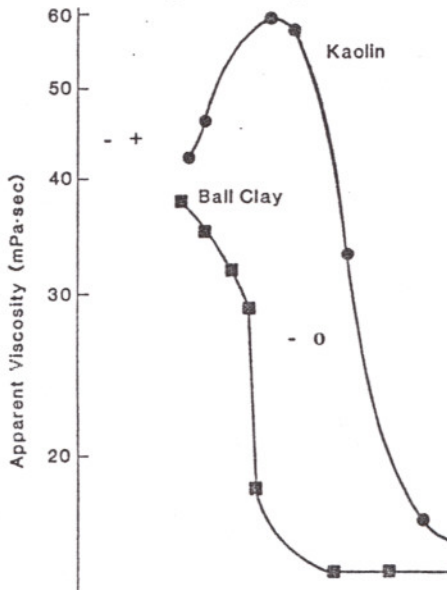


Figure 5.5 : Viscosity of clay slips decreases with increasing pH above IEP of edges of clay particles, but viscosity remains high at low pH because faces remain negative.[27]

## 5.2 Sedimentation

If the particles are larger (diameter  $> 1 \mu\text{m}$ ) than in typical colloids (diameter  $< 0.1 \mu\text{m}$ ) there is no difference in rate of sedimentation between stable and flocculating systems but there is a pronounced difference in the behaviour of the sediments.

Stable suspensions sediment slowly, with a fuzzy boundary between supernatant and sedimenting suspension because the particles sediment individually with speeds varying according to their sizes. Generally suspensions are separated into three regions; a layer of more or less clarified fluid referred to as the "supernatant", a "falling" or "clarification" zone where the suspension settles, and a "sediment" layer named the "compression" or "consolidating" zone where the solid volume fraction increases as the liquid between the particles is slowly squeezed out by the weight of solids. The sediment is very compact since the particles can glide along one another until the packing is as dense as possible. Such a sediment makes re-dispersion difficult and time consuming. If attraction prevails, the suspension coagulates while sedimenting. The sedimentation is faster. The boundary between supernatant and suspension is sharp, since the smaller particles are also caught in the flocs and sediment together with the larger ones. The final sediment is open. If the particles are not too small they can be easily redispersed by shaking or stirring. (Figure 5.6)

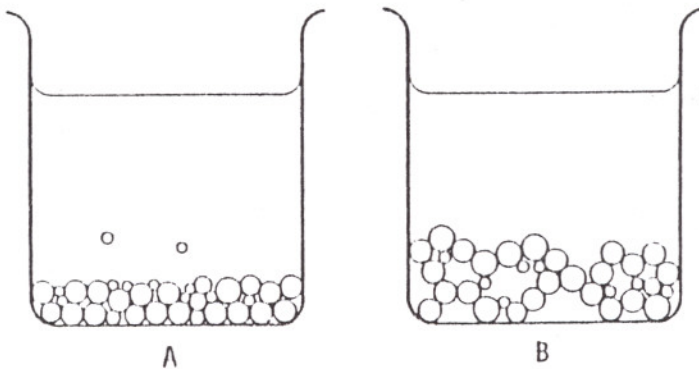


Figure 5.6 : Structure of sediments. A-) compact sediment from stable suspension  
B-) loose sediment from flocculated suspension. [24]

# CHAPTER VI

## EXPERIMENTAL

Seven commercial  $\text{TiO}_2$  powders were obtained from three companies and their characteristics are listed in Table 6.1. Only four of these powders (C, E, F, G) were used in this work. Two of these powders had rutile structure (C, G) and the others had anatase structure (F, E). All powders have 99%  $\text{TiO}_2$  content except powder C with 5 wt %  $\text{Al}_2\text{O}_3$  coating. The particle size distributions of these powders as supplied by the companies are given in Figures 6.1 to 6.4.

Powders were dispersed in water at three different solids loadings (5, 10 and 20 vol %) in this work. The pH of these suspensions were changed in the 2-12 range by using  $\text{HNO}_3$  (10 wt %) and  $\text{NaOH}$  (2 wt %) solutions. A separate suspension was prepared for each powder combination of vol % and pH. A high molecular weight block copolymer obtained from BYK Chemie (BYK 182: polyoxyalkyleneglycol-modified polyurethane with tertiary nitrogen groups, low polar, 30000 molecular weight, 43% solids content, 1.03 gr/ml density) was used for steric stabilization of the suspensions. The surfactant concentrations was varied in the 0.1-0.5% by surfactant solids based on dry powder mass in the preparation of 5 different suspensions for each powder and powder volume percentage. In this fashion about 11 suspensions with different pH values and 5 suspensions with different surfactant contents for each powder at a fixed solids loading was prepared. Each suspension was ball-milled for 30 minutes for the dispersion of the powder.

Rheological behaviour of these suspensions were investigated by using a rheometer (Brookfield RV-DV III model) with the UL adapter in shear rate range of  $31.6\text{-}306\text{ s}^{-1}$ . About 16 ml. suspension were loaded into the UL adapter for each run. Torque, viscosity, shear stress for 10 different shear rates (at 10 different selected revolution rpm of the spindle) were reported by the rheometer for each run. This data were further plotted as shear stress vs. shear rate and viscosity vs. shear rate for rheological behaviour analysis.

Two types of test tubes (15,8 cm long and 14 mm inner diameter, 17,7 cm long and 16 mm inner diameter) were used for the sedimentation studies. About 20 ml from each suspension were put into these tubes at about a height of 10 and 12,5 cm by using a syringe. These tubes were labelled and sealed by parafilm and the suspensions were left to settle (time being equal to 0 hours). These suspensions contained 4,8 and 16 gram of  $TiO_2$  for 5,10 and 20 vol% solids, respectively. The height of the sediments were recorded in various periods and this data were used for the preparation of sedimentation heights (H/cm) vs. time (t/h) plots. Extreme care were taken for undisturbing these settling suspensions during sediment height measurements. These observations were made for up to about 21 days or 500 hours. FTIR spectra of these powders were obtained by Shimadzu FTIR -1600 for phase identification by preparing KBr pellets.

Two types of test tubes (15,8 cm long and 14 mm inner diameter, 17,7 cm long and 16 mm inner diameter) were used for the sedimentation studies. About 20 ml from each suspension were put into these tubes at about a height of 10 and 12,5 cm by using a syringe. These tubes were labelled and sealed by parafilm and the suspensions were left to settle (time being equal to 0 hours). These suspensions contained 4,8 and 16 gram of  $TiO_2$  for 5,10 and 20 vol% solids, respectively. The height of the sediments were recorded in various periods and this data were used for the preparation of sedimentation heights (H/cm) vs. time (t/h) plots. Extreme care were taken for undisturbing these settling suspensions during sediment height measurements. These observations were made for up to about 21 days or 500 hours. FTIR spectra of these powders were obtained by Shimadzu FTIR -1600 for phase identification by preparing KBr pellets.

Table 6.1 : Powders used in Preparing Dispersions

CODE	SOURCE	TRADE NAME	TiO <sub>2</sub> CONTENT	COATED WITH COMPOUNDS BASED ON	DENSITY (gr/cm <sup>3</sup> )	APPLICATIONS
POWDER A	KRONOS	KRONOS 2310	93	Al <sub>2</sub> O <sub>3</sub> (4%),SiO <sub>2</sub> (0.5%)	4	Automotive paints,coil coatings,radiation cured finishes,industrial and decorative coatings
POWDER B	KRONOS	KRONOS 2160	90	Al <sub>2</sub> O <sub>3</sub> (3%),SiO <sub>2</sub> (4%)	3.9	Automotive paints, coil coatings, radiation cured finishes, industrial and decorative coatings
POWDER C	MILLENIUM	TiONA 535	95	Al <sub>2</sub> O <sub>3</sub> (5%)	4.1	Industrial, emulsion and powder coatings
POWDER D	BAYER	R-U-2	98	Al <sub>2</sub> O <sub>3</sub> (2%)	4.1	Primers, decorative coatings, emulsion paints, plastic-based plasters, wallpaper inks, road marking paints
POWDER E	BAYER	A	99	--	3.9	paper, rubber enamels, primers, indoor emulsion paints, cement
POWDER F	BAYER	A-E	99	--	3.9	Enamels, ceramics
POWDER G	BAYER	T	99	--	4.2	Glass, ceramics, electro-ceramics, welding electrodes

DISC CENTRIFUGE RESULTS					
Sample code	Mean (microns)	Mode (microns)	Modal Wt %	%>0.5 microns	Std.Dev.
RCL-535	0.314	0.266	11.144	4.895	0.109

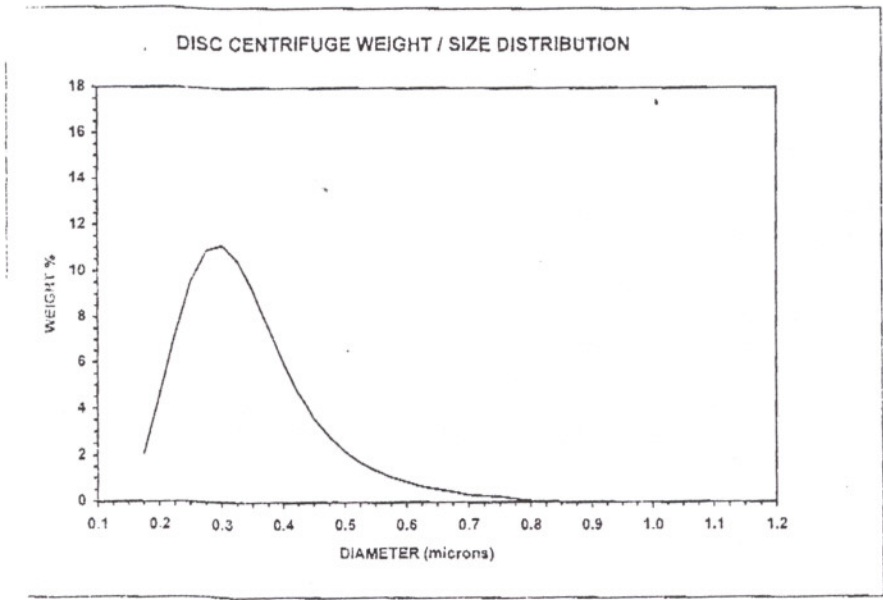


Figure 6.1 : Particle Size Distribution Diagram for Powder C

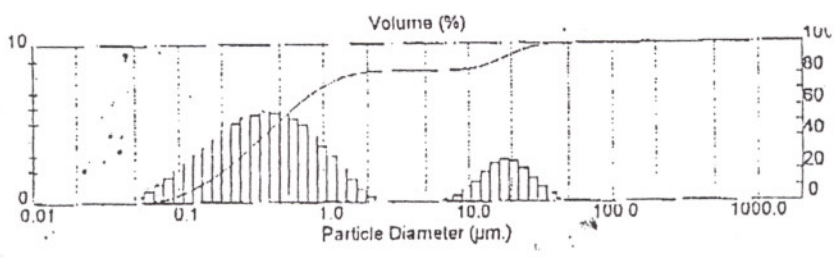


Figure 6.2 : Particle Size Distribution Diagram for Powder G

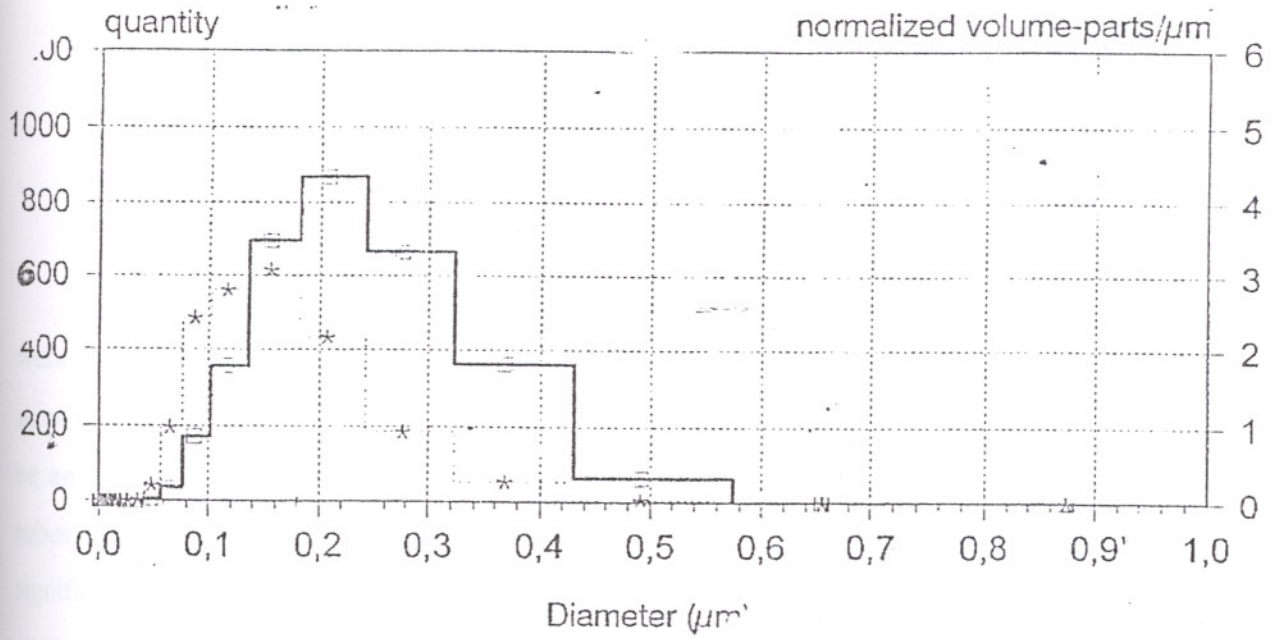


Figure 6.3 : Particle Size Distribution Diagram for Powder F

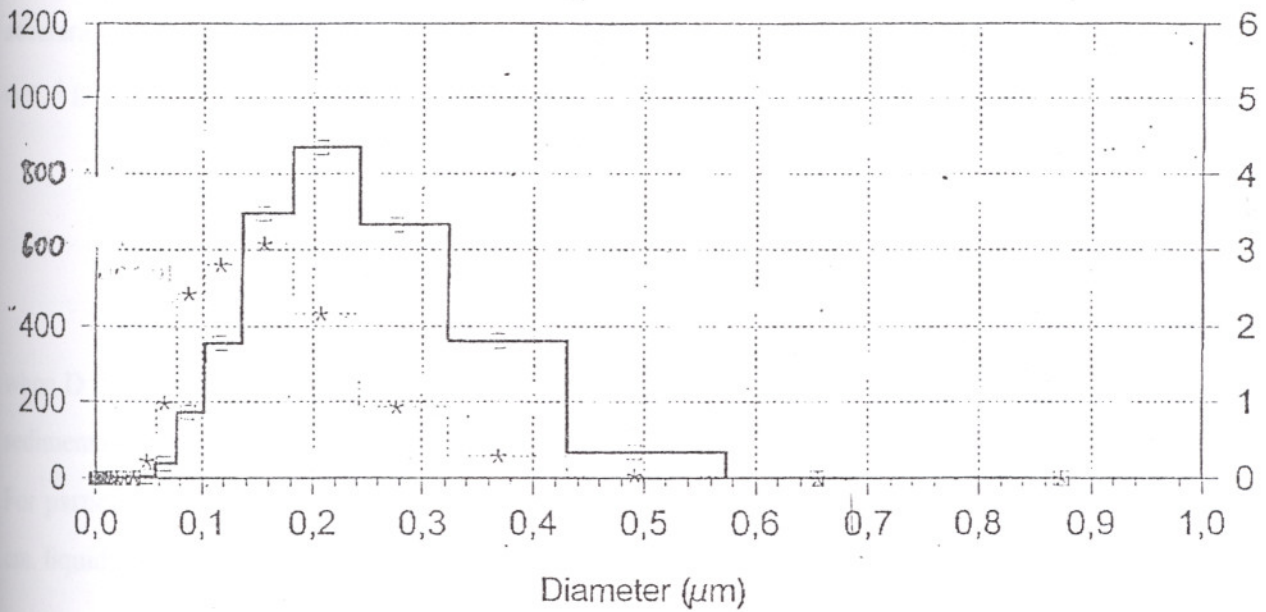


Figure 6.4 : Particle Size Distribution Diagram for Powder E

# CHAPTER VII

## RESULTS AND DISCUSSIONS

The particle size distributions as supplied by the companies for all 4 TiO<sub>2</sub> powders were given in Figures 6.1 to 6.4. These powders have about 0.3 μm. average particle sizes. If all the powders are assumed to have monosize particles of about 0.3 μm., there will be an approximate sedimentation time to reach to the bottom of the sedimentation test tubes. The presence of finer-coarser particles than this particular size also would significantly effect the sedimentation and the rheological behaviour of these suspensions. Assuming spherical particles this sedimentation time can be determined by evaluating the sedimentation velocity from Stokes Law using the following equation:

$$D^2 = 18\eta v / (\rho_s - \rho_f)g \quad 7.1$$

where D is the particle diameter, η is the fluid viscosity, v is the sedimentation velocity, ρ<sub>s</sub> - ρ<sub>f</sub> is the difference in the densities of the particles and the fluid and g is the gravitational acceleration. Plugging in the following values:

ρ<sub>s</sub> = 4 g/cc, ρ<sub>f</sub> = 1 g/cc, η = 0.89 \* 10<sup>-2</sup> g/cm.s (at 25°C), the above equation becomes:

$$D^2 = 18v(0.89 * 10^{-2}) / (4-1) * 980 \quad 7.2$$

$$D^2 = 5.5 * 10^{-5} v \quad 7.3$$

when D is equal to 0.3 μm., v is 1.6 \* 10<sup>-5</sup> cm/s. For a total height of 12.5 cm. the necessary sedimentation time is about 9 days.

For particles 0.1-1.0 μm range the settling velocities and times necessary for settling 12.5 cm. liquid height is tabulated in Table 7.1.

Table 7.1: Comparison of the sedimentation velocities and time according to the particle size.

$D \cdot 10^4$ (cm)	$v \cdot 10^4$ (cm/s)	t(h)	t(day)
0.1	0.0182	1910	80
0.2	0.0727	477	20
0.3	0.164	212	9
0.4	0.291	119	5
0.5	0.455	76	3
0.7	0.891	39	1.62
0.9	1.470	24	1
1.0	1.820	19	0.80

Particles below 0.3  $\mu\text{m}$  will increase the necessary settling time above 9 days and bigger particles, flocs-coagulates would cause a faster sedimentation. The sedimentation experiments were carried over 9 days up to 21 days in order to let 0.2  $\mu\text{m}$  particles settle if they are present in the powders. The variation of falling zone height with time for powders containing monosize  $\text{TiO}_2$  spheres of 0.2, 0.3, 0.4 and 0.5  $\mu\text{m}$  is schematically shown in Figure 7.1 for 10% solids loading.

During the sedimentation experiments generally three regions; sediment, falling zone and supernatant zone is expected. In most of the experiments only two regions, sediment and supernatant zone were observed, but in others the distinction between the falling zone and sediment was not possible and only the change in the height of the falling zone was followed and used in the analysis. These observations were used in the preparation of sedimentation heights (H) vs. time (t) plots. Visual observations on the nature of the prepared suspensions are given in Table 7.2. Suspensions were characterized as D (dispersed) or F (flocculated) by observing their behaviour. If quick settling and rapid formation of a clear supernatant zone occurred the suspension was labeled as F. The presence of a falling zone, gradual decrease in the height of this zone and the presence of a bluish supernatant caused labeling as D. These visual observations will be compared with the sedimentation and rheological behaviour of the suspensions in the following pages.

The H vs.t data at about a final t of 500 hours was used for the evaluation of Packing Density % for each suspension. The packing densities of the sediment were calculated simply by using the following relations:

$$PD\% = (V_{TiO_2} / V_{sed}) * 100 = n * (V_T / V_{sed}) = n * (H_T / H_{sed}) * 100 \quad 7.4$$

$$V_{TiO_2} = n * V_T = (\pi/4 * D^2 * H_T) * n \quad 7.5$$

$$V_{sed} = \pi/4 * D^2 * H_{sed} \quad 7.6$$

$H_T = 10$  or  $12.5$  cm.

$H_{sed}$  = sedimentation height

D = tube diameter

$n = 0.05, 0.1, 0.2$  (solid fractions)

The PD% 's for all suspensions were evaluated and plotted as a function of pH or surfactant content. Evidently, H is inversely proportional to PD% and if the sediment height is high, PD% is low and the suspension has a flocculated structure .

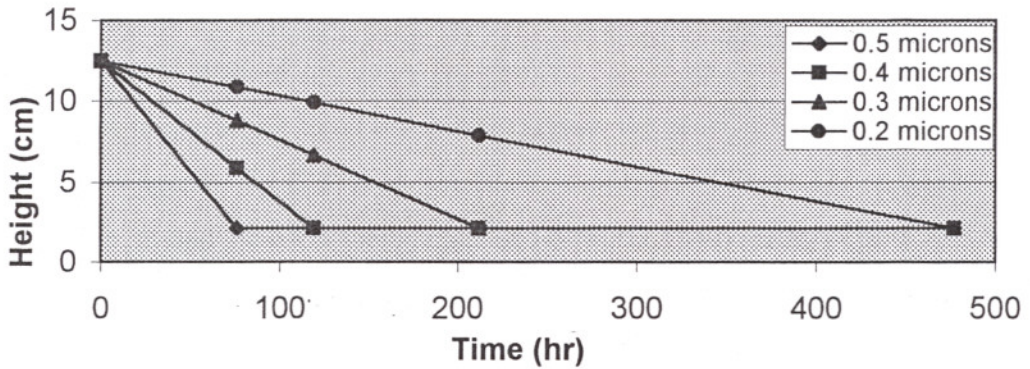


Figure 7.1 : Schematic representation of H vs. t for monosize particles for 10% solids.

## 7.1 Characterization of Powder C :

It is an  $\text{Al}_2\text{O}_3$  coated rutile powder. The H vs. t curves for selected 3 pH values (especially chosen from acidic, basic and neutral regions) are given in Figure 7.2. The height of the sediments were about constant at pH=7 for all solids loadings at successively higher H values. In the acidic (pH=3) and basic zones (pH=10), H varies with time. At 5 vol% solids loadings, H decreases only after 500 hours at pH=3 and stabilizes sharply above 300 hours at pH=10. At higher solids loadings, similar trend is observed at pH=10, but H stabilizes quickly at pH=3. The packing density of the suspensions were very low in the neutral pH range (pH=5-8) but is in the 40-60% range in the acidic and basic zones as shown in Figure 7.3. The viscosities of the suspensions at pH=7 and 10 are rather high showing a pseudoplastic type behaviour at 5 vol% solids loadings. The presence of these zones in the viscosity and stress vs. shear rate curves at pH=9 can be seen in Figure 7.4. The suspension is pseudoplastic below a shear rate of about  $100 \text{ s}^{-1}$ , Newtonian in between  $100-240 \text{ s}^{-1}$  and becomes dilatant above  $250 \text{ s}^{-1}$ . The 5 vol% powder C suspension becomes dilatant (dispersed) at pH=11 and displays similar shear stress, viscosity vs. shear rate behaviours with pH=3 suspension. The behaviour of the 10 and 20 vol% suspensions at pH=3 and 10 are similar and have a dilatant nature (shear thickening). This is an indication of dispersed systems.

The effect of surfactant at all levels were similar the powder C dispersions. The pH of the suspensions became 7.5-7.8 upon the addition of the surfactant. The sediment were densely packed at 10 and 20 vol% solids at around 60%PD. The packing density of 5 vol% were significantly lower at about 20 % as shown in Figure 7.7 and 7.8. These results were not in agreement with the rheological characterizations given in Figures 7.9, 7.10 and 7.11. The suspension is dilatant with a shear-thickening behaviour and relatively low viscosity at 5 vol% solids indicative of a relatively dispersed system. The 10 vol% suspension have Bingham type shear stress-shear rate behaviour and viscosity was relatively high and shear-thickening can be seen indicative of a flocculated suspension. The reason of this contradiction may have something to do with the floc structure. The formation of relatively dense flocs settling relatively quickly to form dense cakes can be responsible from the relatively high viscosities. The H vs. t datas were taken starting with

about 3 days after the preparation of suspensions. The changes in the height of these suspensions from  $t=0$  to  $t=70$  hours might have given some information about the size of these flocs and the  $H$  vs.  $t$  curves would look like those given in Figure 7.1 with the approximated floc size.

### **7.2 Characterization of Powder E :**

The first anatase powder, powder E, behaves differently and disperse systems were not prepared at low pH. The  $H$  vs.  $t$  curves for powder E are given in Figure 7.12. The sediment height at  $pH=3$  is high and quickly stabilizes at around 10. This behaviour changes above  $pH=7$  with the formation of 3 sedimentation layers and a more dispersed suspension. The  $PD\%$  vs.  $pH$  curves given in Figure 7.13 clearly show the presence of a very loosely packed cake below  $pH=6$  and relatively dense cake in the 7-11 pH range. The rheological behaviour of these suspensions given in Figures 7.14, 7.15 and 7.16 in general show a shear thickening behaviour indicative of disperse systems in the basic region except at 5 vol% solids loading where Bingham type of fluid and shear-thinning is observed. The visual observations also state the formation of disperse systems above  $pH=7$ .

The powder E suspensions with surfactant addition forms mostly flocculated suspensions. The  $H$  vs.  $t$  curves given in Figure 7.17 and  $PD\%$  curves given in Figure 7.18 shows that the  $PD\%$  's are very low at 5 and 10 vol% suspensions but relatively high (about 60%) at 20 vol% solids. The viscosities of all of these suspensions are relatively high and the suspensions do show shear-thinning behaviour. This is the typical character of flocculated systems (Figures 7.19, 20, 21).

### **7.3 Characterization of Powder F :**

The second anatase powder, powder F, which was obtained from Bayer was stated to be useful for ceramic applications had a wider dispersed pH range from visual observations as stated in Table 7.2. The suspensions below  $pH=6$  have a low packing density and the final  $H$  values are relatively high as shown in Figures 7.22 and 7.23. The packing densities in the 6-11 pH range in around 40% is relatively lower than some of the previous powder suspensions. The rheological behaviour of only the 5 vol% powder F suspensions were characterized. The  $pH=4$  suspension has a typical Bingham type shear-

thinning behaviour as shown in Figure 7.24. The behaviours of pH=7 and 10 suspensions are very similar and they have a shear thickening-dilatant behaviour. The rheological behaviours of these powders E and F are different at 5 vol% solids loadings. This may be due to particle size distribution differences. This information was taken from the Bayer Company, so the powder F is higher grade than the powder E.

The powder E has much more impurities than the powder F.

The surfactant addition to powder F suspensions caused the formation of flocculated suspensions and very low packing density compacts in the 10-30% packing densities as shown in Figures 7.25 and 7.26. The flocs formed in 5 vol% suspension were probably weak-loose-high porosity flocs as evidenced by the rheological behaviour given Figure 7.27. The suspension is pseudoplastic (shear-thinning) at low shear rate but becomes dilatant above about  $150 \text{ s}^{-1}$  rate and shear thickening happens above this value. This was considered to be an indication of the presence of relatively weak and easily dispersible flocs.

Table 7.2: Visual observations on the nature of the suspensions. D:disperse, F:flocculated

pH	Powder C			Powder E			Powder F			Powder G		
	5%	10%	20%	5%	10%	20%	5%	10%	20%	5%	10%	20%
2	D	F	F	F	F	-	F	F	-	D	D	D
3	D	F	F	F	F	-	F	F	-	D	D	D
4	D	F	F	F	F	-	D	F	F	F	F	F
5	F	F	F	F	F	-	D	F	F	F	F	F
6	F	F	F	F	F	F	D	D	D	F	F	F
7	F	F	F	D	D	F	D	D	D	F	F	F
8	F	F	F	D	D	D	D	D	D	D	F	F
9	D	D	D	D	D	D	D	D	D	D	F	D
10	D	D	D	D	D	D	D	D	D	D	D	D
11	D	D	D	D	D	D	D	D	D	D	D	D
12	D	D	D	F	D	D	D	D	D	D	D	F
% surf	5% pH: 7.8	10% pH: 7.75	20% pH: 7.5	5% pH: 7	10% pH: 7	20% pH: 7	5% pH: 10	10% pH: 10	20% pH: 10	5% pH: 4	10% pH: 4	20% pH: 4
0,1	F	D	D	F	F	D	F	F	F	F	F	F
0,2	F	D	D	F	F	D	F	F	F	F	F	F
0,3	F	D	D	F	F	F	F	F	F	F	F	F
0,4	F	D	D	F	F	F	F	F	F	F	F	F
0,5	F	D	D	F	F	F	F	F	F	F	F	F

#### 7.4 Characterization of Powder G :

The final powder, powder G, was a rutile powder the H vs. t and packing density plots are given in Figures 7.28 and 7.29. The suspension were visually observed to be dispersed at pH=2 and also had high packing densities in these acidic solutions. The packing densities are low in the pH=3 to 9 range. The pH=3 and 7 solutions have a shear-thinning Bingham type behaviour as shown in Figure 30. pH=10 suspension is dilatant which was in agreement with visual observations and packing densities. The addition of surfactant to powder G suspensions caused the formation of flocculated suspensions and low packing densities as shown in Figure 7.31 and 7.32. The rheological behaviour of 5 vol% suspensions was Bingham type as shown in Figure 7.33 in agreement with about 15 PD%. The final pH values of these suspensions was about 4.5 which also is in the unstable region. The suspension behaviour was not dependent on the surfactant percentages which was varied in the 0.1-0.5% based on TiO<sub>2</sub> solids content.

The experiments done in the basic, acidic and neutral regions gave some typical results. In rheological measurements, the shear-thinning or pseudoplastic structure means a flocculated suspension and shear-thickening and dilatant structure shows a more stable and more dispersed suspensions. In sedimentation measurements, it is expected the formation of three sedimentation layers (sedimentation, supernatant and falling zone) for a dispersed systems. Three sedimentation layers means more compact sediment and high packing density percentages. This was seen in different pH values for four titania powders. In the suspensions having surfactant, it was generally seen the flocculated suspensions, that is, two sedimentation regions, sediment and clear solution, in sedimentation measurements and pseudoplastic nature in rheological measurements. There were sometimes contradictions due to the nature of floc structure.

İZMİR YÜKSEK TEKNOLOJİ ENSTİTÜSÜ  
REKTÖRLÜĞÜ  
Kütüphane ve Dokümantasyon Daire Bşk.

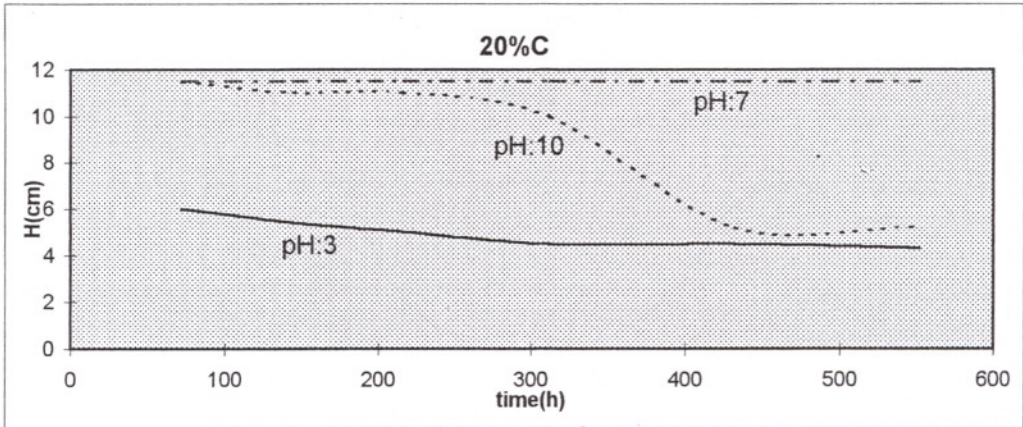
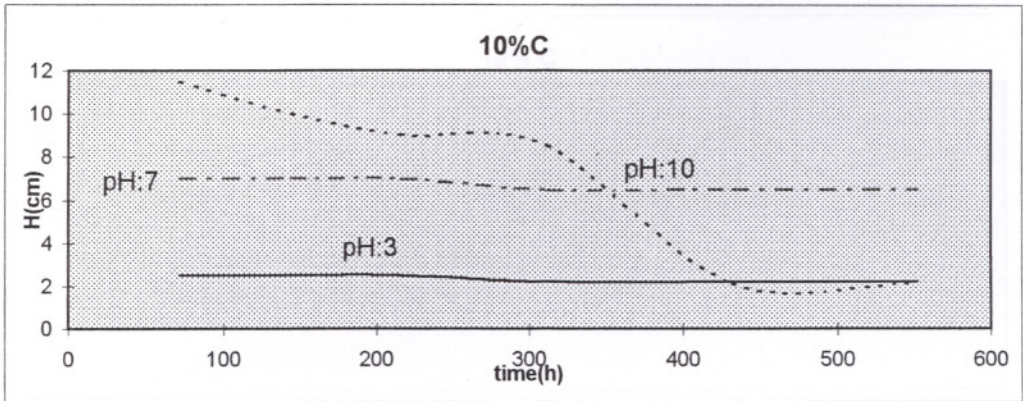
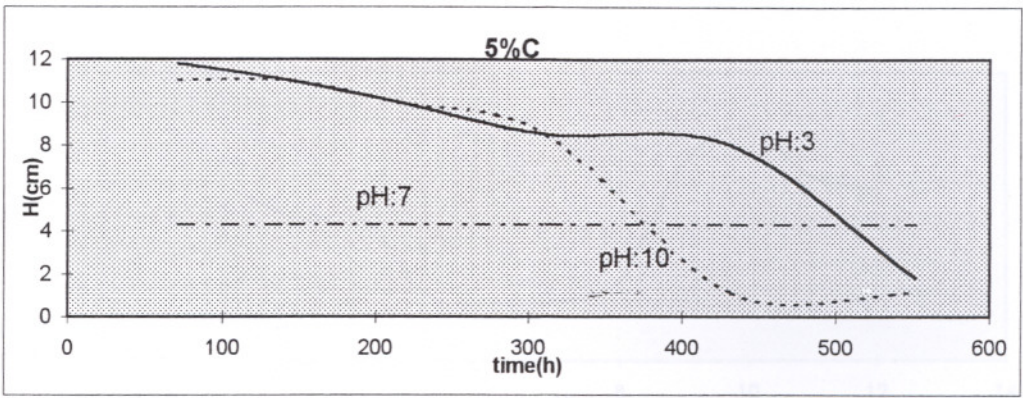


Figure 7.2 :  $H$  vs.  $t$  at 3 different pH for powder C without surfactant

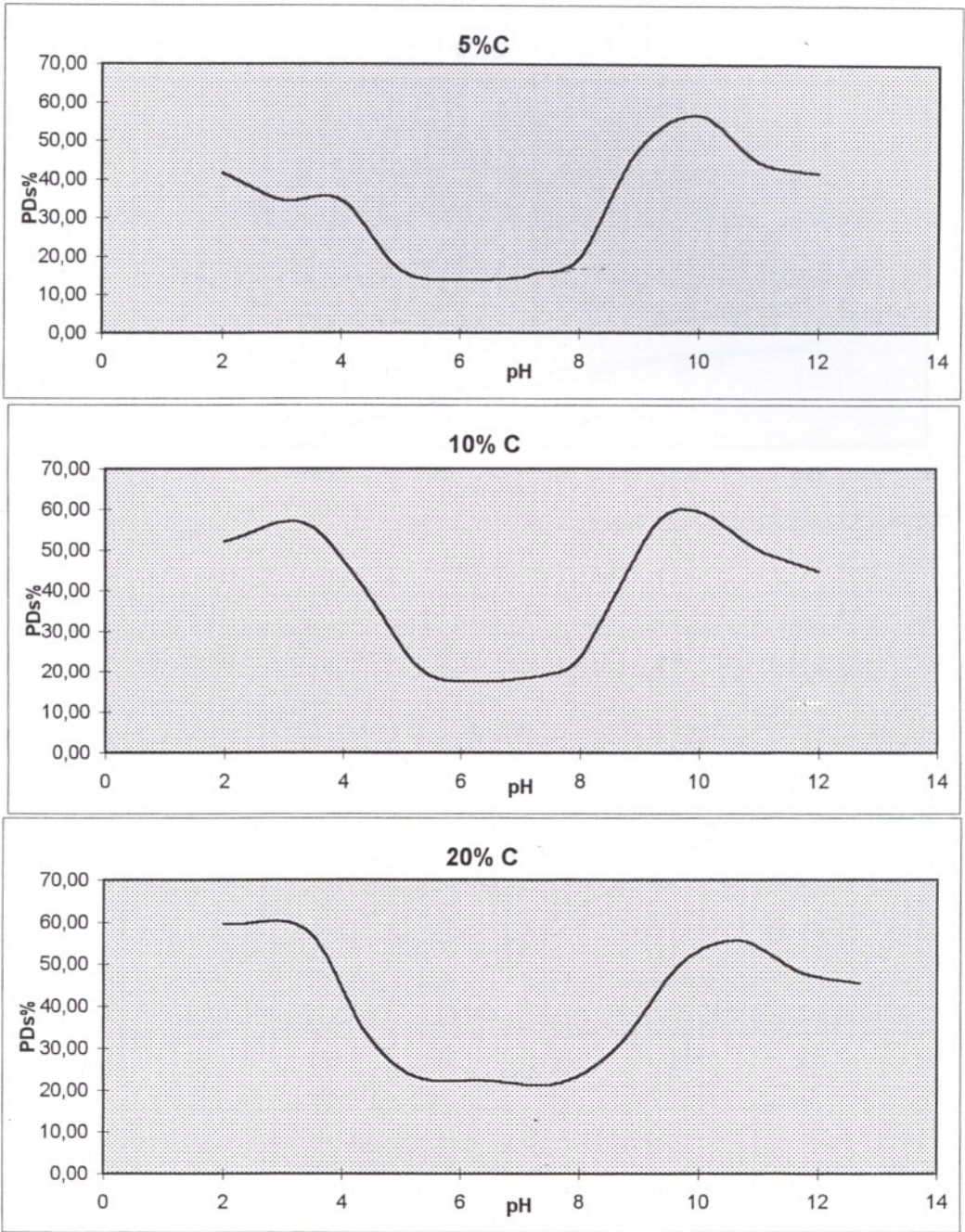


Figure 7.3 : PD% vs.pH at saturation time for powder C without surfactant

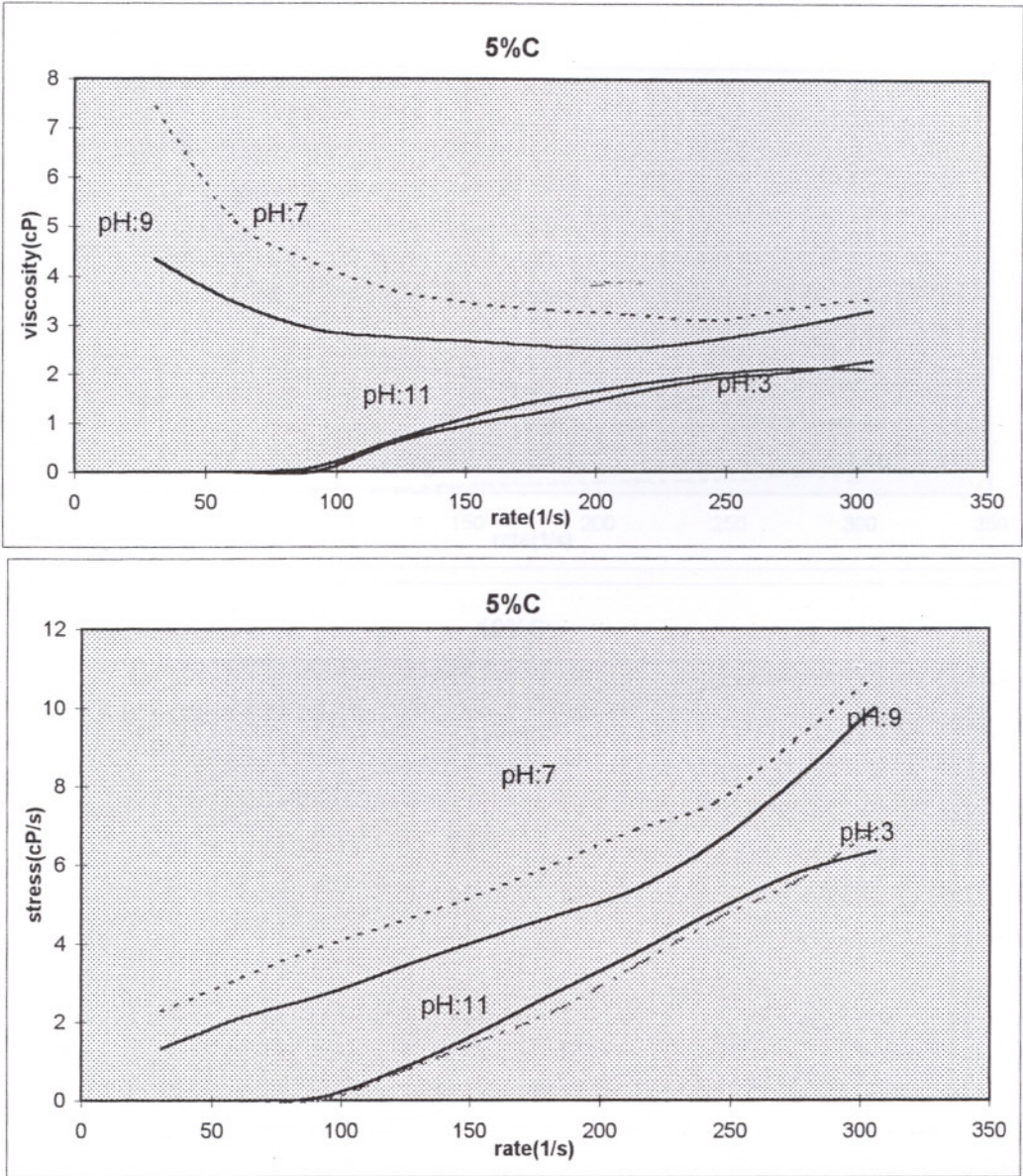


Figure 7.4 : Viscosity vs.rate and rate vs.stress graphs for powder C having 5% solid

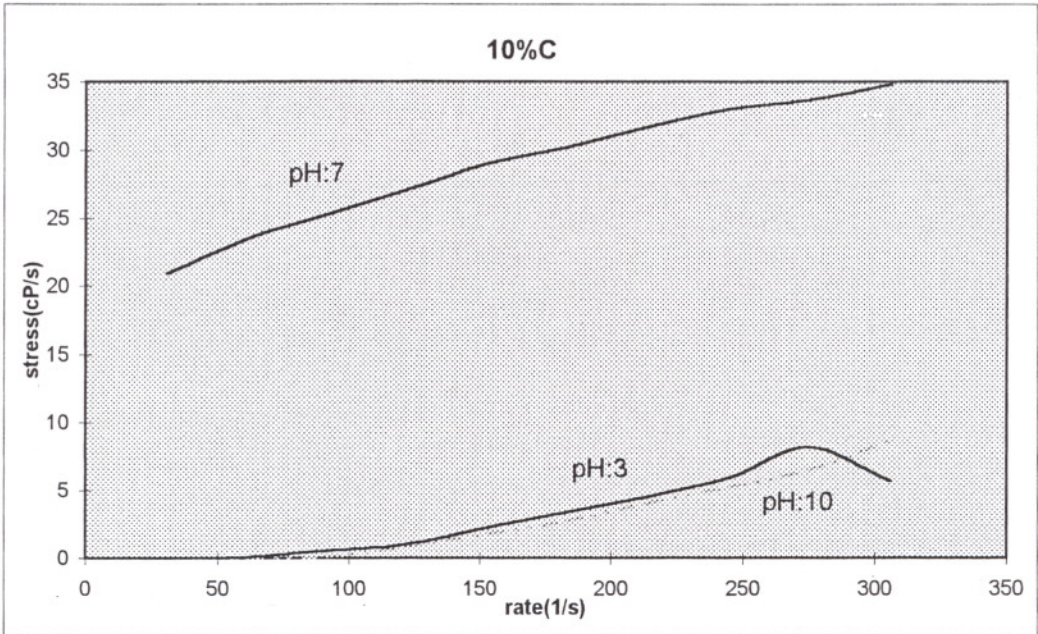
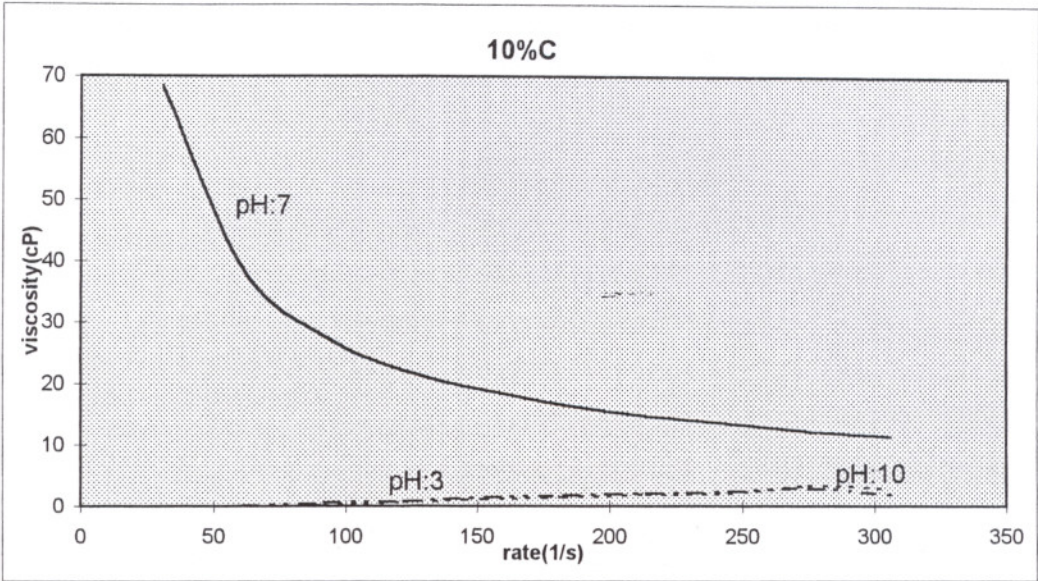


Figure 7.5 : Viscosity vs.rate and rate vs.stress graphs for powder C having 10% solid

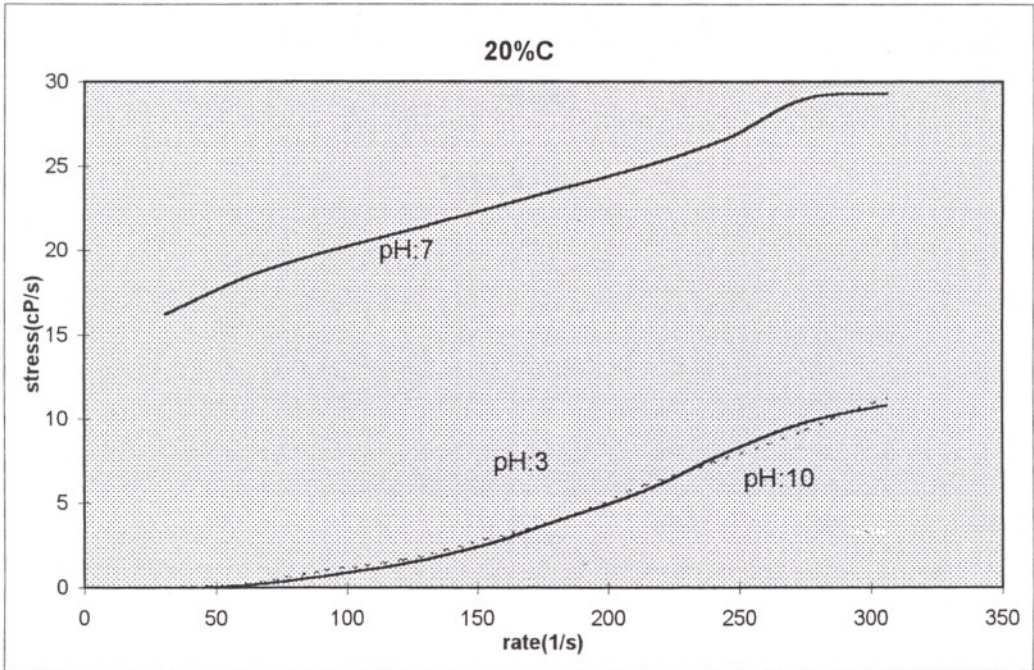
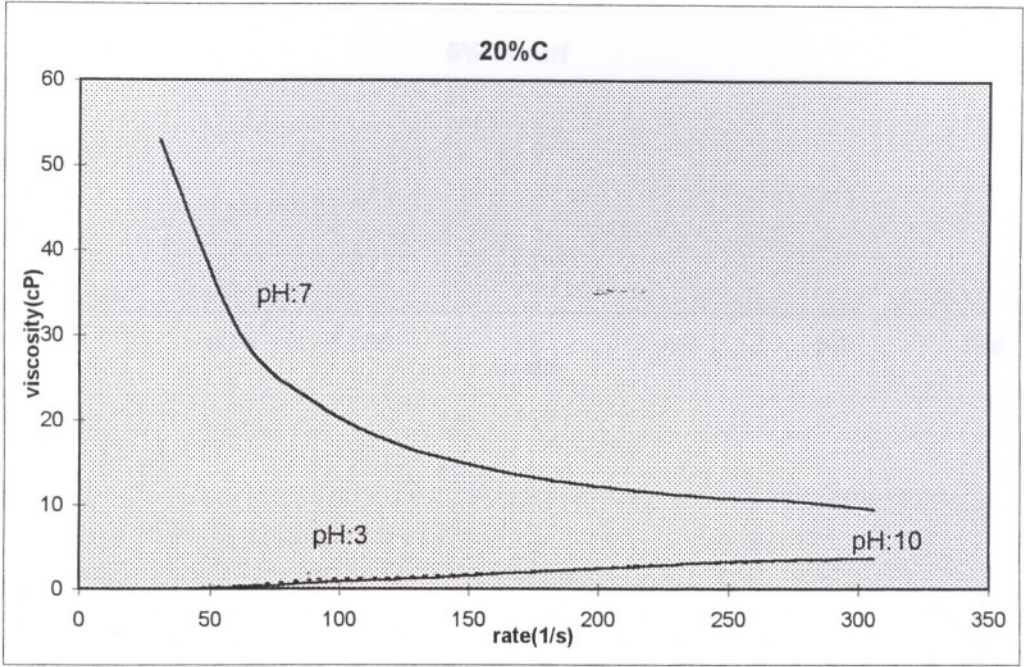


Figure 7.6 : Viscosity vs.rate and rate vs.stress graphs for powder C having 20% solid

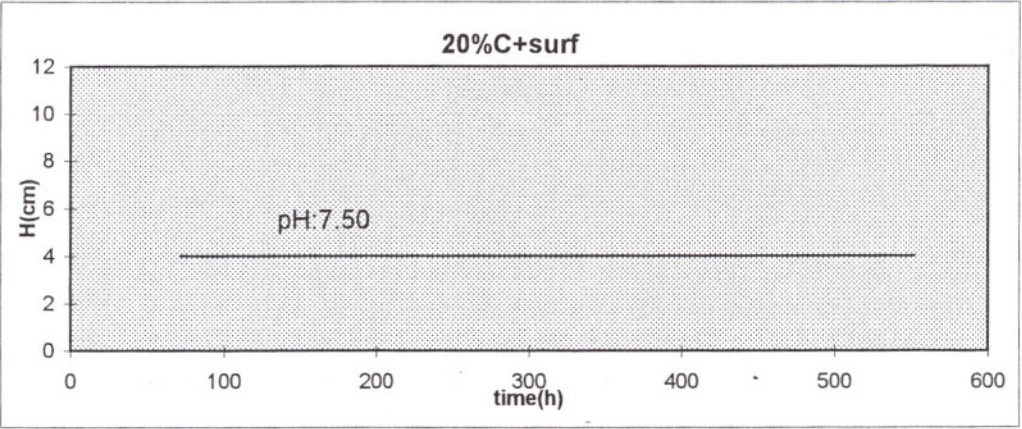
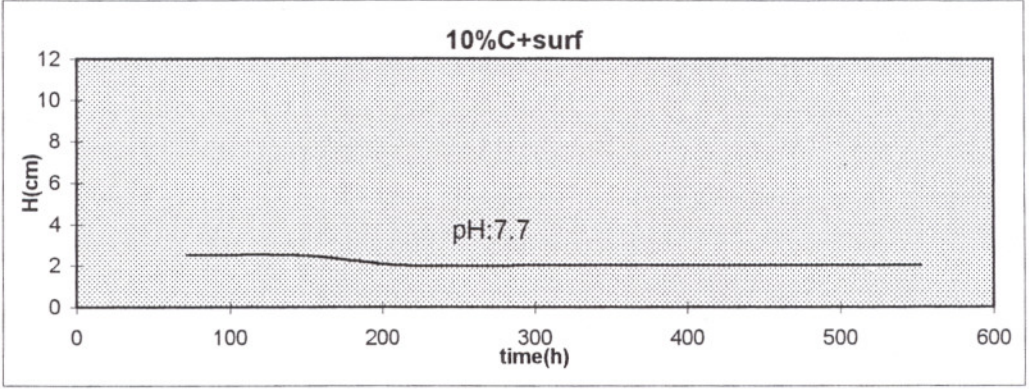
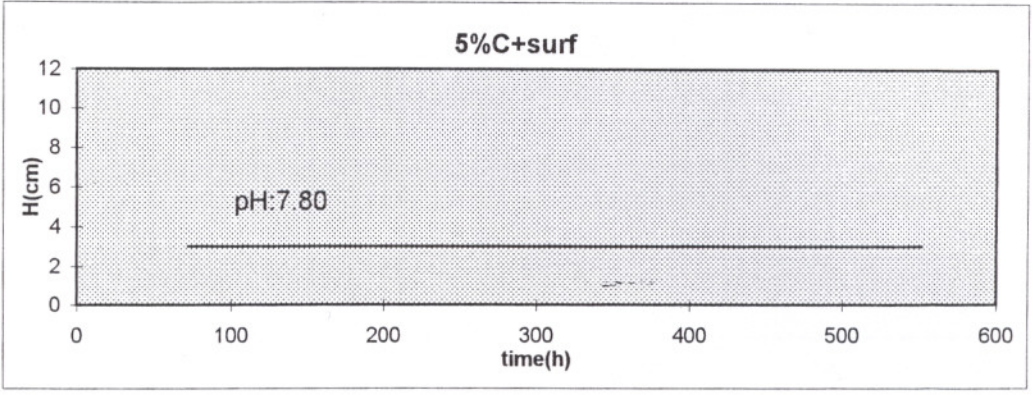


Figure 7.7 : The trend of H vs.t for titania powder C having surfactant

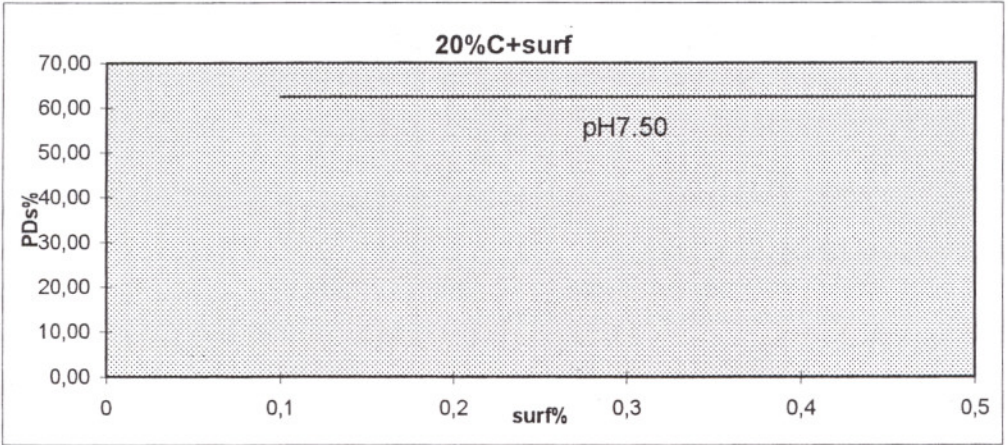
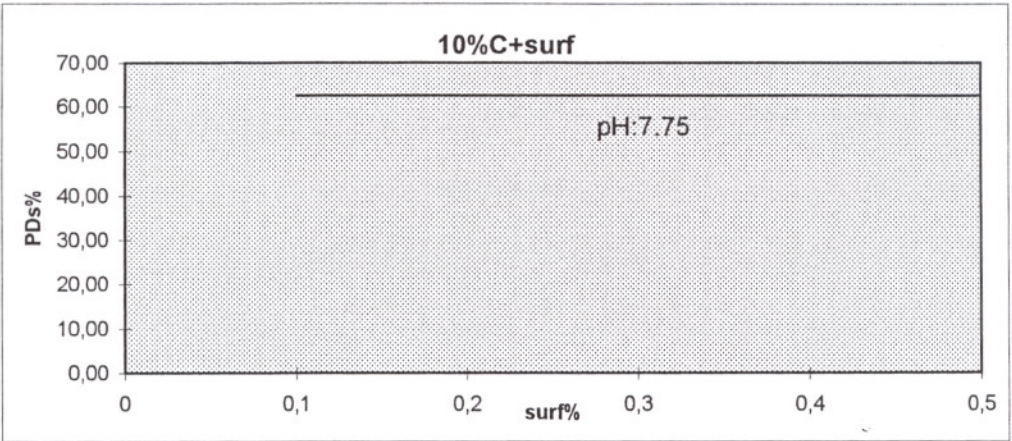
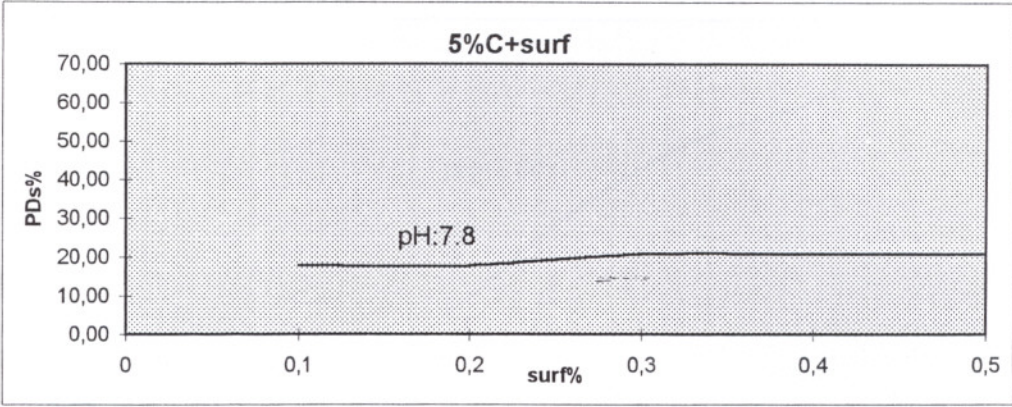


Figure 7.8 : PD% vs.surf% for powder C at saturation time

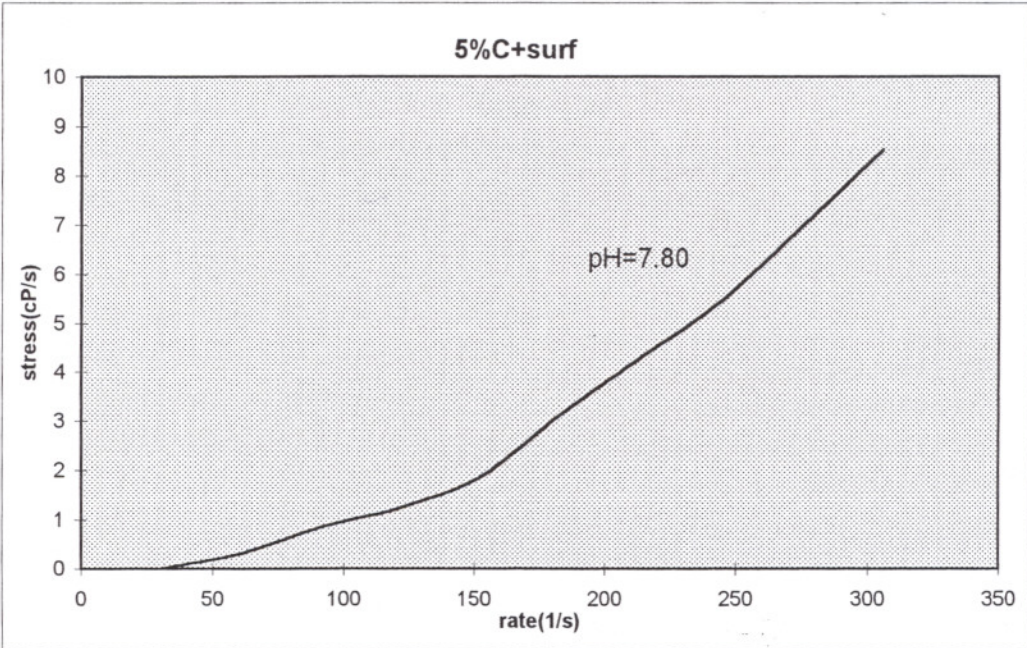
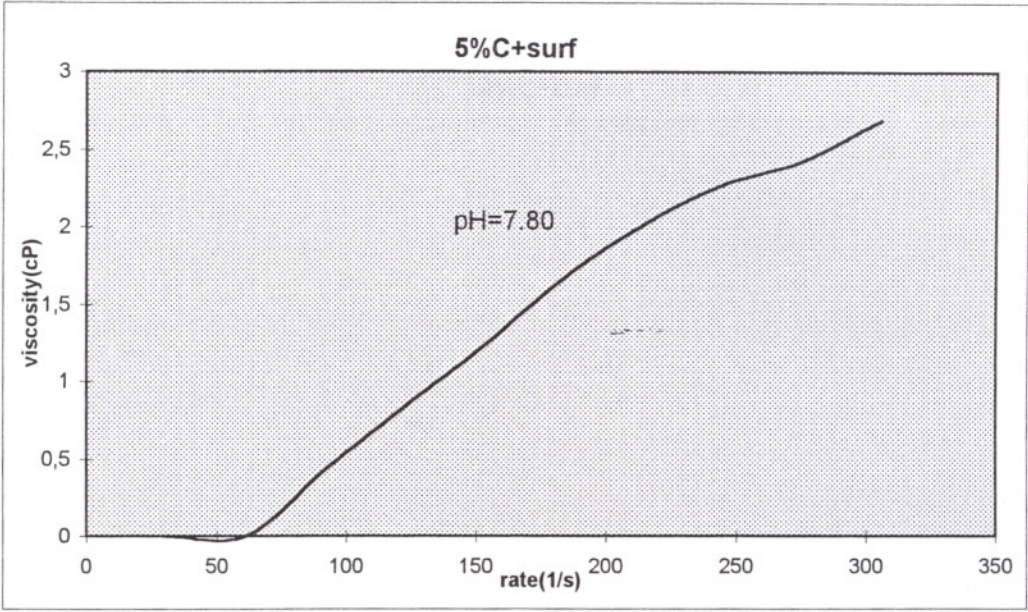


Figure 7.9 : Viscosity vs.rate and rate vs.stress graphs for powder C having surfactant

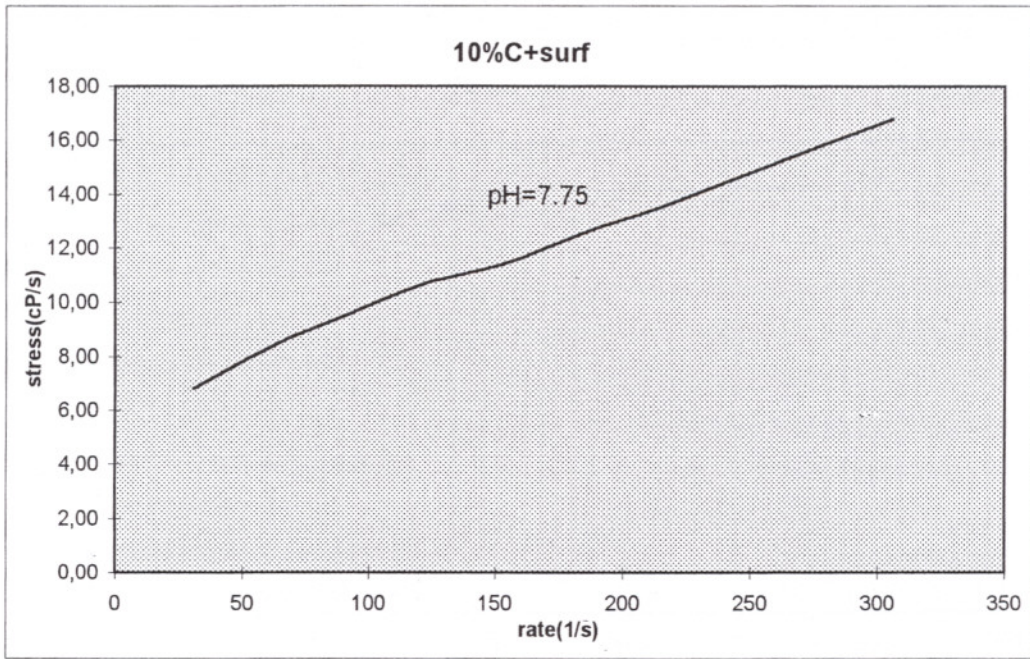
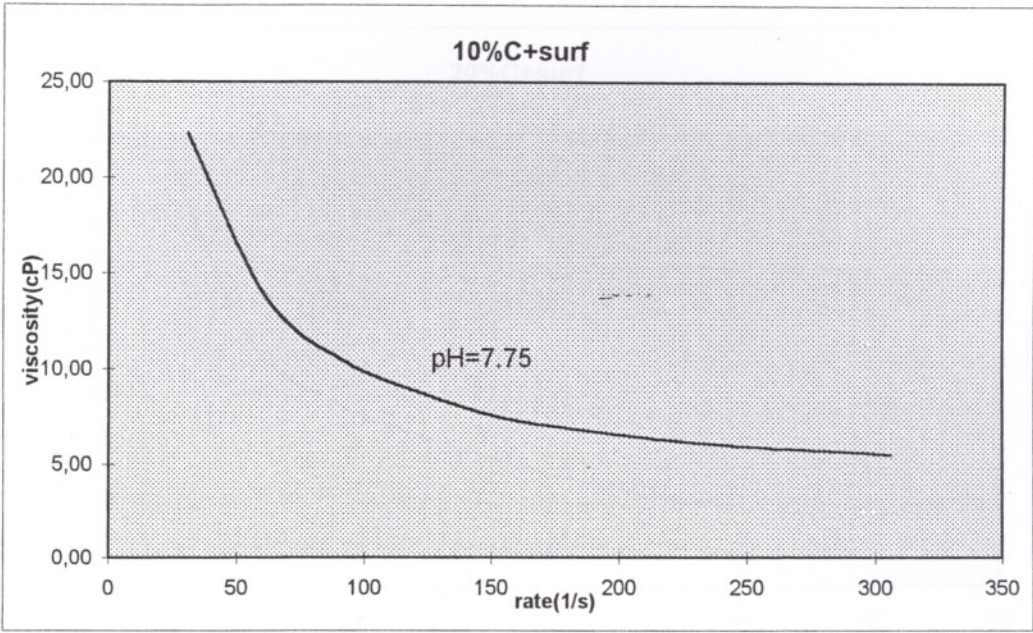


Figure 7.10 : Viscosity vs.rate and rate vs.stress graphs for powder C (10% solid) having surfactant

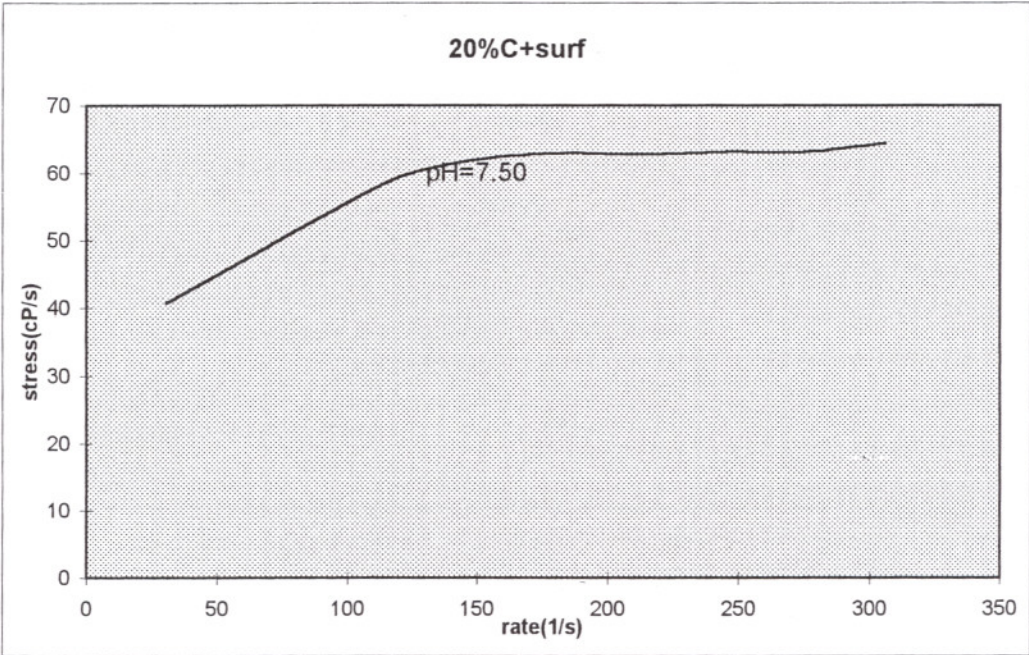
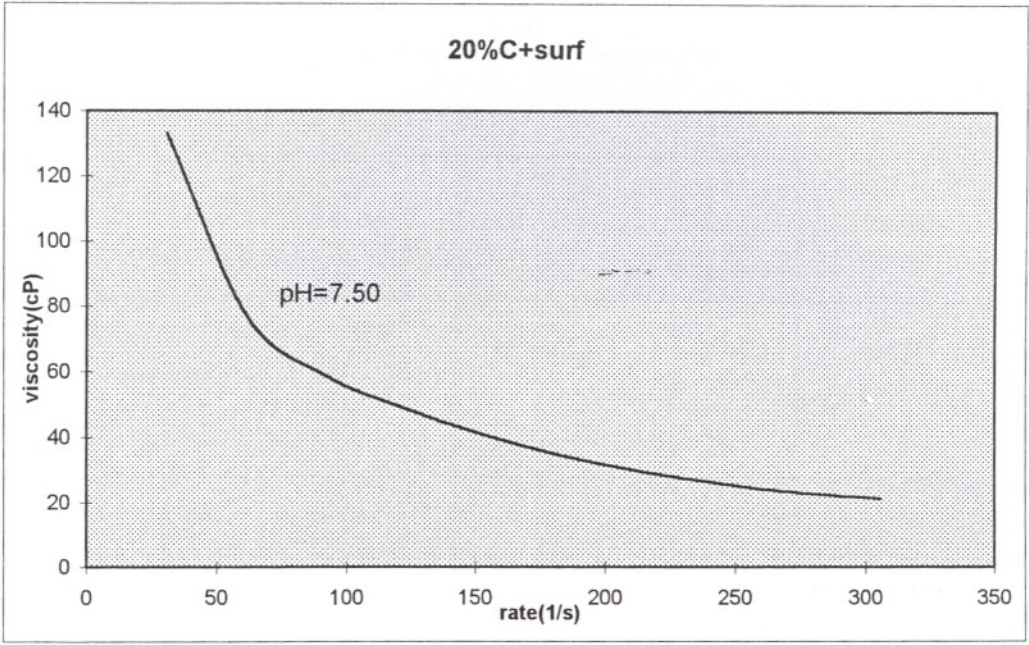


Figure 7.11 : Viscosity vs.rate and rate vs.stress graphs for powder C (20% solid) having surfactant

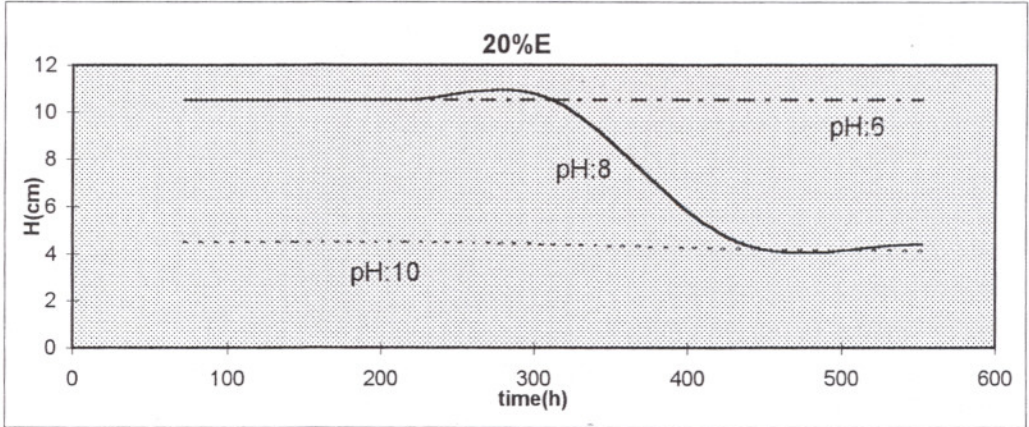
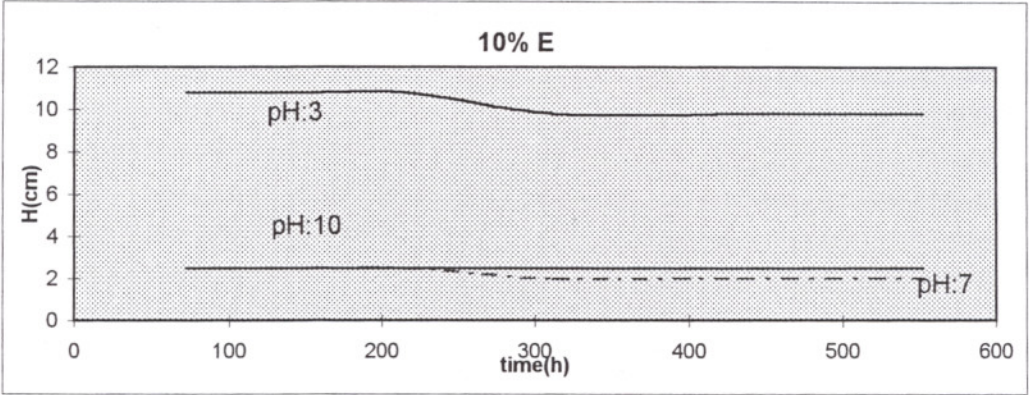
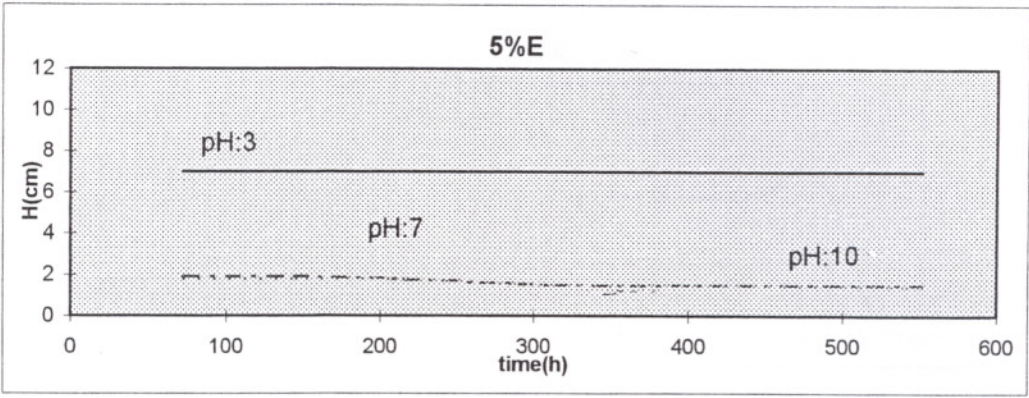


Figure 7.12 : H vs.t at 3 different pH for powder E without surfactant

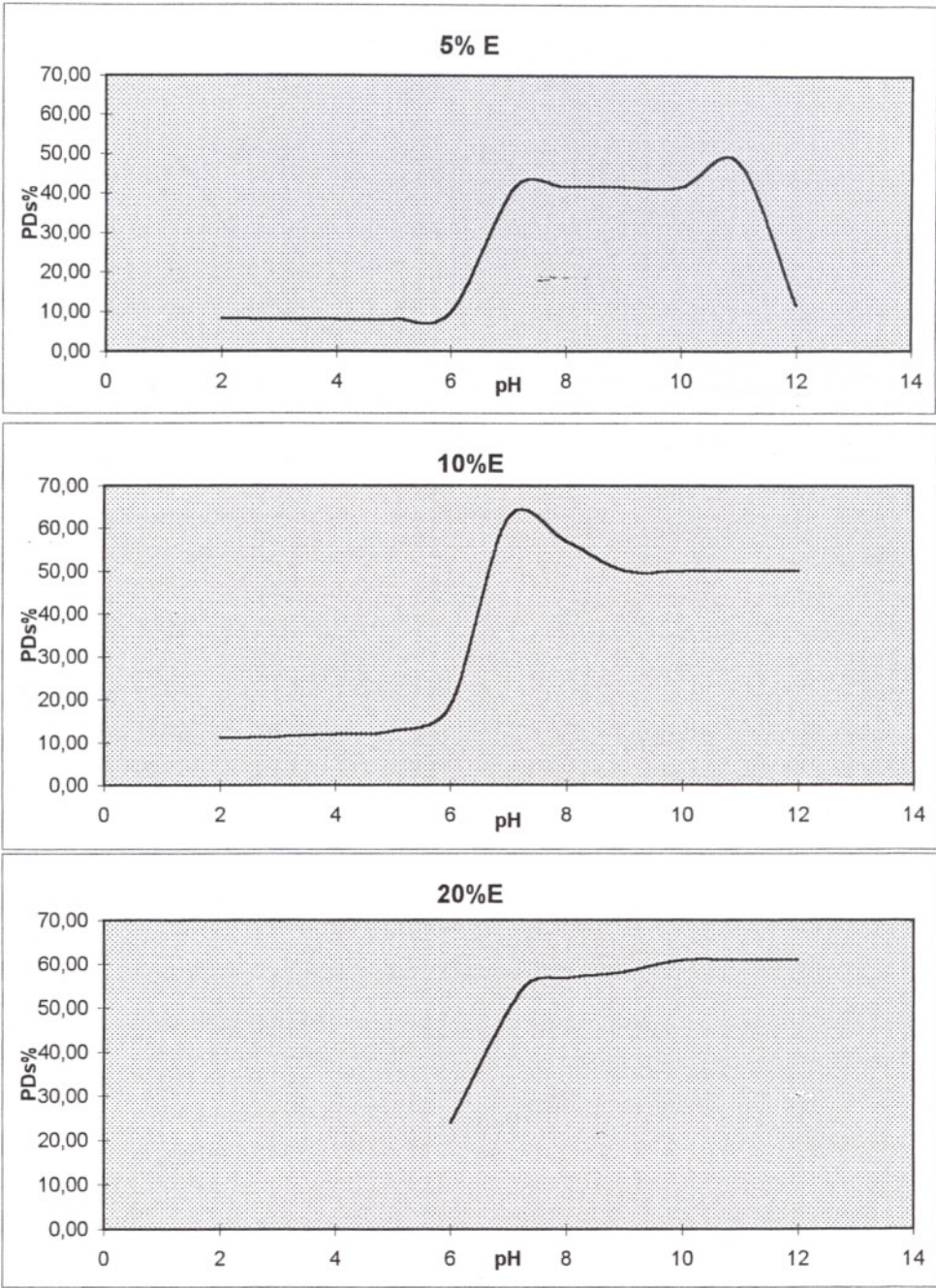


Figure 7.13 : PD% vs.pH at saturation time for powder E without surfactant

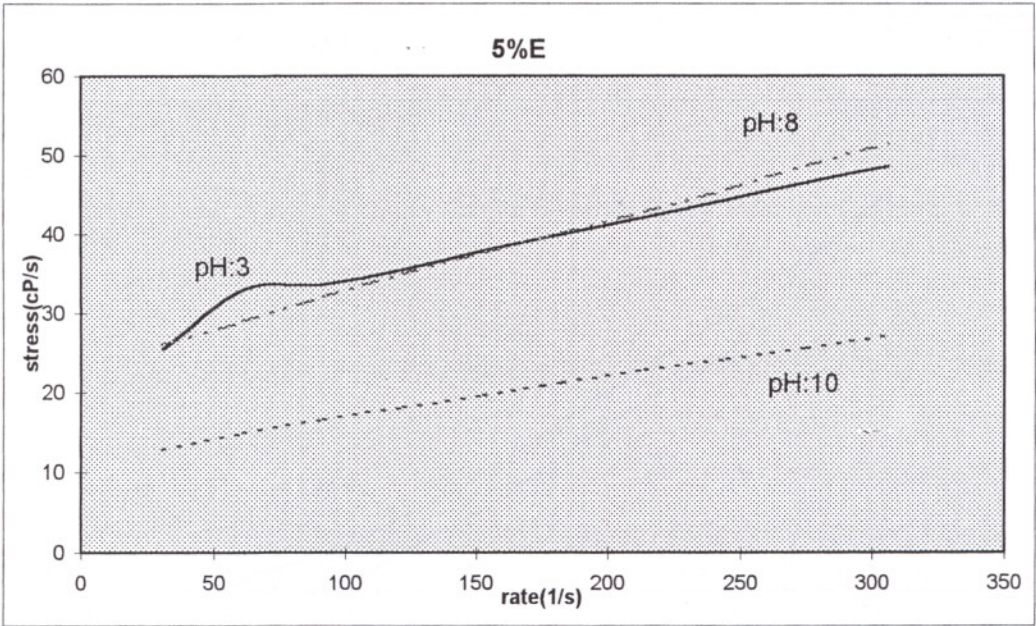
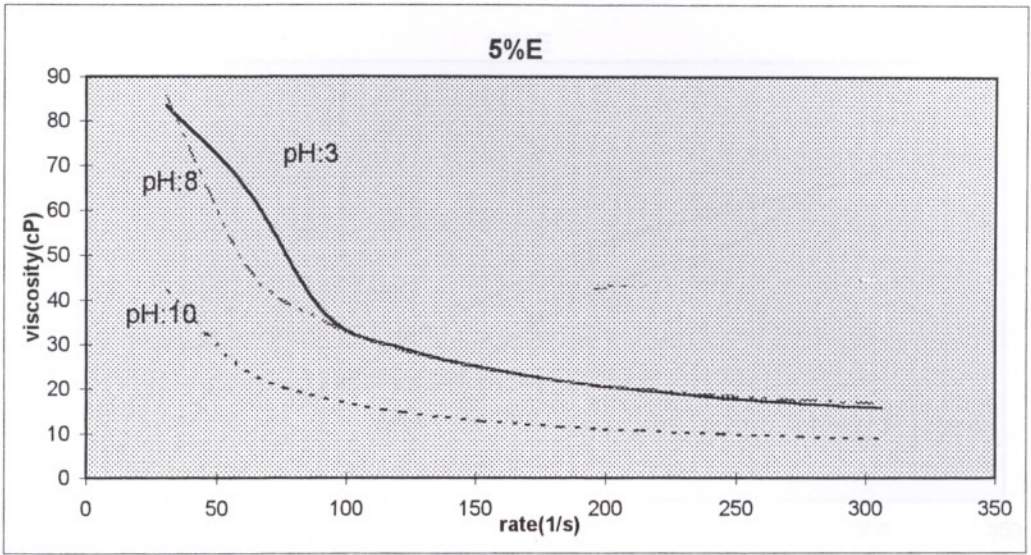


Figure 7.14 : Viscosity vs.rate and rate vs.stress graphs for powder E having 5% solid

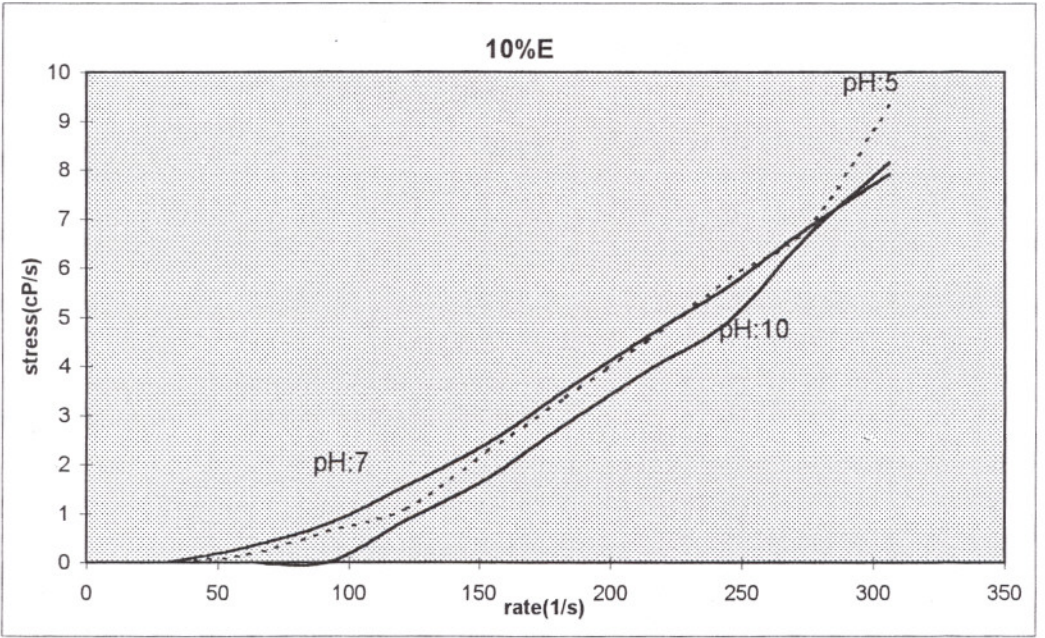
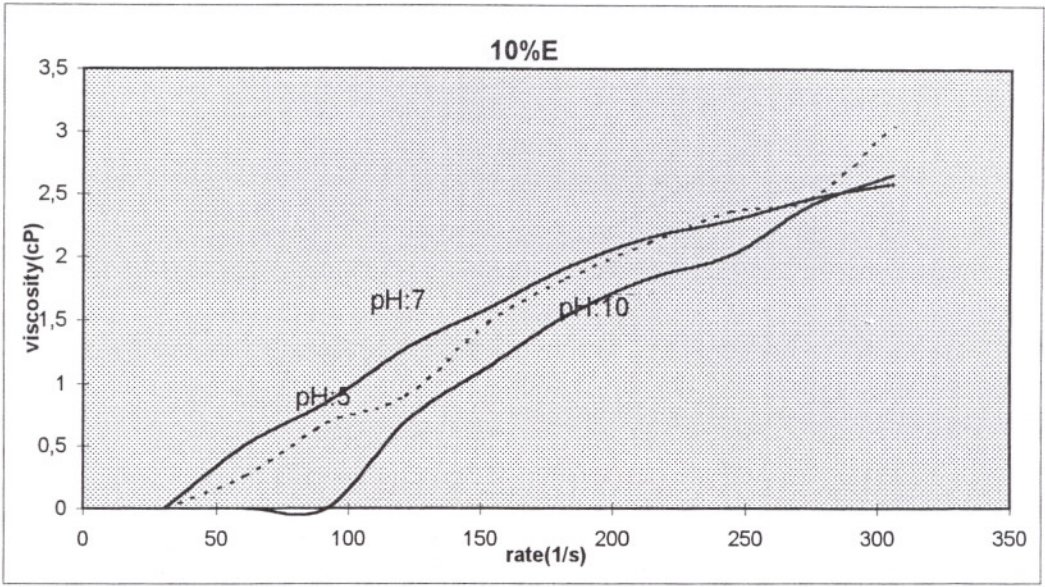


Figure 7.15 : Viscosity vs.rate and rate vs.stress graphs for powder E having 10% solid

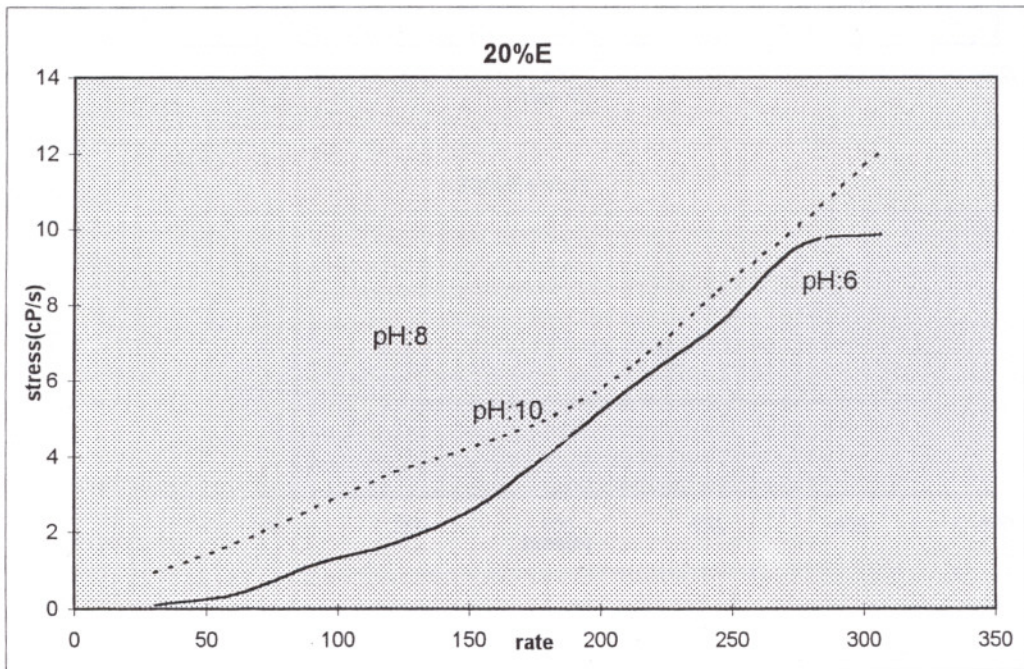
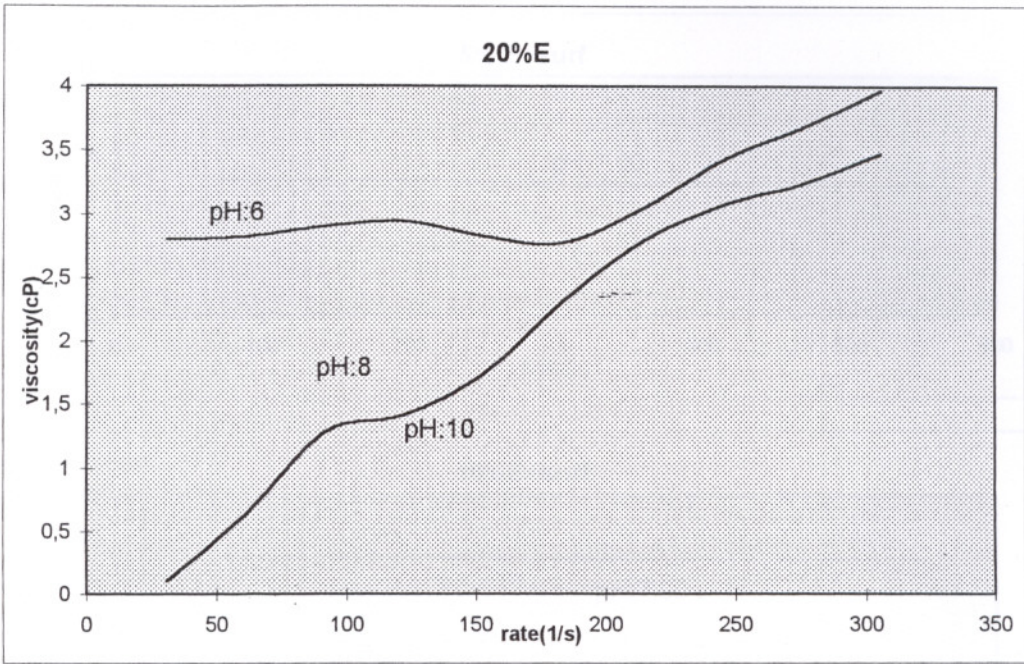


Figure 7.16 : Viscosity vs.rate and rate vs.stress graphs for powder E having 20% solid

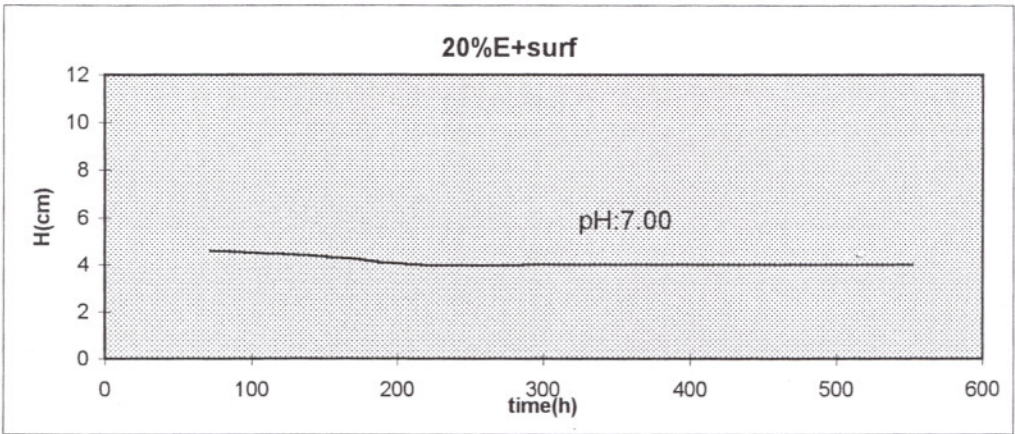
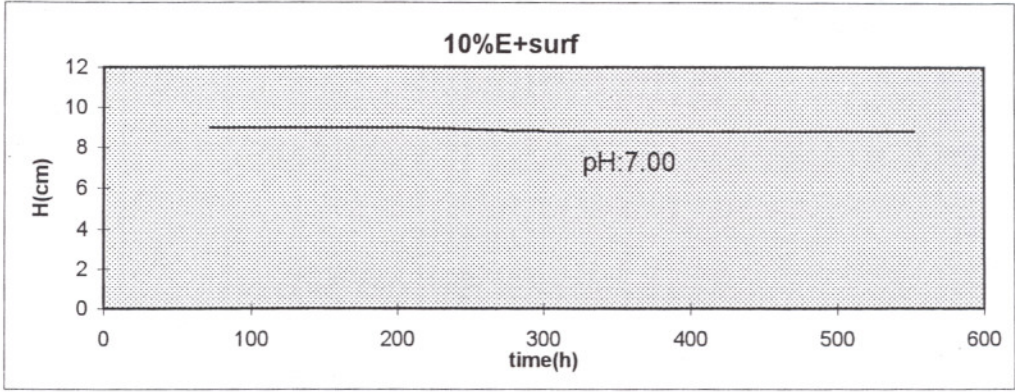
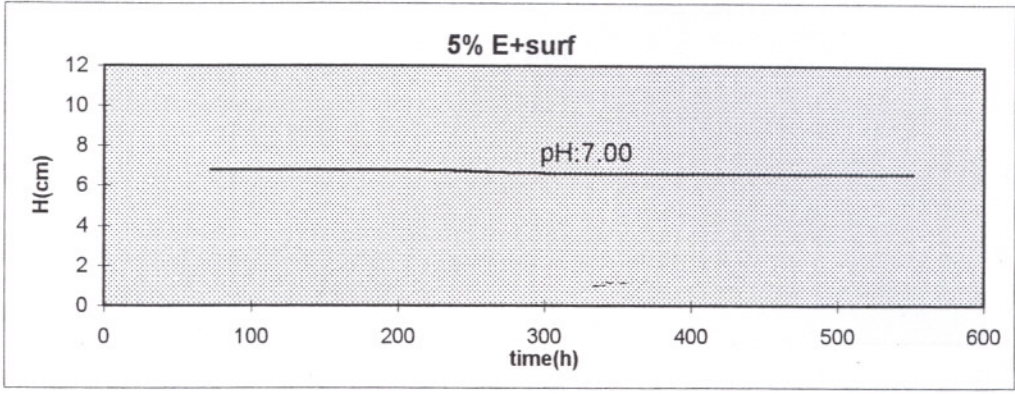


Figure 7.17 : The trend of H vs.t for titania powder E having surfactant

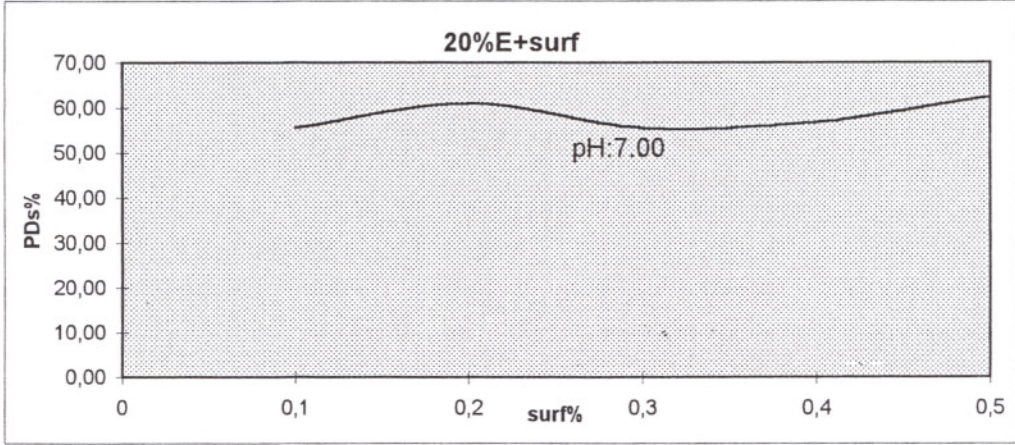
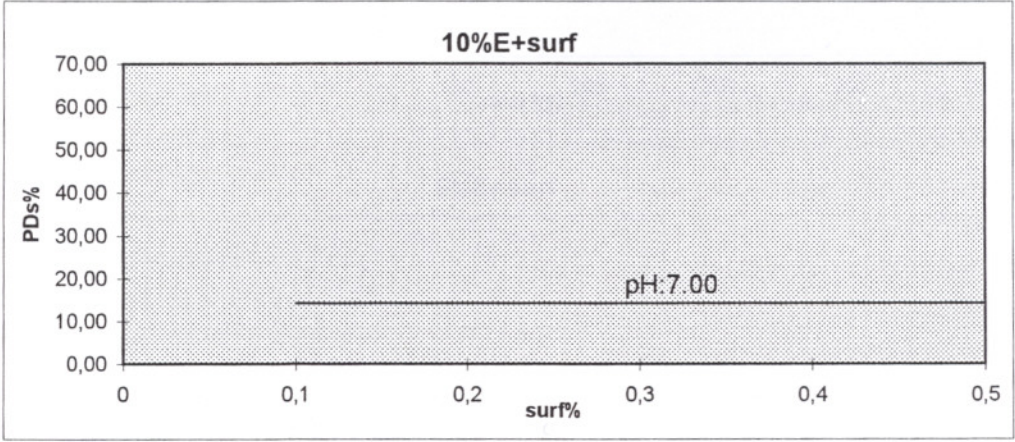
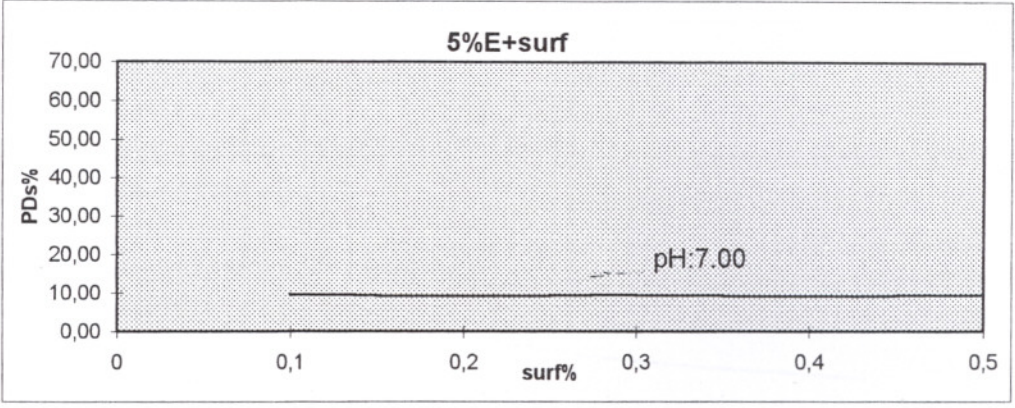


Figure 7.18 : PD% vs.surf% for powder E at saturation time

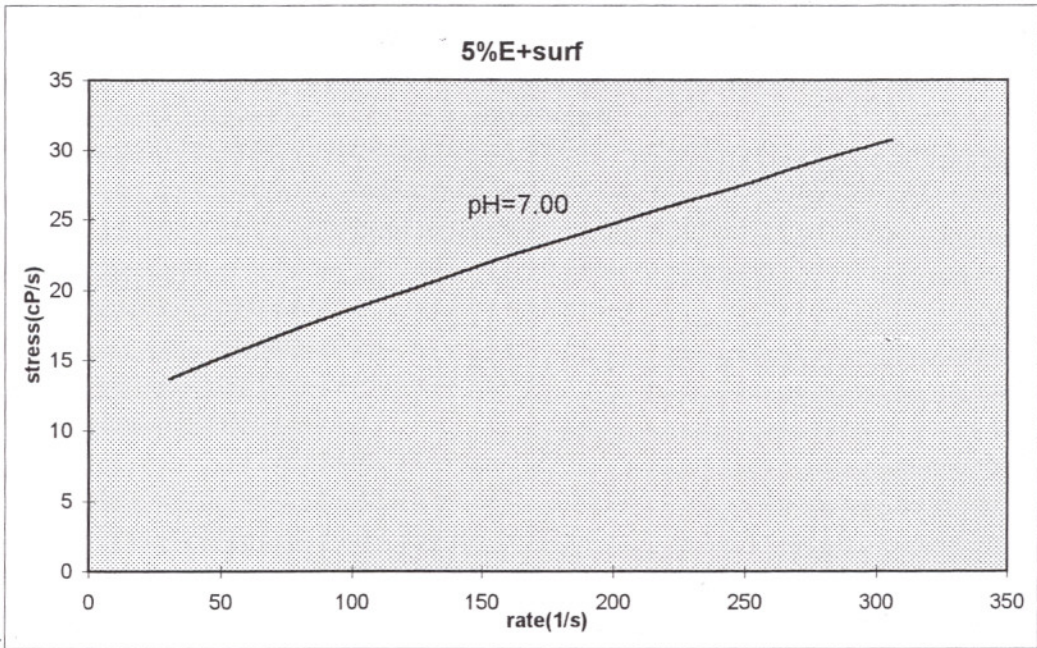
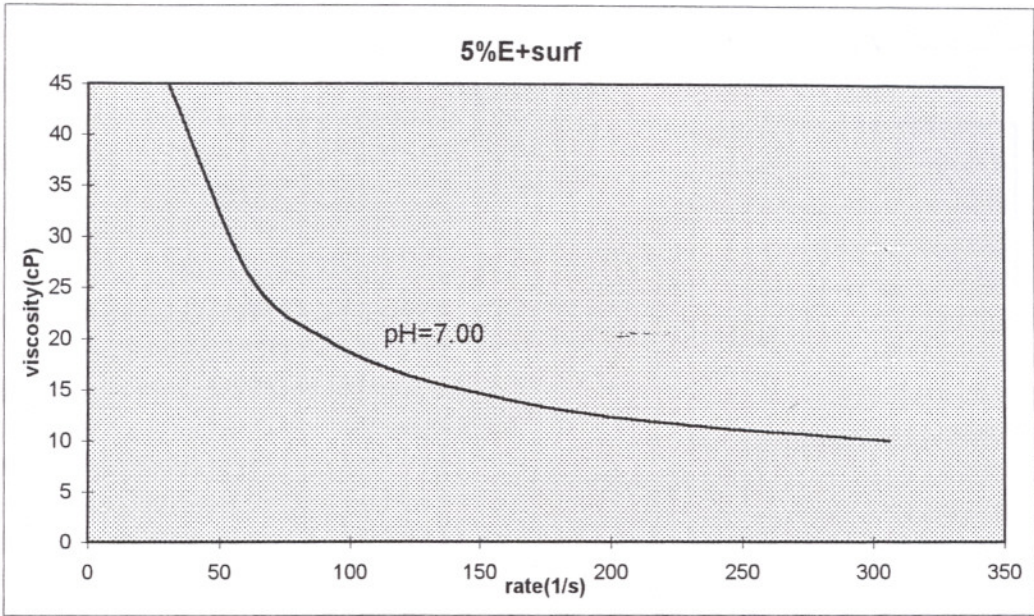


Figure 7.19 : Viscosity vs.rate and rate vs.stress graphs for Powder E having surfactant

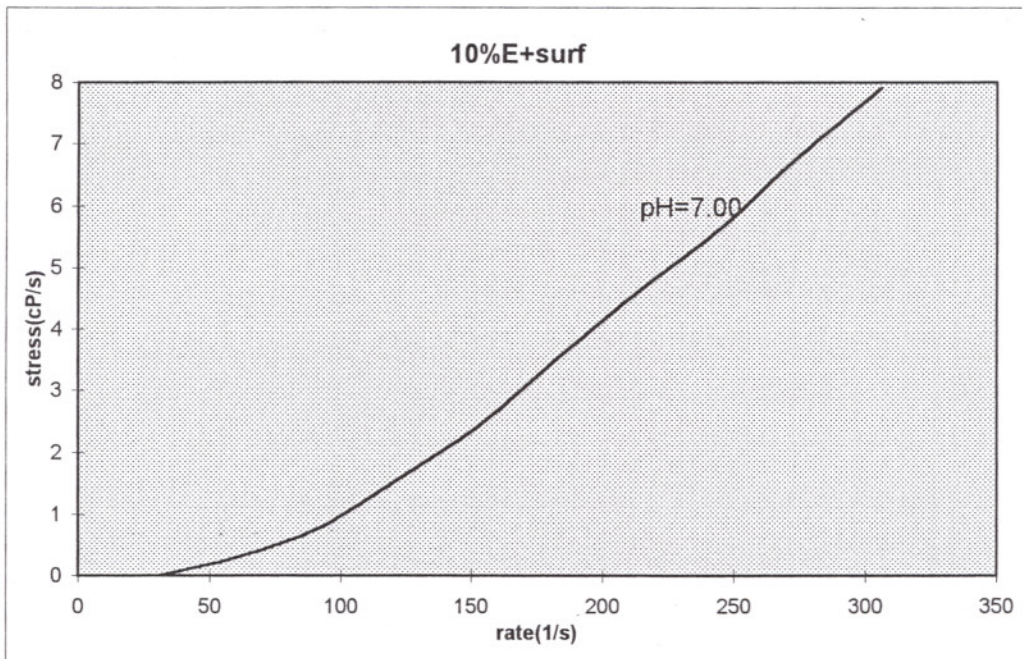
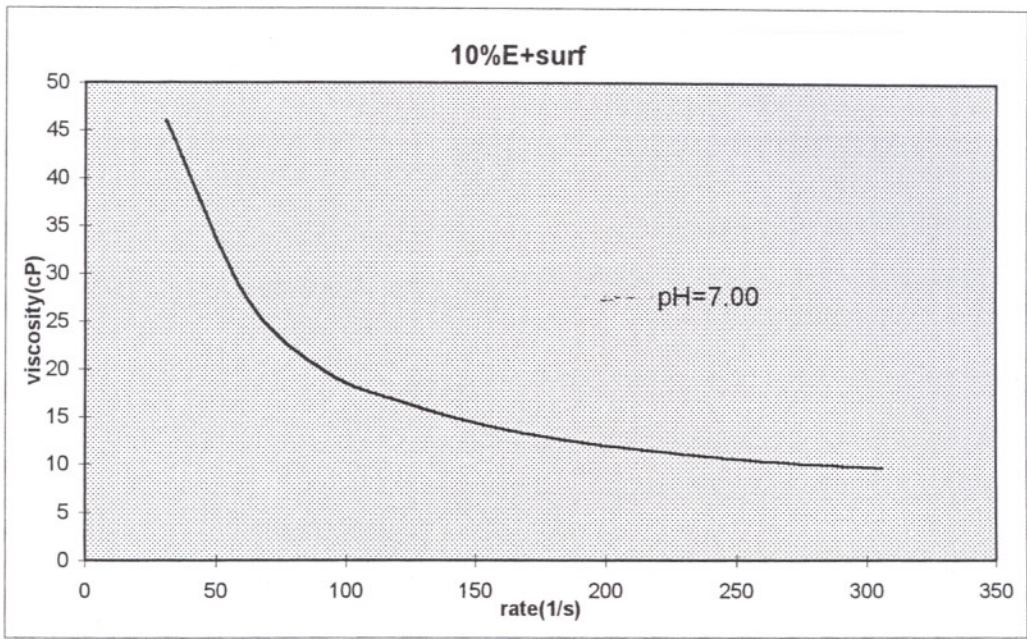


Figure 7.20 : Viscosity vs.rate and rate vs.stress graphs for powder E (10% solid) having surfactant

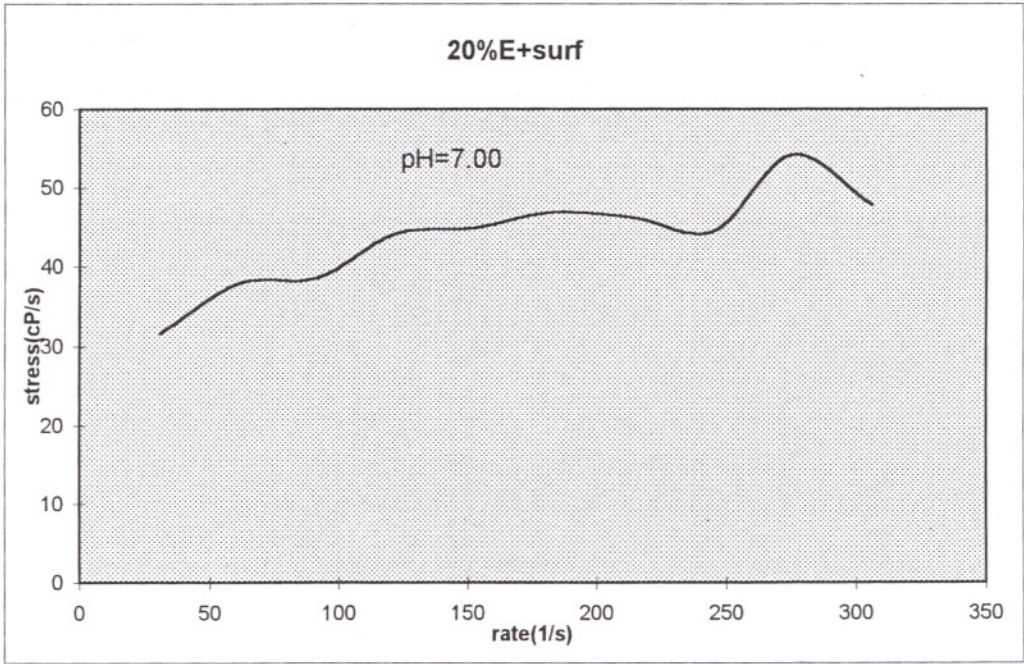
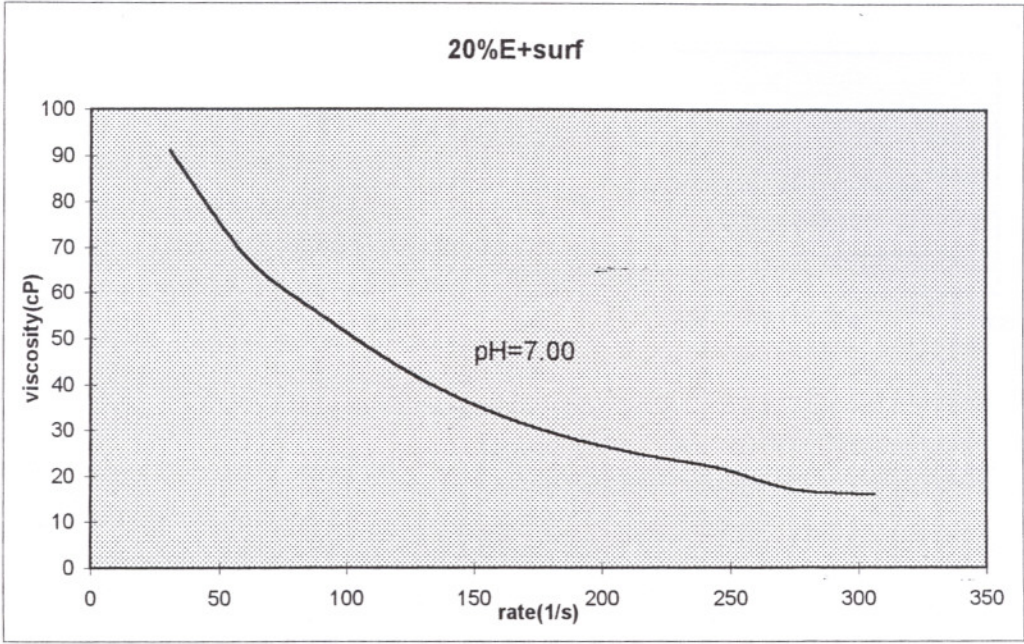


Figure 7.21 : Viscosity vs.rate and rate vs.stress graphs for powder E (20% solid) having surfactant

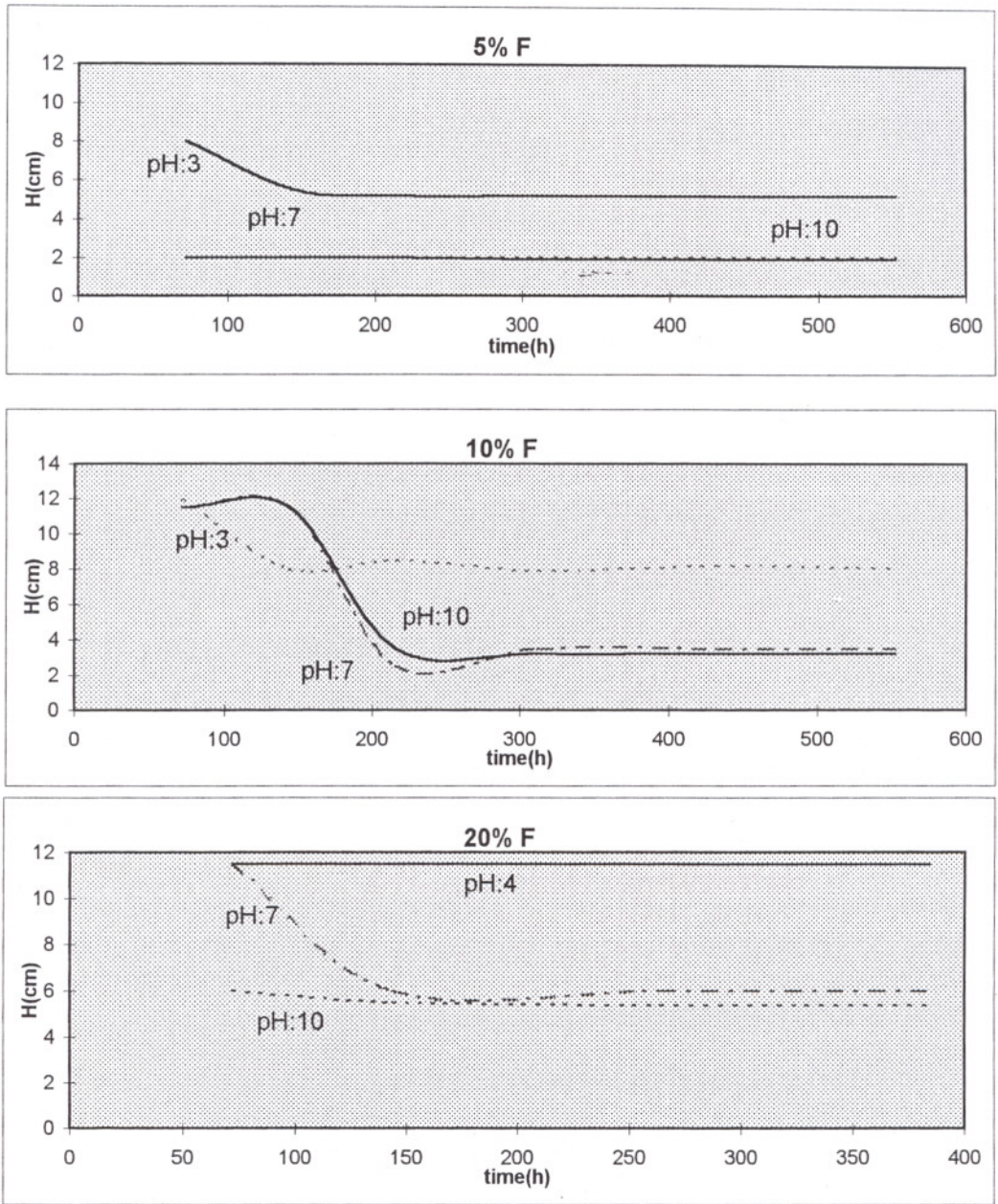


Figure 7.22 : H vs.t at 3 different pH for powder F without surfactant

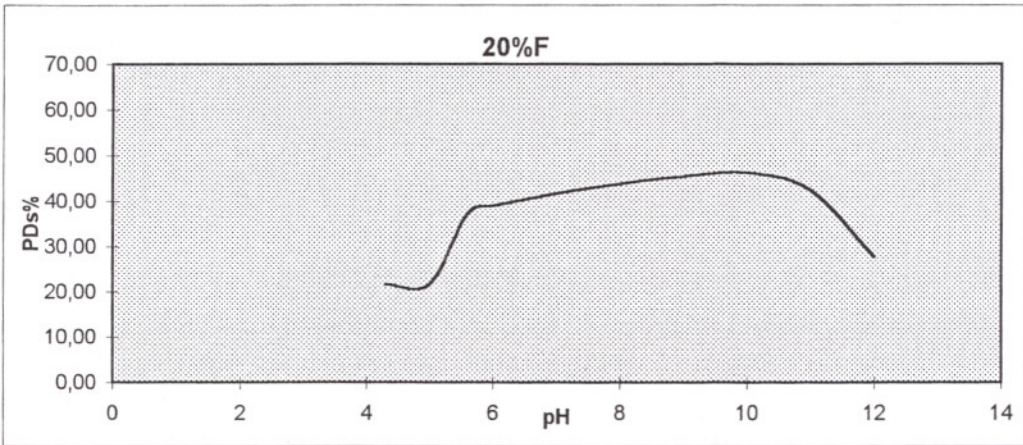
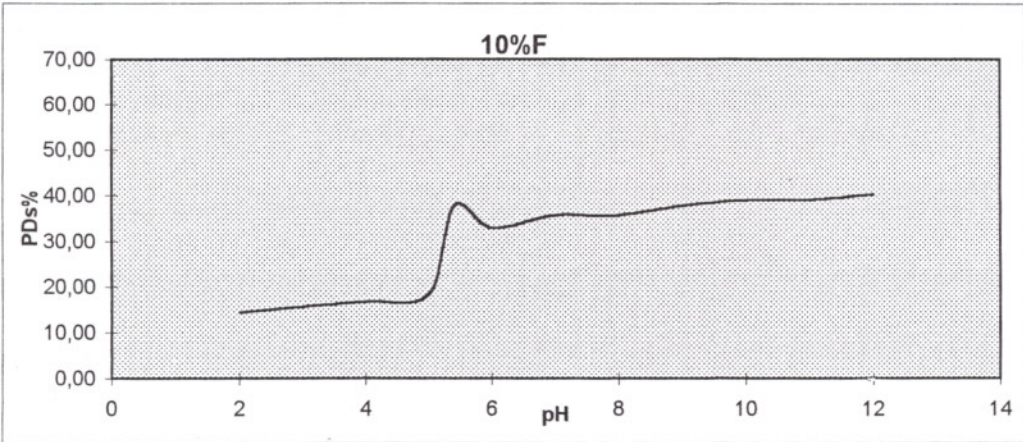
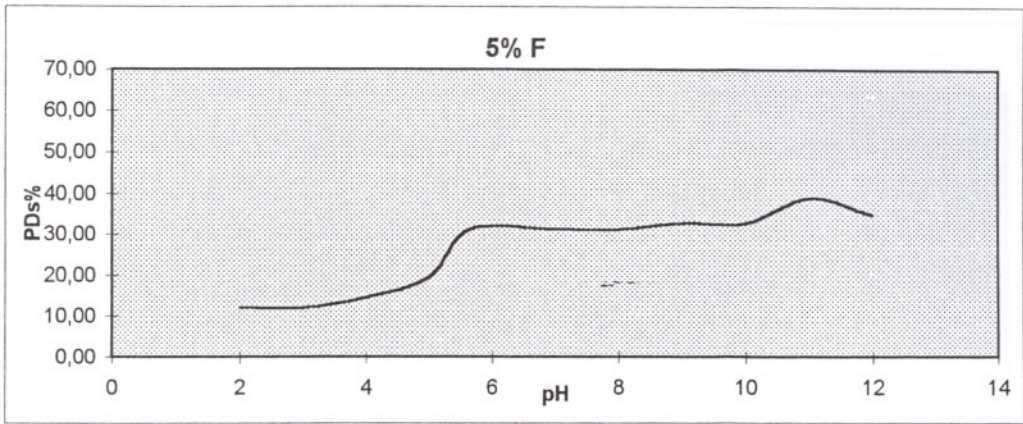


Figure 7.23 : PD% vs.pH at saturation time for powder F without surfactant

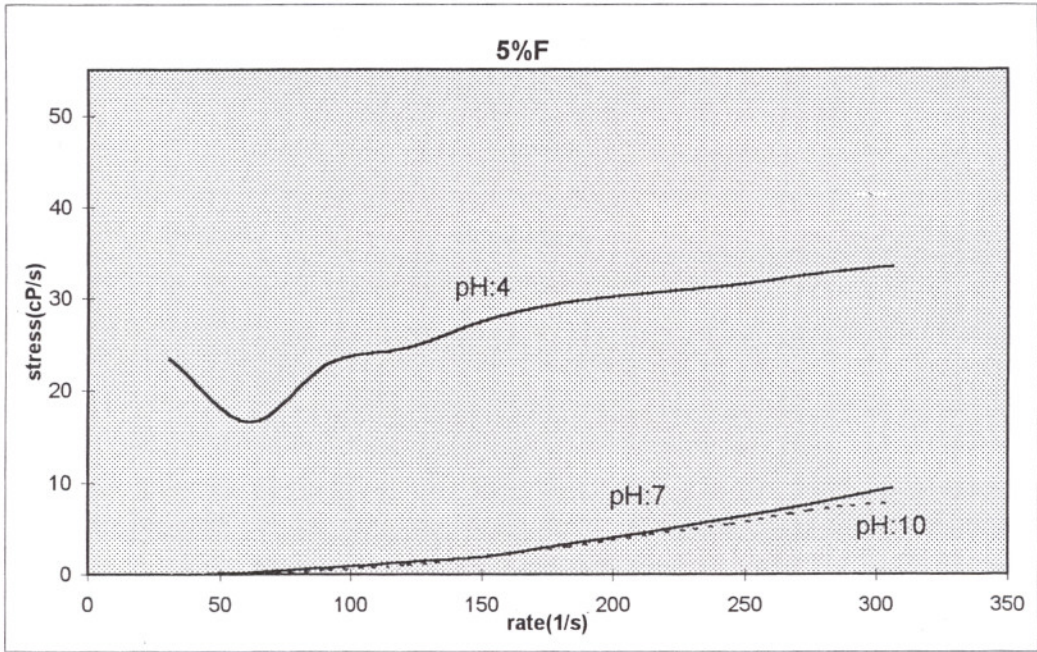
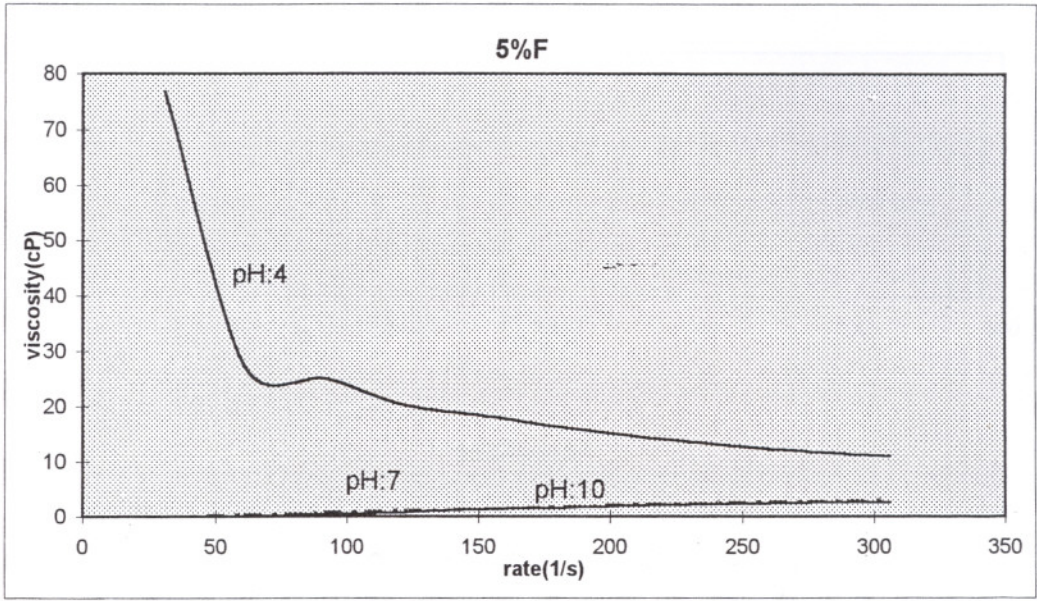


Figure 7.24 : Viscosity vs.rate and rate vs.stress graphs for powder F having 5% solid

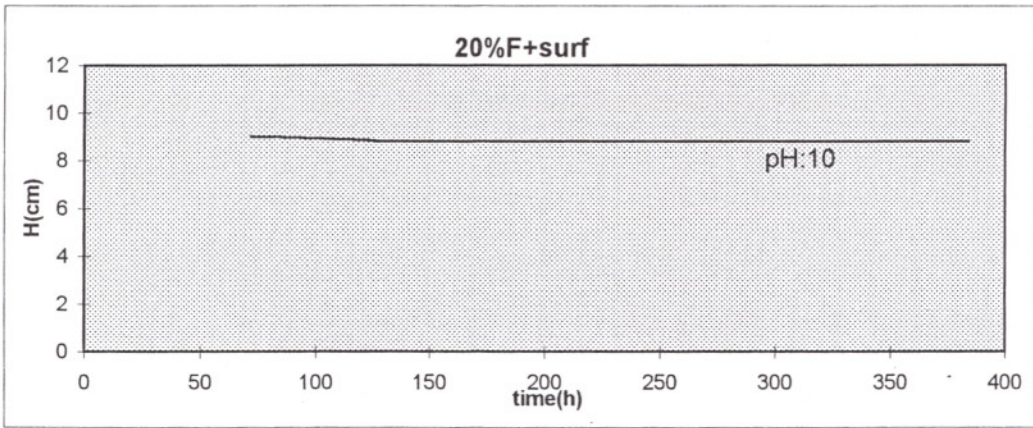
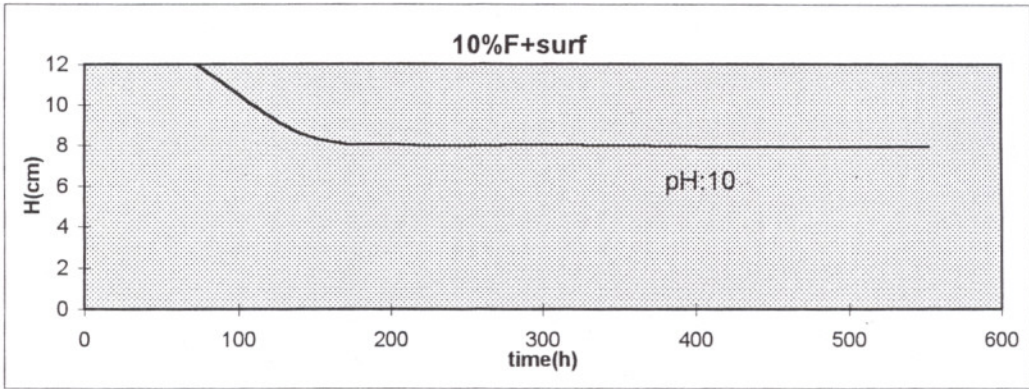
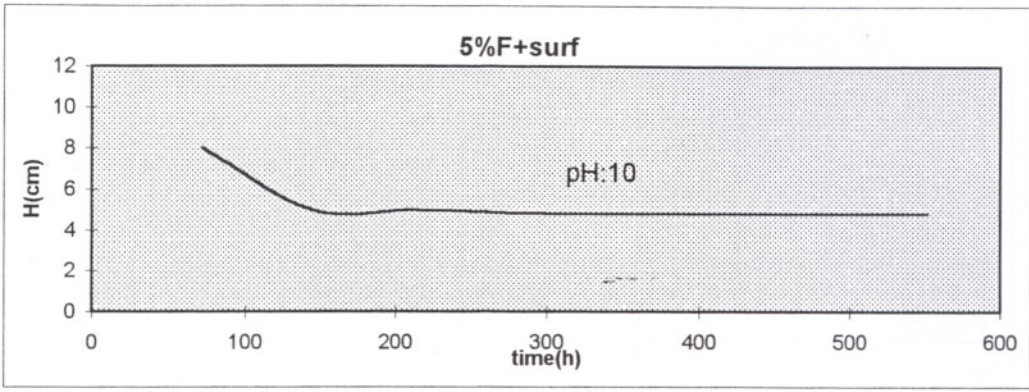


Figure 7.25 : The trend of H vs.t for titania powder F having surfactant

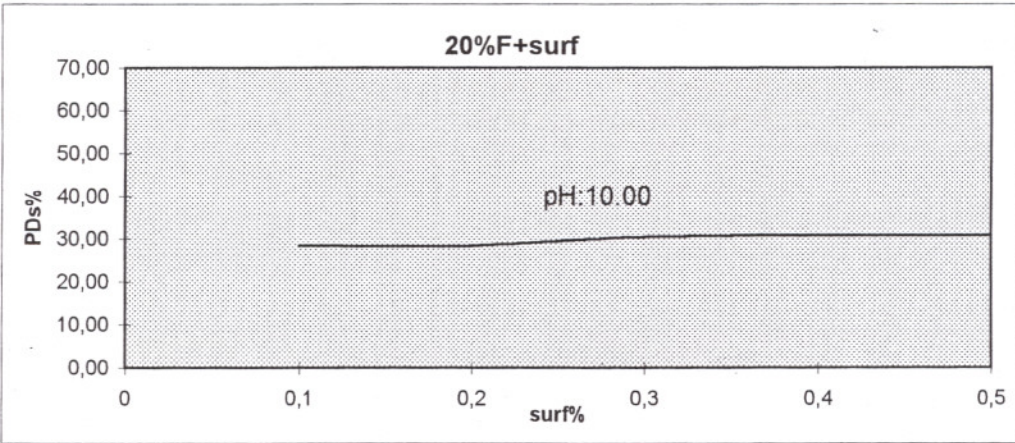
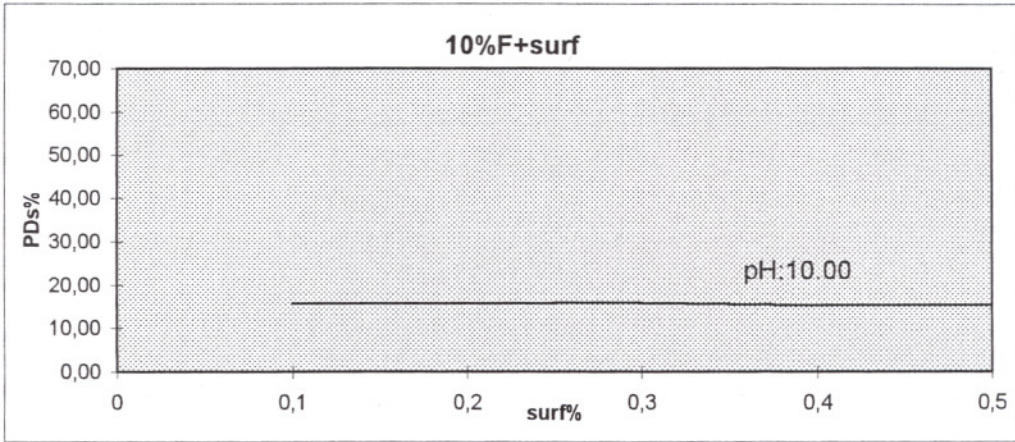
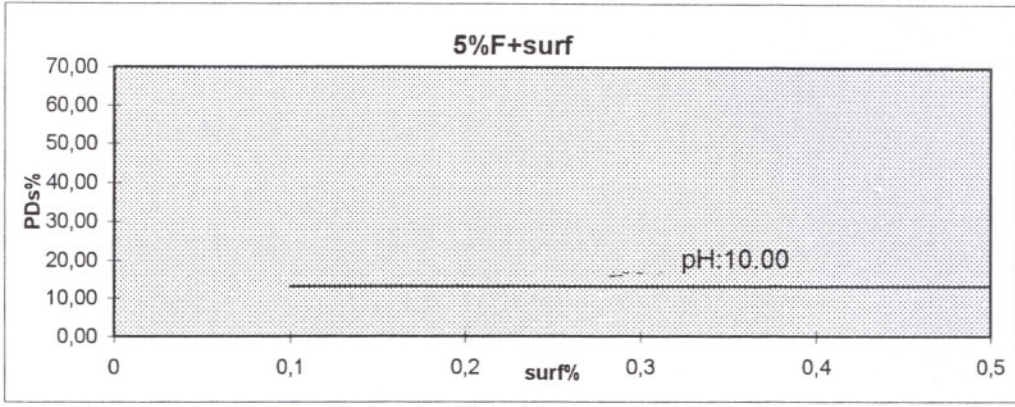


Figure 7.26 : PD% vs.surf% for powder F at saturation time

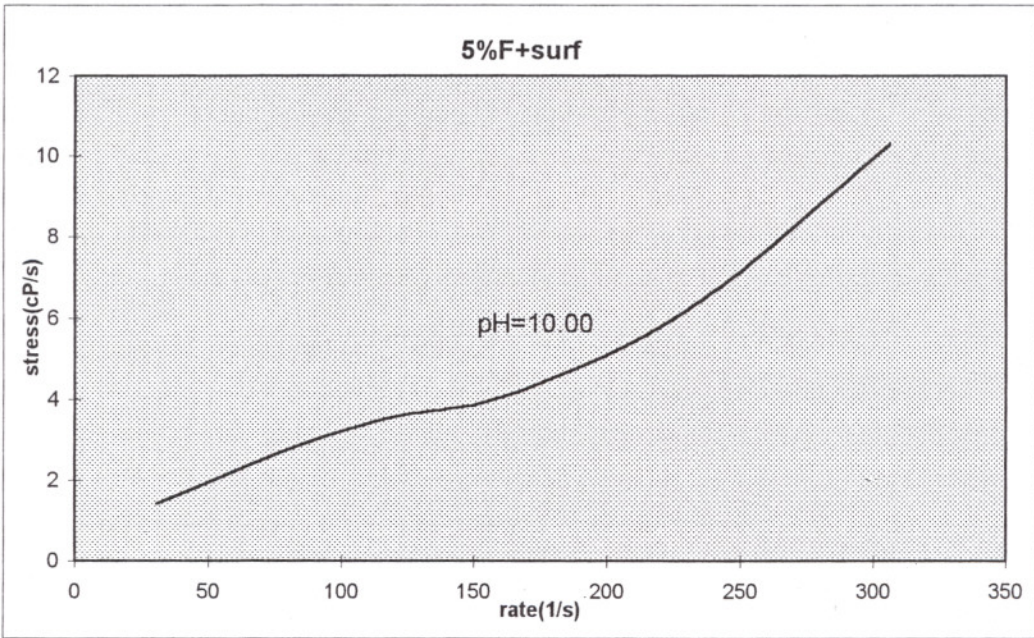
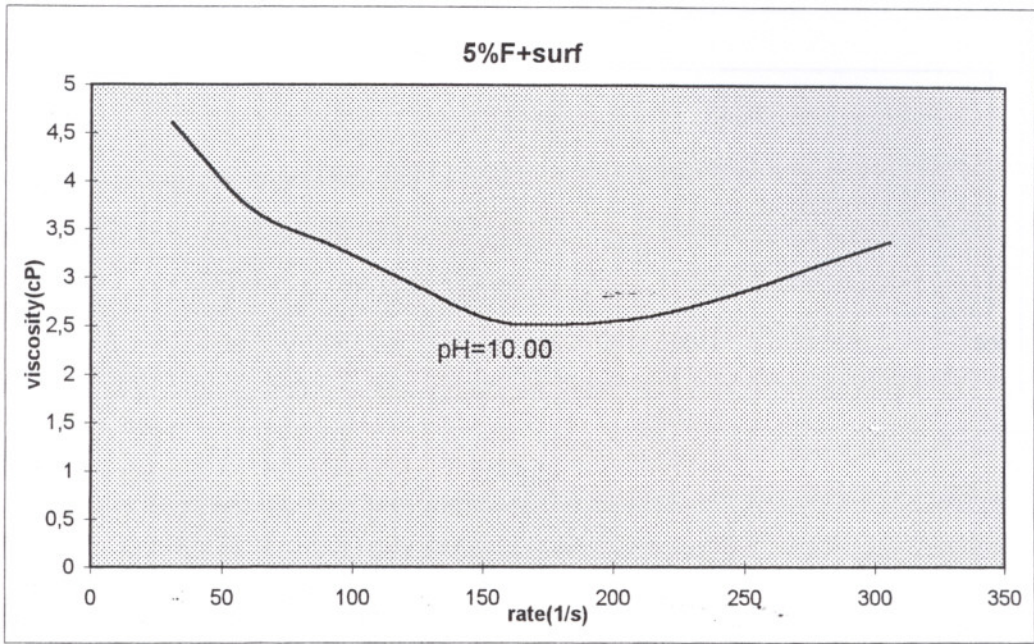


Figure 7.27: Viscosity vs.rate and rate vs.stress graphs for powder F (5%) having surfactant

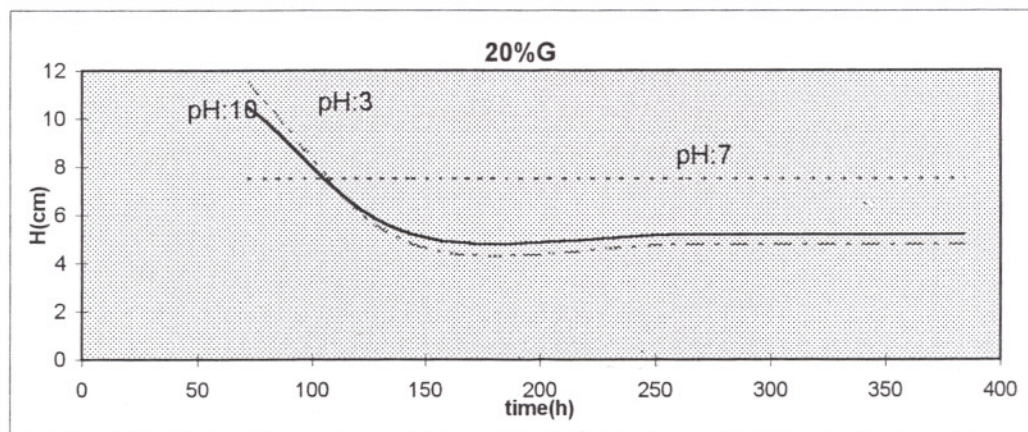
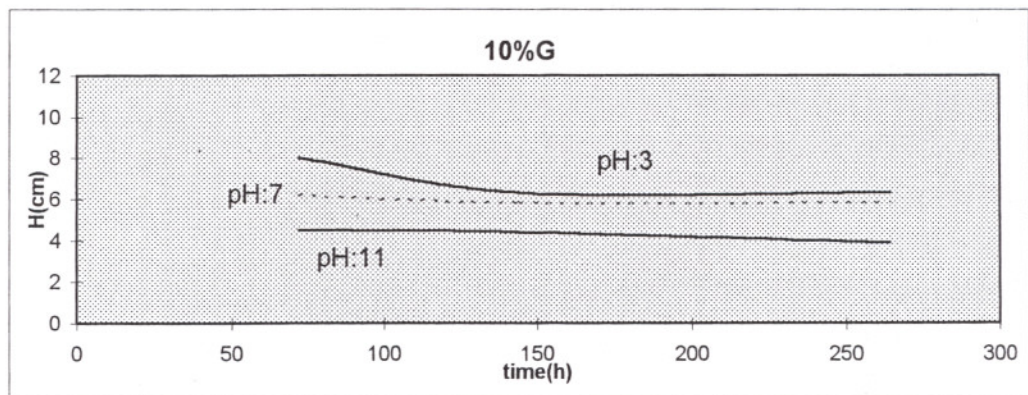
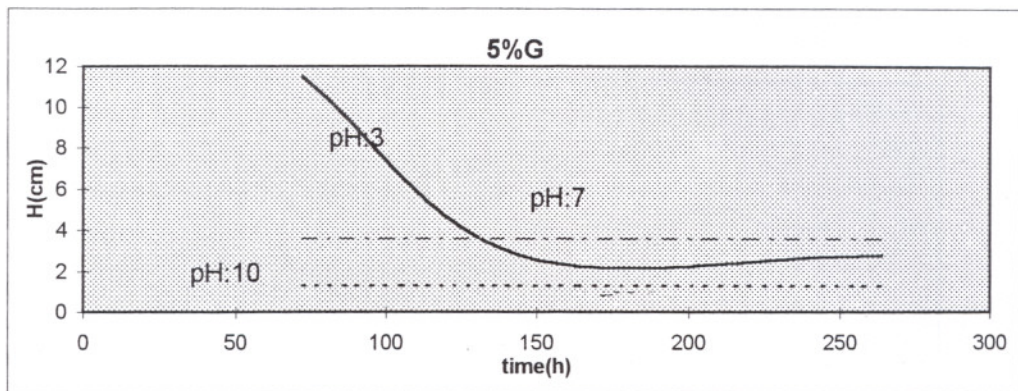


Figure 7.28 : H vs.t at 3 different pH for powder G without surfactant

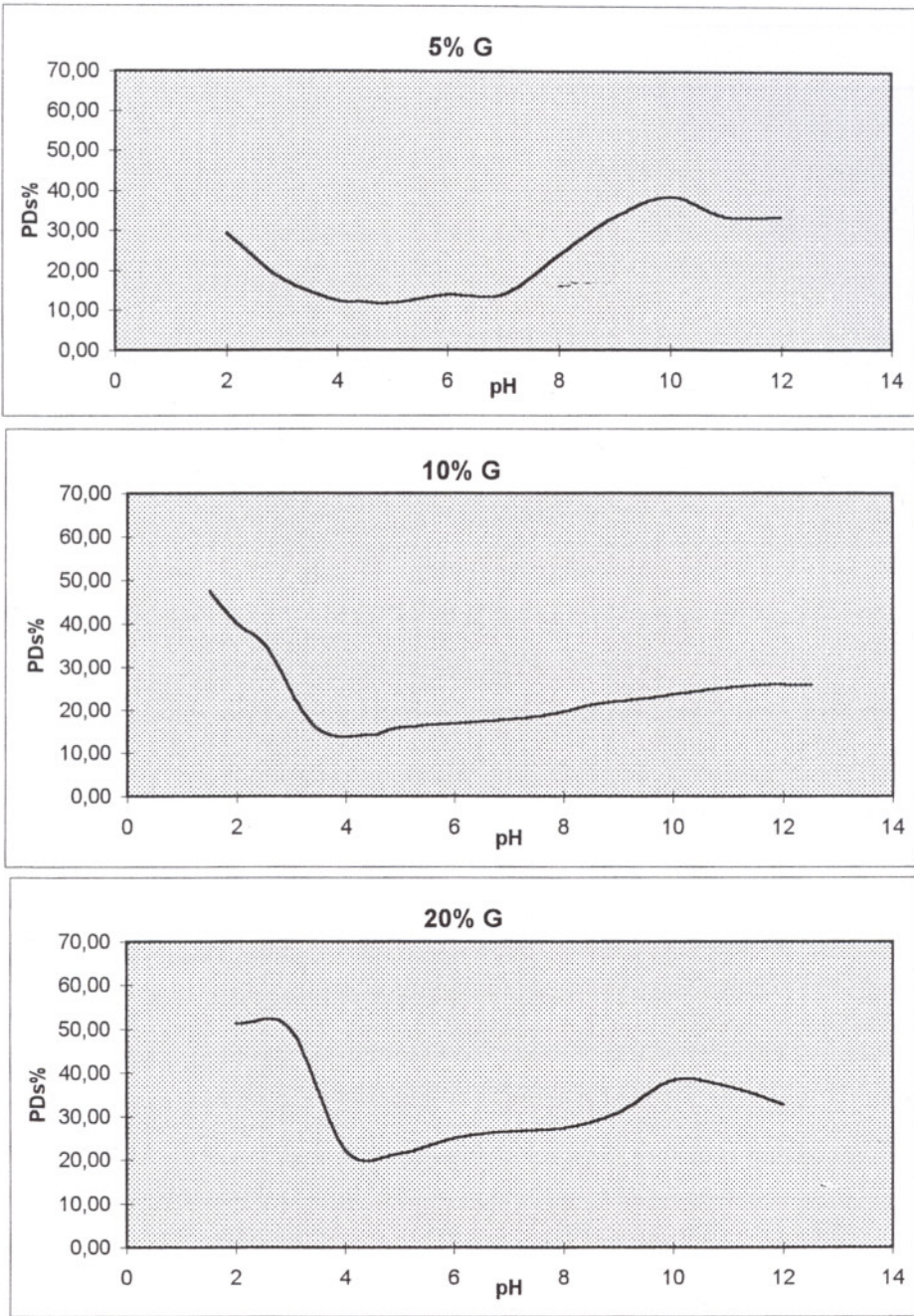


Figure 7.29 : PD% vs.pH at saturation time for powder G without surfactant

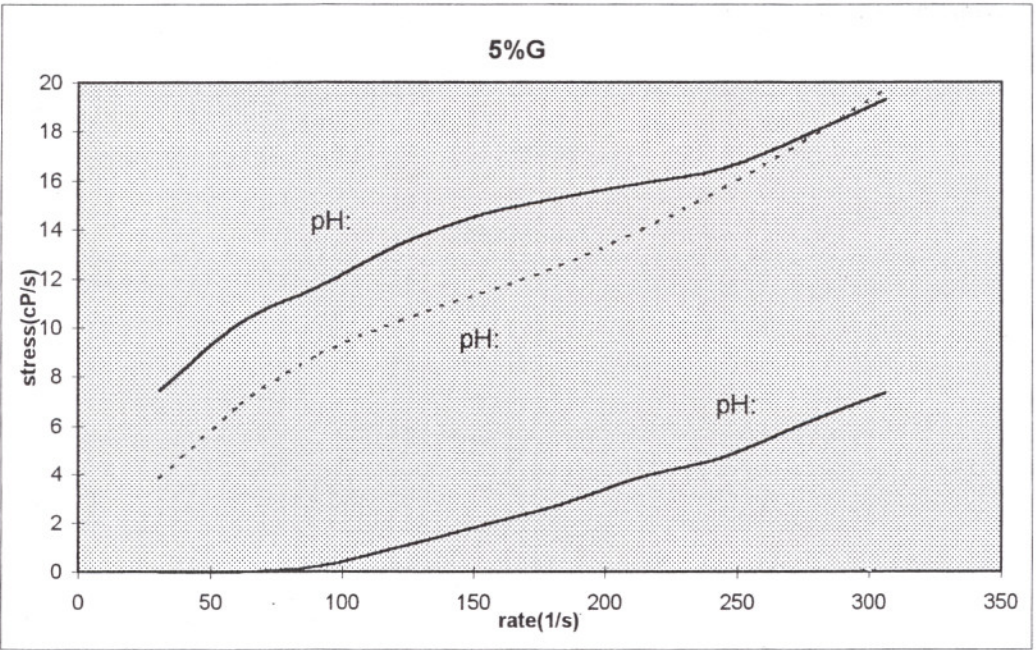
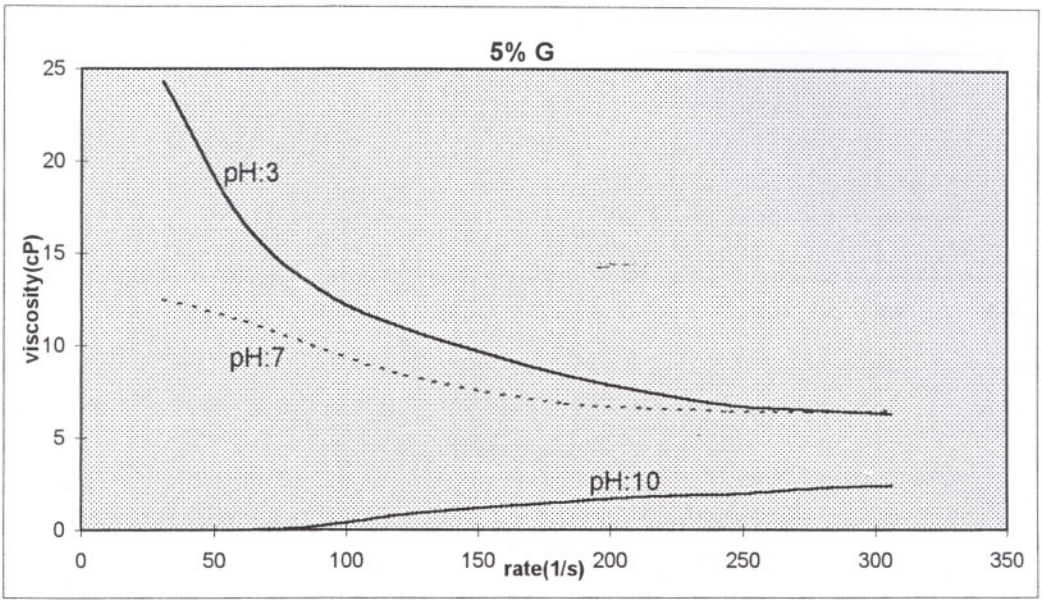


Figure 7.30 : Viscosity vs.rate and rate vs.stress graphs for powder G having 5% solid

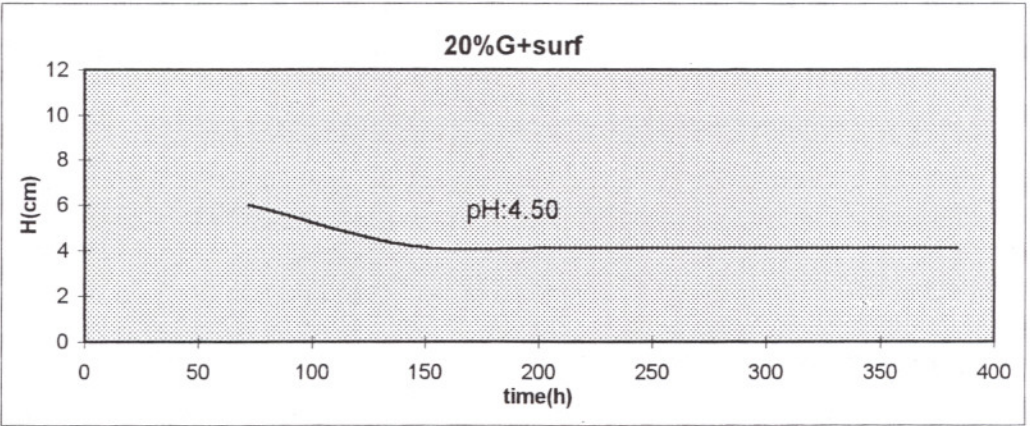
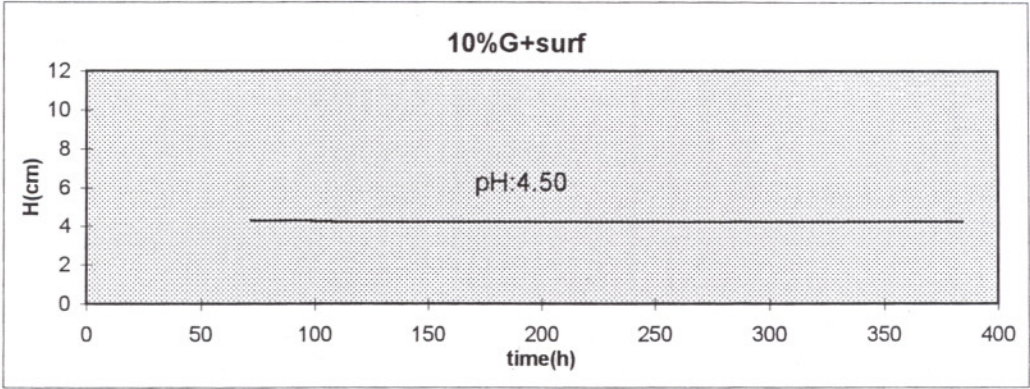
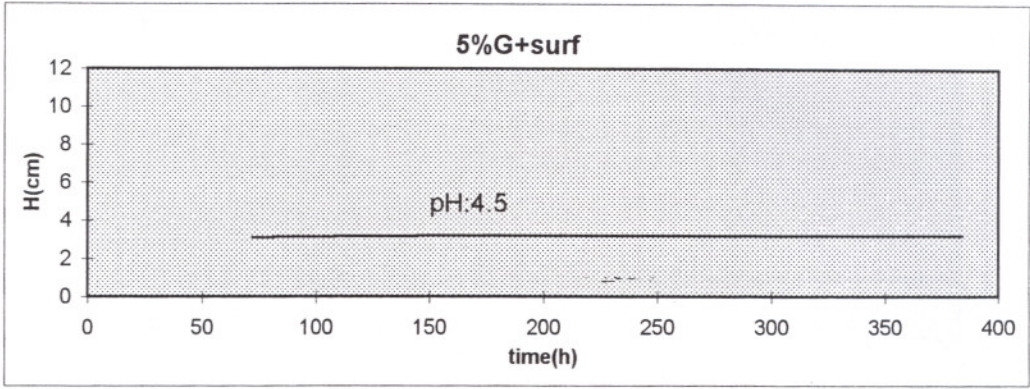


Figure 7.31 : The trend of H vs.t for titania powder G having surfactant

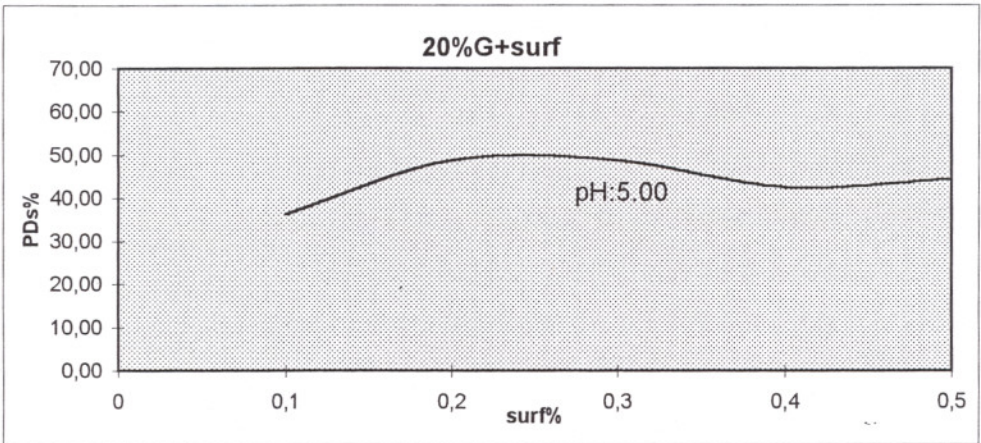
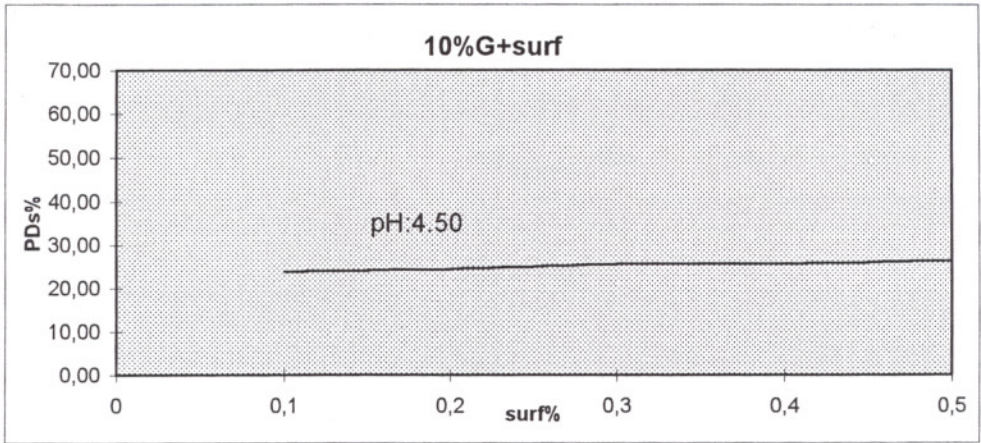
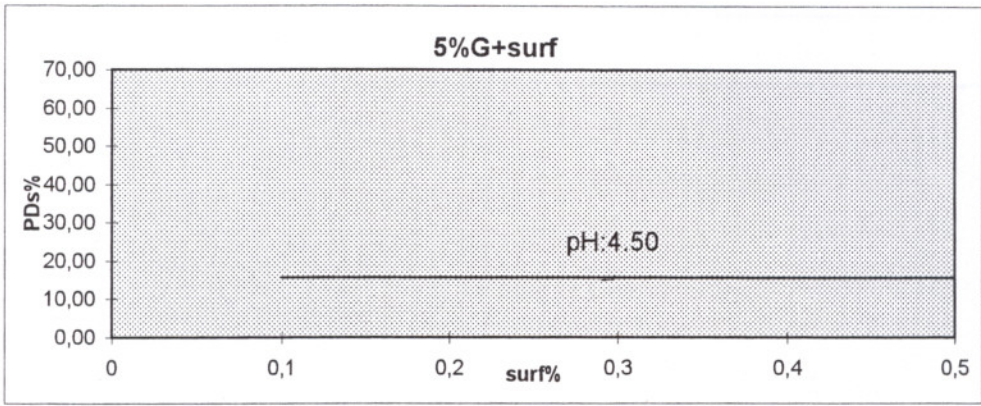


Figure 7.32 : PD% vs.surf% for powder G at saturation time

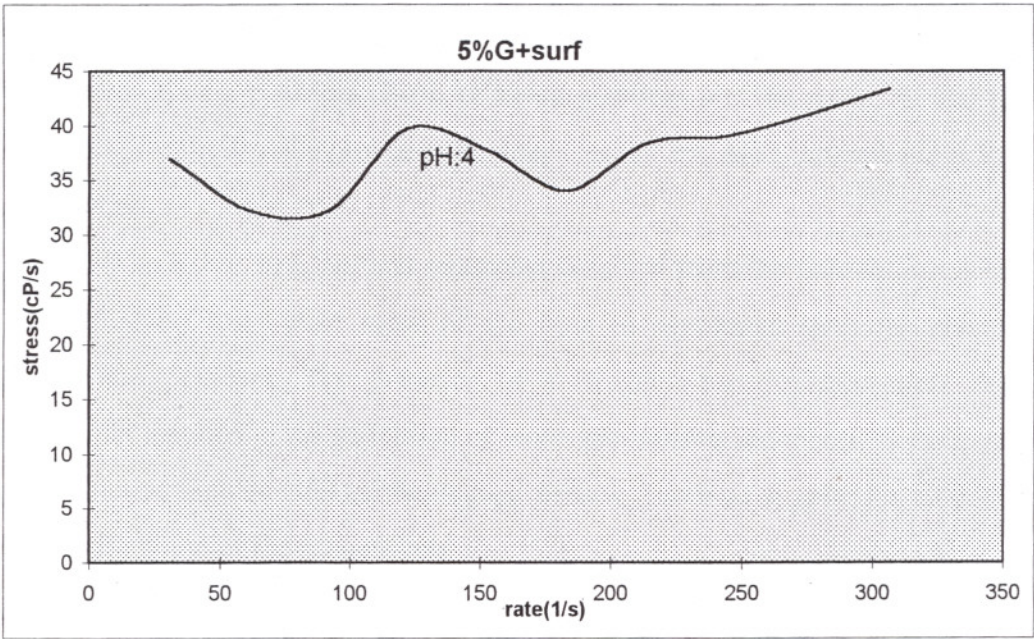
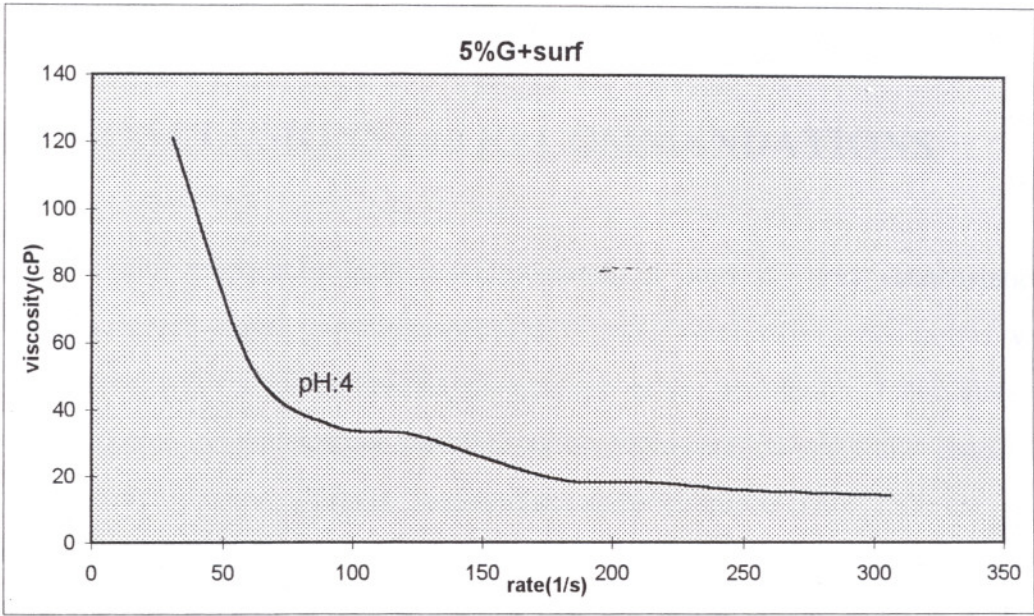


Figure 7.33 : Viscosity vs.rate and rate vs.stress graphs for powder G (5%) having surfactant

# CHAPTER VIII

## CONCLUSIONS and RECOMMENDATIONS

The preparation and characterization of sterically and electrostatically stabilized commercial titania powder suspensions in water were investigated in this work. The experimental work involved the deagglomeration of the powders by ball-milling and the characterization of the powder suspensions by sedimentation tests and rheological behaviour characterization. Titania suspensions were prepared with different solids contents (5,10 and 20 vol%) and the pH of these suspensions were kept in the 2-12 pH range. A commercial block copolymer at 0.1-0.5 wt% of  $\text{TiO}_2$  content was also added to investigate the affect of steric stabilization on stability and rheology. The suspensions were prepared by four titania powders. Both of these powders are the rutile, C and G; the others, E and F, are the anatase powders. Powder C is the 5%  $\text{Al}_2\text{O}_3$  coated and E,F,G are uncoated powders.

The PD% 's of the final sediments obtained from the final sediment heights in the sedimentation tests were most of the time in agreement with the rheological behaviour of the powders. The presence of a Bingham-pseudoplastic-shear thinning behaviour mostly resulted in the formation of loose low density sediments. Sediments with packing densities as high as 60% of rheological density (taken as 4 gr/cc for all powders) was observed for some of the suspensions.

These stable suspensions usually had three zones; sediment, falling zone and bluish supernatant zone. The dispersed suspensions mostly had a dilatant-shear thickening behaviour.

The formation of dense flocs with sizes bigger than 0.3  $\mu\text{m}$ . average  $\text{TiO}_2$  particle size was thought to be responsible from the discrepancies between the sedimentation and rheological analysis. In these suspensions the height of the sediment decreased to a low value a strongly (yielding high packing densities in the 40-60% range) but these suspensions showed shear thinning behaviour typical of flocculated systems.

These flocs may either form during the suspension preparation or may actually be present in the original powder which was not well dispersed during the ball-milling operation.

The results of this work showed that two commercial anatase or rutile powders may behave differently in water suspensions due to differences in particle size distribution or surface-coatings characteristics. This work also indicated that the parallel characterization of suspensions by both sedimentation and rheological characterizations may prove fruitful and contribute significantly to the understanding of powder suspensions.

The determination of the  $H$  vs.  $t$  behaviour in the 0 to 100 hours may yield valuable information on the nature of flocs forming in these suspensions which may not be evident in the rheological characterizations. The use of other surfactants and the combination of electrostatic-steric stabilization by pH fixation in surfactant containing water-based suspensions may yield valuable information.

## REFERENCES

1. Abend S., Bonnke N., Stabilization of emulsions by heterocoagulation of clay minerals and layered double hydroxides; *Journal of Colloid and Polymer Science*, 276,1998,pg.730-737.
2. Amberg R.D; TiO<sub>2</sub>-its importance, yesterday, today and tomorrow; *Polymers Paint Colour Journal* ; October 1985.
3. Bars N.L.,Levitz P.; Deagglomeration and dispersion of BaTiO<sub>3</sub> and Al<sub>2</sub>O<sub>3</sub> powders in an organic medium;*Journal of Colloid and Interface Science*,175,1995,pg.400-410.
4. Becher P.J; *Journal of Paint Technology*; vol.41,No:536,1969.
5. Bleir A.; Stability of ceramic suspensions; pg391-400.
6. Braun J.H.;TiO<sub>2</sub>'s contribution to the durability of paint films; Dupont Series.
7. Cesarano J., Aksay I.A.; Processing of highly concentrated aqueous  $\alpha$ - Al<sub>2</sub>O<sub>3</sub> suspensions stabilized polyelectrolytes;*Journal of American Ceramic Society*,71,1988,pg.1062-1067.
- 8.Everett D.H.;Basic Principles of Colloid Science,The Royal Society of Chemistry,1988,pg.1-5.
- 9.Faers M.A., Luckham P.F; Rheology of PEO-PPO block copolymer stabilized latices and emulsions; *Colloids and Surfaces*,86,1994,pg.317-327.
- 10.Gesenhues U.; Coprecipitation of hydrous Al<sub>2</sub>O<sub>3</sub> and SiO<sub>2</sub> with TiO<sub>2</sub> pigment as substrate; *Journal of Colloid and Interface Science* , 168,1994,pg.428-436.
- 11.Giordano P.F., Denoyel R; Interfacial aggregation of a non-ionic surfactant: Effect on the stability of SiO<sub>2</sub> suspensions; *Journal of Colloid and Interface Science* , 175,1995, pg.400-410.
- 12.Gregory J.; Flocculation and Filtration of colloidal particles; pg.59-69.
- 13.Heimenz.P.C.; Principles of Colloid and Surface Chemistry; 3<sup>rd</sup> Ed.; 1997; Marcel Dekker, Inc.
- 14.Hemar Y., Horne D.; Electrostatic interactions in adsorbed protein layers probed by a sedimentation technique; *Journal of Colloid and Interface Science* , 206,1998,pg.138-145.

15. Keh H.J., Liu Y.C.; Sedimentation velocity and potential in a dilute suspension of charged composite spheres; *Journal of Colloid and Interface Science*, 195, 1997, pg. 169-191.
16. Lee J.W, Lee H.M, Park O.O; Rheology and dynamics of water-in-oil emulsions under steady and dynamic shear flow; *Journal of Colloid and Interface Science*, 185, 1997, pg. 297-305.
17. Lyklema J.; The colloidal background of agglomeration; pg. 23-35
18. Martin M.; Sedimentation equilibrium of suspensions of colloidal particles at finite concentrations; *Journal of Colloid and Polymer Science*, 272, 1994, pg. 1582-1589.
19. Myers D.; Surfaces, interfaces and colloids, Principles and Applications, VCH, 1991
20. Napper D.H.; Steric Stabilization; *Journal of Colloid and Interface Science*, 58, 1977, pg. 390-406.
21. NL Industries; *Rheology*; pg. 3-9.
22. Novich B., Pyatt D.H.; Consolidation behaviour of high performance ceramic suspensions; *Journal of American Ceramic Society*, 73, 207-212, 1990
23. Ohshima H.; Sedimentation potential in a concentrated suspension of spherical colloidal particles; *Journal of Colloid and Interface Science*, 208, 1998, pg. 295-301.
24. Overbeek J.; How colloid stability affects the behaviour of suspensions; pg. 25-41.
25. Parfitt G.D; Science and technology of pigment dispersion; Congress on 28-31 May, 1985 in Switzerland.
26. Paul S.; Surface Coatings; Wiley & Sons, 1985
27. Reed J.S.; Principles of ceramics processing; second ed., 1989, Wiley & Sons, pg. 277-307
28. Prunet F.B., Legay D.F; Influence of lipidic coating on the sedimentation of metallic powders; *Journal of Colloid and Interface Science*, 145, 1991, pg. 524-538.
29. Rosen M.; Surfactants and Interfacial Phenomena; 2<sup>nd</sup> Ed., 1989, Wiley & Sons.
30. Rubin A.J.; Formation and stability of colloidal dispersions of fine particles in water; pg. 45-56.
31. Spanos N., Geogiadou I.; Investigation of rutile, anatase and industrial TiO<sub>2</sub>/water solution interfaces using potentiometric titration and microelectrophoresis; *Journal of Colloid and Interface Science*, 172, 1995, pg. 374-382.
32. Stoye D.; Paints, Coatings and Solvents, VCH, 1991

33. Tagawa M., Gotoh K., Ohmura Y.; An experimental trial for the determination of the CCC using sedimentation method; 273,1995,pg.1065-1070.
34. Weiss A., Hartenstein M.; Preparation and Characterization of well-defined streically stabilized latex particles with narrow size distribution; *Journal of Colloid and Polymer Science*,276,1998,pg.794-799.
35. Williams R. A.; Colloid and Surface Engineering,; Chapter 1.

İZMİR YÜKSEK TEKNOLOJİ ENSTİTÜSÜ  
REKTÖRLÜĞÜ  
Kütüphane ve Dokümantasyon Daire Bşk.

# APPENDIX

## FTIR CURVES OF FOUR TITANIA USED IN TESTS

The FTIR curves of commercial anatase and rutile titania powders are given in Figures A1 to A4. These FTIR spectra show that powders C and G have rutile structure whereas powders E and F have anatase structure as was reported by the companies. O-Ti-O group may absorb around 700-420  $\text{cm}^{-1}$  absorption band. The peak located at 540  $\text{cm}^{-1}$  may show Ti-O stretching for anatase structure. The absorption band includes strong peaks at 700, 650, 550, 470 and 410  $\text{cm}^{-1}$ . The absorption located at 700-420  $\text{cm}^{-1}$  may define as O-Ti-O group. The absorption band has medium peaks at 550 and 520  $\text{cm}^{-1}$  and a strong peak at 410  $\text{cm}^{-1}$ .

### POWDER G

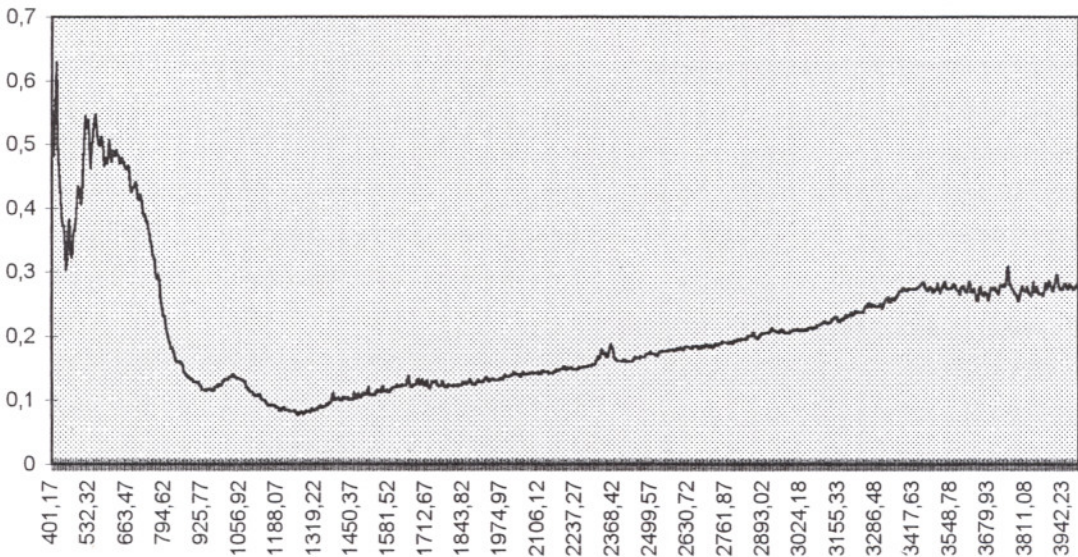


Figure A.1: FTIR Spectra of rutile powder G

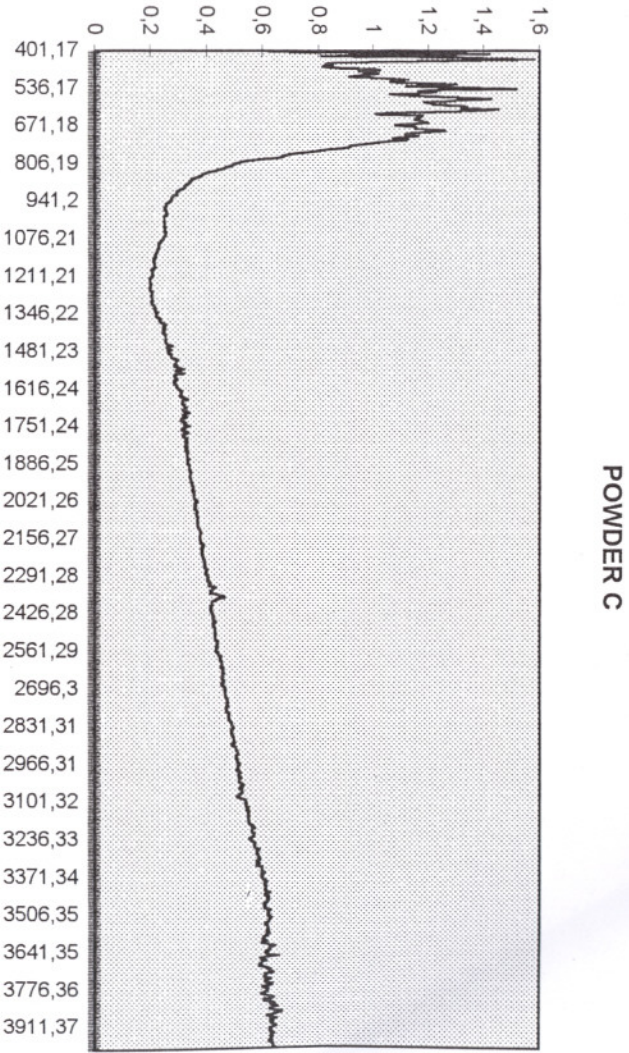
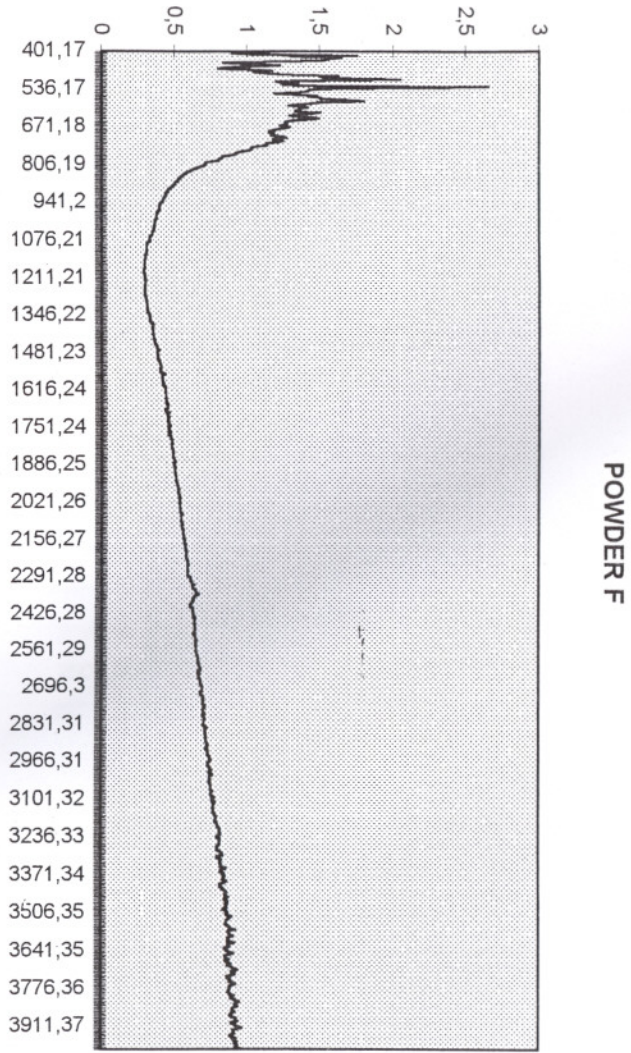


Figure A.3 : FTIR Spectra of anatase powder C

## POWDER E

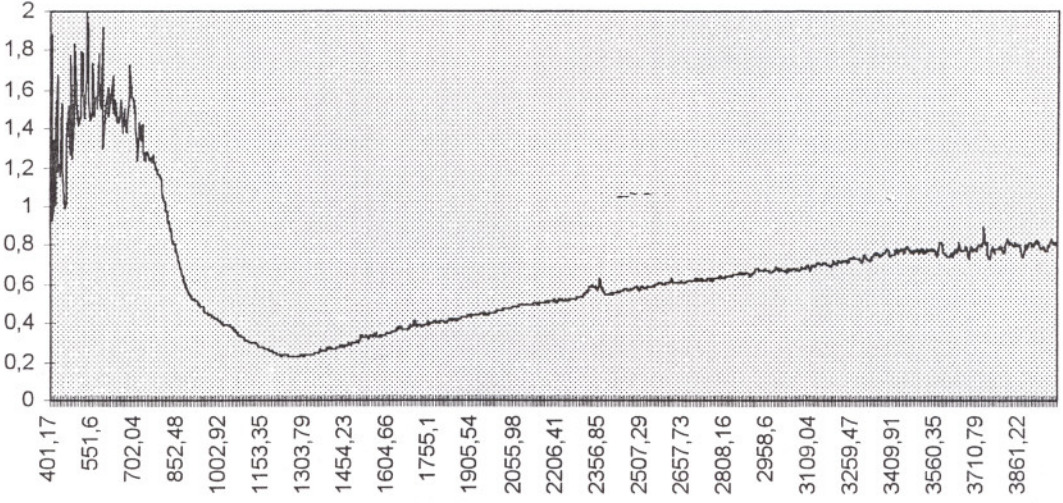


Figure A.4 : FTIR Spectra of anatase powder E